

**STUDY OF CALCIUM SPARKS IN SKELETAL AND  
SMOOTH MUSCLE CELLS IN NORMAL AND  
PATHOLOGICAL CONDITIONS**

**Inauguraldissertation**

zur

Erlangung der Würde eines Doktors der Philosophie  
vorgelegt der  
Philosophisch-Naturwissenschaftlichen Fakultät  
der Universität Basel

von

Rubén José López Dicurú  
aus Maracay (Venezuela)

Basel, 2016

Original document stored on the publication server of the University of Basel [edoc.unibas.ch](http://edoc.unibas.ch)



This work is licensed under a [Creative Commons Attribution-NonCommercial 4.0 International License](http://creativecommons.org/licenses/by-nc/4.0/).



Genehmigt von der Philosophisch-Naturwissenschaftlichen Fakultät  
auf Antrag von

Prof. Dr. Jean Pieters, Fakultätsverantwortliche

Prof. Dr. Susan Treves, Dissertationsleiterin

Prof. Dr. Christoph Handschin, Korreferent

Basel, den 19. April 2016

Prof. Dr. Jörg Schibler, Dekan



---

## ACKNOWLEDGEMENT

The Doctorate is for me without doubt more than a big intellectual challenge. It was a enormous life test that involved many sacrifices, lots of patience and perseverance and dramatic changes in the way to see and think about life and of course a lot, of work.

In this section I would like to recognize some people (and others that may have escaped from my memory) that generously gave me the tools to make my path through the PhD an enjoyable journey.

I wish to express my deepest acknowledgment to Francesco Zorzato and Susan Treves for the trust they deposited in me to board this fantastic project and to be part of the splendid team of the research laboratory of the Department of Anesthesia and Perioperative and Patient Safety. Their endless patience and will to teach are virtues that I have always appreciated especially in my difficult early times when I was starting the great challenge that accompanied this challenge. More than the innumerable intellectual and technical knowledge inputs that they place at my disposal, the critical thinking and holistic focus to analyze and solve problems are only a few of the many teachings I received from them and I will never stop thanking them.

Antonio, I could not be happy if I did not properly mention you. My assistant, my helper, my translator, my friend, my family. I have a big debt with you. Beside all the technical support that you offered me, your confidence, friendship, goodwill and the like-no-other happy and young spirit and humor gave me strength and a lot of happiness during this experience. I will never stop thanking you for all that you have done.

I deeply thank all the valuable technical and practical teachings that I kindly receive from Anne Sylvie Monnet.

I would of course also like to thank the members of the laboratory whom have shared with me these past 4 unforgettable years, especially Ori. I think we are notably different but we went through similar challenges, changes and experiences that formed us and made us both mature and find a deep respect for each other. I would also like to thank Maja, Alexis and more recently Chris and Jan, as well as Martine, Asensio, Thierry and Albi; your kindness made the atmosphere in the laboratory a happy and enjoyable place to work.

---

I would like to also thank other people inside and out of the Department of Biomedicine that, even though they were not directly involved in the realization of this project, have contributed by giving their priceless moral and spiritual support.

I am in deep debt with Heidi Hoyer mann that with her kindness and friendly smile helped me with the administrative support, useful advices and always-brilliant ideas that played a key role in my development in the laboratory.

The boys from the mechanical and electrical workshop, particularly Martin and Volker, they always were present with excellent goodwill to solve with incomparable professionalism the many technical problems that I would have never solved on my own.

Beyond all the immense technical and intellectual support that I received from many people, I would like to thank all those coworkers outside of the Laboratory that gave me their smiling, charisma, kindness, motivation and hope in those difficult moments. To them: Mary and their friends and Frank and el Gallego (from the cleaning service), Saida (from the Centrino) and others, my sincerest recognition for your priceless human value that you shared with me along this journey.

Beyond the borders of the ZLF I want to mention some people that offered strength to reach this goal. My very much-appreciated Sifu (Sabine) with her wisdom she taught me not only lessons in self-defense but also lessons to confront everyday life eventualities.

Kay Salathé, how not to cite you! You opened the doors of the heart of Basel and its surrounding areas showing the best that it has: its people. Without the family that warmly and selflessly you introduced me to (Basti, Vera, Beni, Zwicky brothers, Karin, Pepi, Dimi, Dominick, Ryf and Rachel, Lea, Vivi, Stefi and others that I easily forget their names), my journey would have not been a professional and personal success. You guys always make me feel at home. To all of you, my Swiss family, my deepest thank you.

Eliane Schneider, I am particularly in great debt with you for all your support.

Finally, I want to save the last lines of this section to thank my family. My mother Algeria, Santiago, Frederick, My aunts Saida, Anaelisa, la Sra Toribia, Nico, Everlin, my beloved nephews and nieces and particularly my father. Their wise advices, moral support, motivation and infinite love kept me standing firmly along this experience. I owe them to a great extent the success of this great experience. Thank you for being there.

---

## SUMMARY

mTOR signaling influence a wide range of cellular process including protein synthesis (Iadevaia et al., 2012; Ma and Blenis, 2009; Thoreen et al., 2012), lipids synthesis (Lamming and Sabatini, 2013), transcription (Dibble and Manning, 2013; Vazquez-Martin et al., 2011), nucleotides biosynthesis (Ben-Sahra et al., 2013; Robitaille et al., 2013) and cellular energetics (Albert and Hall, 2015; Duvel et al., 2010; Inoki et al., 2012). In muscle, suppression of mTORC1 signaling results in several phenotypic changes including decreased life expectancy, increased glycogen deposits and alterations of the twitch kinetics of slow fibres (Bentzinger et al., 2008), however it is unclear what is its specific role in the excitation contraction (EC) coupling. Likewise, the ryanodine receptor (RyR), the calcium release channel of the sarcoplasmic reticulum, plays a fundamental role in calcium homeostasis in a variety of cells and particularly in muscle (Lanner et al., 2010). Mutations in the gene encoding this channel have been associated with a number of debilitating or life-threatening neuromuscular pathologies including malignant hyperthermia (Kolb et al., 1982; Rosenberg et al., 2015; Treves et al., 2005), but little or no knowledge is known about their pathophysiological influence in mild bleeding disorders. In this thesis we investigated in greater detail 1) the effect of the mTORC1 signalling pathway on the integrity of the protein participants in skeletal muscle EC coupling and calcium homeostasis by using a muscle specific Raptor KO mouse model. 2) The calcium homeostasis of vascular smooth muscle cells of an MH mouse model and its association to mild bleeding disorders as also observed in MH patients.

As far as the mTOR is concerned, we found that in raptor knockout (RamKO) mice, the bulk of glycogen phosphorylase (GP) is mainly associated in its cAMP-non-stimulated form with sarcoplasmic reticulum (SR) membranes. In addition, radio ligand binding assay showed a ryanodine to dihydropyridine receptors (DHPRs) ratio of 0.79 and 1.35 for wild-type (WT) and raptor KO skeletal muscle membranes respectively, which was confirmed by Western Blot analysis. Peak amplitude and time to peak of the global calcium transients evoked by supramaximal field stimulation were not different between WT and raptor KO. However, the increase in the voltage sensor-uncoupled RyRs leads to an increase of both frequency and mass of elementary calcium release events (ECRE) induced by hyper-osmotic shock in flexor digitorum brevis (FDB) fibres from raptor KO. These findings together with previous reports

---

should be taken into consideration in the clinical practice when rapamycin or its analogs (rapalogs) is administrated to patients.

As far as *RYR1*-mutations in human patients and its relationship to bleeding abnormalities is concerned, 8/20 mutation carriers revealed abnormal bleeding scores compared with their healthy relatives (0/11). Similarly, MHS *RYR1*<sub>Y522S</sub> knock in mice exhibited 3 times longer bleeding times compared to their wild type littermates. The bleeding defect of MHS mice could be reversed by pre-treatment with the ryanodine receptor 1 antagonist dantrolene. Primary vascular SMCs from *RYR1*<sub>Y522S</sub> knock-in mice exhibited a higher frequency of subplasmalemmal Ca<sup>2+</sup> sparks leading to a more negative resting membrane potential. Furthermore, Ca<sup>2+</sup> sparks were blocked by pre-treatment with ryanodine or dantrolene. These results stimulated us to generate a model that could explain how impaired calcium homeostasis addressed by *RyR1* mutation could affect bleeding without influencing platelet or coagulation factor function. Our results on impaired calcium homeostasis caused by *RyR1* mutations could extend to other tissues that functionally express this channel.

In conclusion, the present study shows that the protein composition and function of the molecular machinery involved in skeletal muscle excitation-contraction (EC) coupling is affected by mTORC1 signaling and that *RYR1* mutations cause prolonged bleeding by altering vascular SMC function and emphasize the potential therapeutic value of dantrolene in the treatment of such bleeding abnormalities.



---

# TABLE OF CONTENTS

<b>ACKNOWLEDGEMENT</b> .....	I
<b>SUMMARY</b> .....	III
<b>INTRODUCTION</b> .....	1
<i>mTOR signaling in skeletal muscle</i> .....	2
mTOR: a brief overview .....	2
mTORC1 signaling in different pathological conditions .....	4
The mTORC1 pathway influences skeletal muscle .....	4
<i>An overview to skeletal muscle physiology</i> .....	7
Structural organization of skeletal muscle .....	7
Muscle fiber type .....	8
EC coupling .....	9
<i>Major proteins involved in skeletal muscle EC coupling</i> .....	13
RyR .....	14
<i>RyR1 function and Malignant Hyperthermia</i> .....	15
DHPR .....	17
SERCA .....	18
Calsequestrin .....	19
Calreticulin .....	20
Sarcalumenin .....	21
Albumin .....	21
SR protein of 35 KDa (SRP-35) .....	22
JP-45 .....	22
<i>Calcium Homeostasis</i> .....	24
Quantal calcium release unit: The Elementary Calcium Release Event (ECRE) as a fundamental calcium signal .....	24
Initiation and termination of ECREs in muscle .....	25
ECRE as a physiological signal for normal EC coupling integrity .....	26
<i>Overview of vascular smooth muscle cell physiology</i> .....	27
Vascular smooth muscle cell function and organization .....	27

---

Vascular smooth muscle cell structure .....	28
Excitation contraction coupling in smooth muscle cells .....	29
<i>Hemostasis and bleeding disorders associated to impaired vascular response</i> .....	33
<b>RESULTS</b> .....	35
Manuscript I: mTORC1 signaling on EC coupling and Ca <sup>2+</sup> homeostasis of skeletal muscle .....	35
<i>Summary of publication 1</i> .....	35
Raptor ablation in skeletal muscle decreases Cav1.1 expression and affects the function of the excitation–contraction coupling supramolecular complex <sup>¶</sup> .....	36
Abstract .....	36
Introduction .....	38
Materials and Methods .....	40
RamKO mice .....	40
RNA extraction, reverse transcription and PCR reactions .....	40
SR isolation, Western blotting and biochemical assays .....	40
In vitro muscle strength assessment .....	41
Isolation of extensor digitorum longus and soleus muscle fibres .....	41
Calcium measurements .....	42
ECRE analysis .....	43
Glycogen phosphorylase activity measurement .....	43
Luciferase reporter assay .....	44
Results .....	44
Mechanical properties of isolated fibres and content of proteins involved in excitation–contraction coupling in skeletal muscles of RamKO mice .....	44
Protein composition of skeletal muscle sarcoplasmic reticulum from RamKO mice .....	45
RamKO ablation affects the excitation–contraction coupling macromolecular complex .....	45
Glycogen phosphorylase is targeted to sarcoplasmic reticulum membrane in skeletal muscle from RamKO mice .....	47
Calcium transients on isolated EDL and soleus fibres .....	47

---

---

Elementary calcium release events in WT and RamKO FDB fibres.....	49
Discussion.....	50
Ca <sub>v</sub> 1.1 content in RamKO mice.....	50
RyR/Ca <sub>v</sub> 1.1 ratio in skeletal muscle of RamKO mice.....	51
Global calcium signals and elementary calcium release events in WT and RamKO fibres.....	52
Compartmentalization of glycogen phosphorylase to SR membrane.....	53
Figures, Legends and Tables.....	55
Figure 1. Mechanical properties of isolated EDL and soleus muscles from RamKO and control littermates.....	55
Figure 2. Biochemical characterization of SR proteins from RamKO mice.....	56
Figure 3. Ca <sub>v</sub> 1.1 is decreased in RamKO mice.....	57
Figure 4. Ca <sub>v</sub> 1.1 decrease in RamKO mice is not due to a decrease in transcription of Ca <sub>v</sub> 1.1 mRNA.....	58
Figure 5. RyR content and functional characteristics are not changed in RamKO mice.....	59
Figure 6. GP is accumulated in the SR of RamKO mice and represents mainly the enzymatically-inactive form.....	60
Figure 7. Changes in the myoplasmic [Ca <sup>2+</sup> ] of individual, enzymatically dissociated EDL and soleus fibres.....	61
Figure 8. Osmotic-shock triggered ECRE are more frequent in FDB fibres from RamKO than WT mice.....	62
Table 1. Kinetic properties of calcium transients of isolated EDL and soleus fibres from control and RamKO mice.....	63
Table 2. Morphology of ECREs in skeletal muscle fibres.....	63
Supplementary Material.....	64
Supplementary Figure.....	64
Figure S1. Global Ca <sup>2+</sup> transients in mouse FDB fibers isolated from WT and RamKO littermates elicited before and after hyperosmotic stress-induced-ECREs.....	64
Supplementary Videos.....	65
Supplementary video 1.....	65
Supplementary video 2.....	65

---

---

Supplementary video 3 .....	65
Supplementary video 4 .....	65
Supplementary video 5 .....	65
Supplementary video 6 .....	65
Author Contribution .....	66
Aknowledgements .....	66
Funding .....	66
References .....	66
Manuscript II: MH-linked <i>RyR1</i> mutation and arterial smooth muscle $Ca^{2+}$ homeostasis on bleeding disorders .....	75
<i>Summary of publication 2</i> .....	75
<i>RYR1</i> mutations are a newly identified cause of prolonged bleeding abnormalities <sup>¶</sup> .....	77
Abstract .....	78
Overview, results and finding implications .....	79
Methods .....	83
Patients .....	83
Animal Model .....	83
Bleeding time assay .....	84
Isolation of single smooth muscle cells .....	84
Calcium imaging and Spark analysis .....	84
Immunofluorescence .....	84
Real Time qPCR and RT PCR .....	85
Membrane potential measurements .....	85
Statistical analysis and graphical software .....	86
Figures, legends and Table .....	87
Figure 1. <i>RYR1</i> mutations are associated with prolonged bleeding times .....	87
Figure 2. RyR1 is expressed in aorta and tail arteries and has a sub- plasma membrane localization .....	88
Figure 3. Arterial SMC from the <i>RYR1</i> <sub>Y522S</sub> mouse exhibit smaller intracellular $Ca^{2+}$ stores and a higher frequency of spontaneous $Ca^{2+}$ sparks .....	89

---

---

Figure 4. The resting membrane potential in SMC from the RYR1 <sub>Y522S</sub> mouse is significantly different from that of WT cells. Schematic representation of RyR1 function in arterial smooth muscle cells. ....	91
Table 1. Genetic details, neuromuscular features, MCMDM-1VWD bleeding questionnaire scores and bleeding phenotypes from patients with <i>RYR1</i> -related myopathies and their non-mutated relatives. ....	92
Supplementary material .....	94
Supplementary Figures .....	94
Supplementary Figure 1. Female RYR1 <sub>Y522S</sub> knock in MHS mice show prolonged bleeding times. ....	94
Supplementary Figure 2. Specificity of the anti-RyR1 antibodies used for IHC: western blots of skeletal and cardiac total sarcoplasmic reticulum membranes using isoform specific anti-RyR antibodies. ....	95
Supplementary Figure 3. Membrane potential measurements using the fluorescence potentiometric probe Bis-Oxonol. ....	96
Supplementary Table .....	97
Supplementary Table 2.4. Effect of Dantrolene and Ryanodine on the frequency of spontaneous Ca <sup>2+</sup> Sparks.....	97
Supplementary Videos.....	98
Supplementary video 1 .....	98
Supplementary video 2 .....	98
Supplementary video 3 .....	98
Supplementary video 4 .....	98
Supplementary video 5 .....	98
Supplementary video 6 .....	98
Supplementary video 7 .....	99
Supplementary video 8 .....	99
Author Contribution .....	100
Acknowledgements .....	100
Funding.....	100
References.....	101
<b>CONCLUSIONS AND PERSPECTIVES .....</b>	<b>105</b>
<b>APPENDIX.....</b>	<b>107</b>

---

---

<i>Blood pressure assessment in RyR1Y522S mice</i> .....	107
<i>Detailed kinetics Analysis of ECREs activity in VSMCs</i> .....	109
Table A1. Detailed Analysis of full kinetics parameters of ECREs activity quantified in VSMCs from WT and RyR1Y522S animals respectively. ....	110
Table A2. Detailed Analysis of full kinetics parameters of ECREs activity quantified in VSMCs from WT and RyR1Y522S animals respectively treated with Dantrolene.....	111
<i>Effect of Tetracain 150 <math>\mu</math>M on ECREs activity in VSMCs</i> .....	112
Video A1 .....	112
Video A2.....	112
<b>REFERENCES</b> .....	113
<b>CURRICULUM VITAE</b> .....	137

---

## INTRODUCTION

Muscle is a soft tissue, whose main purpose is to produce motion and force in animals. The generation of limb and trunk movements, the control of breathing as well as involuntary visceral movement, heart beating and vascular tone are controlled by muscles.

Morphological, structural and functional features allow to classify them grossly in three main types: skeletal, cardiac and smooth muscles. The first two share a common feature: a regular striation pattern easily observable under the microscope, while smooth muscles lack such a remarkable characteristic.

All muscles cause motion by cycles of contraction and relaxation that are tightly controlled by complex protein machineries, however, different muscle types differ in the ways these cycles are triggered and terminated and interference of its delicate homeostasis may lead to severe diseases (Lanner, 2012; Le Rumeur, 2015; Timchenko, 2013).

In the past decades a number of experimental evidence has uncovered the important role of mTOR signaling in a wide range of cellular anabolic process including protein synthesis (Iadevaia et al., 2012; Ma and Blenis, 2009; Thoreen et al., 2012), lipid synthesis (Lamming and Sabatini, 2013), transcription (Dibble and Manning, 2013; Vazquez-Martin et al., 2011), nucleotides biosynthesis (Ben-Sahra et al., 2013; Robitaille et al., 2013) and cellular energetics (Albert and Hall, 2015; Duvel et al., 2010; Inoki et al., 2012). It is also no surprise that skeletal muscle, representing approximately 40 percent of our body weight, is also influenced by the mTOR signalling pathway. This is also supported by the growing number of publications relating to mTOR signaling in muscle pathophysiology in recent years (Bentzinger et al., 2013; Bentzinger et al., 2008; Bodine et al., 2001a; Khurana and Davies, 2003; Lawrence, 2001; Leger et al., 2006; Ribeiro et al., 2015).

## ***mTOR signaling in skeletal muscle***

mTOR: a brief overview

mTOR is a protein kinase that belongs to the family of Phosphoinositide 3-kinase (PI3K)-related kinases (PIKKs) (Baretic and Williams, 2014). This group of proteins shares a common structure consisting of a conserved kinase core domain; a short conserved segment referred to as FATC domain, which is located just at the C-terminal of the kinase domain, and a long series of variable helical repeats forming the  $\alpha$ -solenoid domain. mTOR, as the other family member of PIKKs, is characterized by the fact that it preferentially phosphorylates its substrate on a serine or threonine residue (Kang et al., 2013).

In order to function and exert its enzymatic activity mTOR requires a set of accompanying proteins. Thus, mTOR forms two multicomponent distinct catalytic complexes: mTOR complex 1 (mTORC1) composed by the mTOR kinase active core, and additional regulatory proteins including the regulatory associated protein of mTOR (RAPTOR), the mammalian lethal with SEC13 protein 8 (mLST8), the Proline-Rich Akt Substrate of 40 KDa (PRAS40) and the DEP-domain-containing mTOR interacting protein (DEPTOR). This complex is best known for being the target of rapamycin (Heitman et al., 1991), a suppressor of eukaryotic cell proliferation produced by the bacterium *Streptomyces hygroscopicus* (Vezina et al., 1975) and clinically used as an immunosupresant (Brattstrom et al., 2000; Kahan et al., 1998).

The other functional complex referred to as mTOR complex 2 (mTORC2) is equipped with the catalytic unit mTOR and the associated proteins rapamycin-insensitive companion of mTOR (RICTOR), mLST8, the protein observed with RICTOR 1/2 (PROTOR 1/2) and DEPTOR. This complex was initially believed to be independent of rapamycin (Jacinto et al., 2004), however new evidence shows that it can be affected by this drug depending on the cell types, dose and in a time-dependent fashion. (Sarbasov et al., 2006).

Thus, mTORC1 and mTORC2 contain both distinct and shared proteins. However, they differ markedly as to their upstream stimulants, as well as their regulatory and functional output (see Figure 1).

mTORC1 responds to a set of upstream signals including growth factors, stress, oxygen, energy status and amino acids, to promote cell growth by regulating positively anabolic



processes including protein and lipid synthesis, energy metabolism and negatively catabolic process such as autophagy and lysosome biogenesis (for extended and detailed reviews on mTOR signaling see (Cornu et al., 2013; Hall, 2008; Laplante and Sabatini, 2012). Once mTORC1 is activated, it phosphorylates several substrate including the translational regulators eukaryotic translation initiation factor 4E (eIF4E)-binding protein 1 (4E-BP1) and ribosomal protein S6 kinase 1 (S6K1) to coordinate the initiation of protein synthesis (Ma and Blenis, 2009). Moreover, mTORC1 also operates on sterol regulatory element-binding protein 1/2 (SREBP1/2), which are transcription factors that control the synthesis of genes involved in fatty acid and cholesterol anabolism (Laplante and Sabatini, 2009).

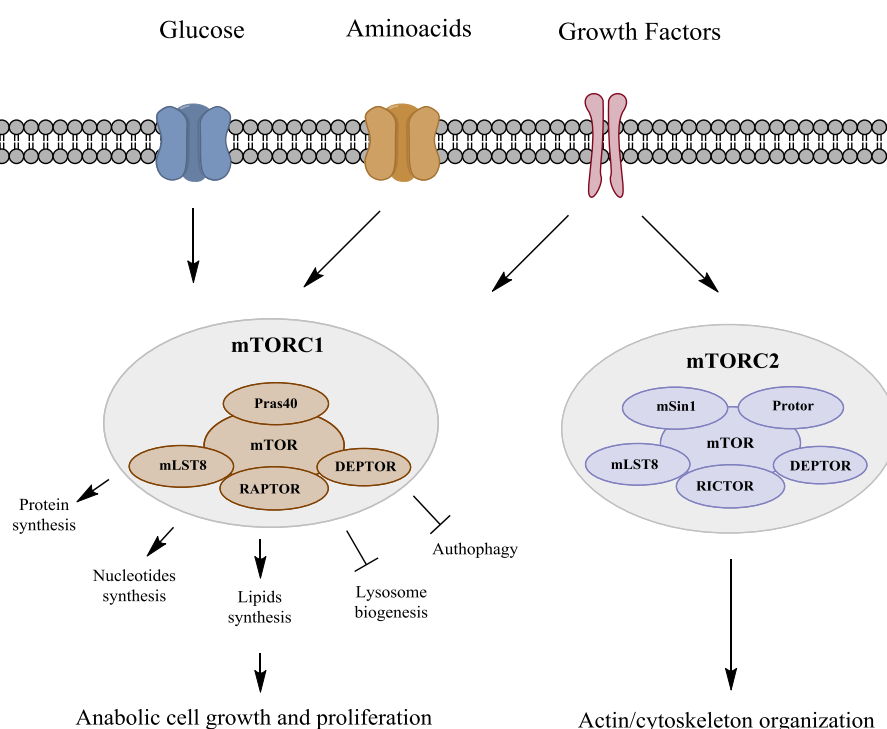


Figure 1. Overview of the mTOR signalling pathway in cellular function with the main upstream input and downstream effectors. For details see the text explanation.

On the other hand, knowledge of mTORC2 function is less clear and reports relating to its functional role are more sparse. Nonetheless, it is known that mTORC2 is more sensitive to growth factors than nutrients and plays an important role in the dynamics of actin cytoskeleton by associating with ribosomes (Jacinto et al., 2004; Sarbassov et al., 2004; Zinzalla et al., 2011) possibly involving Protein Kinase C alpha (PKC $\alpha$ ) and the small GTPases Rho and Rac. Figure 1 shows a summary of the main cellular processes controlled by the mTOR signaling complexes as well as some of its input stimulus.

## mTORC1 signaling in different pathological conditions

Since mTORC1 activation includes a long list of regulatory metabolic pathways that roughly determine cell proliferation, its pharmacological control represents a key tool in understanding not only its functional mechanism but also its significance in the development and prevention of several diseases. The mechanism of action of rapamycin involves the proline isomerase FKBP12 to form the Rapamicin-FKBP12 complex (Heitman et al., 1991; Koltin et al., 1991; Sabatini et al., 1994). This Rapamicin-FKBP12 complex binds to the mTOR N-terminal of the kinase domain (Chen et al., 1995) and acts as an allosteric inhibitor, therefore preventing mTORC1 function.

Rapamycin, (commercially known as Sirolimus or Rapamune) which is used worldwide was FDA approved in the U.S. in 1999 and in Europe is given to patients since 2001 (European Medicines Agency, 2015) and by (U. S. Food and Drug Administration, 2015), it is used to treat a range of impaired mTOR functions including Cancer (Baselga et al., 2012), organ transplantation immunosuppressant (Calne et al., 1989; Lorber et al., 2005; Schuler et al., 1997) and neurological disorders (Cardamone et al., 2014). More recently, it has been discovered to prolong the life span of animals (Ehninger et al., 2014; Fok et al., 2014; Harrison et al., 2009) though there its effect on prolonging human lifespan is controversial (Johnson et al., 2013).

Nevertheless, uses of rapamycin in a clinical context continue growing. The extensive use of rapamycin or its analogs (rapalogs) demands more knowledge to understand better its function in a more systemic approach. To achieve this aim we explored the role of the mTORC1 pathway on skeletal muscle physiology, particularly in controlling calcium homeostasis and the protein complexes involved in this process. In the next section I will describe the finding of the role of mTORC1 in muscle biology.

## The mTORC1 pathway influences skeletal muscle

Skeletal muscle is an organ that has incredible adaptive capabilities in response to several physiological (e.g., exercise) and pathological (systemic diseases, myopathy, and aging)

---

conditions. Some of these adaptive processes include hypertrophy, atrophy, regeneration, fiber type conversion and mitochondrial biogenesis that ultimately result in a change of the muscle performance. Thus for instance, formation of muscle mass, is a complex process determined by the balance between new protein synthesis and degradation; both of them tightly regulated and interrelated (Sandri, 2008). Both systems require energy, a checkpoint where the body decides either to promote growth and hypertrophy or activate protein breakdown and atrophy. mTORC1 plays an important role in muscle growth closely related to the metabolic response. In fact it seems to be involved in the maintenance of mitochondrial oxidative function by directly regulating mitochondrial gene expression through the control of transcription complexes such as like Yin Yang 1 (YY1) and Peroxisome proliferator-activated receptor gamma coactivator 1-alpha (PGC-1  $\alpha$ ) (Cunningham et al., 2007) both master regulators of mitochondrial gene biogenesis.

Additionally, Insulin Factor-like Growth Type 1 (IGF-1) was shown to be able to increase muscle protein synthesis mediated by the PI3K/Akt/mTOR signaling pathway in a rapamycin-sensitive manner (Ohanna et al., 2005; Rommel et al., 2001), linking in this way metabolic input with muscle growth.

Recent evidence has revealed that mTORC1 represents a crucial signaling pathway determining protein synthesis in skeletal muscle. In mechanical-load induced growth Bodine et al. demonstrated that the adaptive hypertrophy of adult skeletal muscles seems to be crucially regulated by the activation of the Akt/mTOR pathway and its downstream targets S6K1 and 4E-BP1 (Bodine et al., 2001b).

In the same line, dramatic changes in muscle phenotype are observed when mTOR or some of its associated proteins are knocked out in animal models. For example at the level of whole body, Knocking Out (KO) mTOR (Gangloff et al., 2004; Murakami et al., 2004) or its companions RAPTOR and mLST8 (Guertin et al., 2006) is embryonically lethal. Furthermore, conditional muscle specific KO of mTORC1 mouse models display a wide range of muscle pathologies. In particular such mice display features of muscular dystrophy (MD) and metabolic changes including increased glucose uptake and glycogen synthesis, associated with reduced glycogen breakdown, increased glycogen accumulation and premature death (Risson et al., 2009).

Consistent with these findings, mice with muscle specific KO of RAPTOR (RAmKO) previously generated by Bentzinger and colleagues, exhibited a reduced life-span as well as some features of dystrophy with elevated numbers of muscle fibers with centralized nuclei

and the presence of central core-like structures, changes in mitochondrial function, increased glycogen content, a higher proportion of fast muscle fibers accompanied by a switch from oxidative to glucolytic metabolism and decreased muscle mass (Bentzinger et al., 2008).

In a more functional approach made in the same study by Bentzinger and colleagues ablation of RAPTOR in muscle not only significantly compromised the voluntary running wheel exercise in these mice but also *in vitro* dissected muscle *extensor digitorum brevis* (EDL) and *soleus* exhibited a diminished performance when submitted to strenuous fatigue protocols. These changes were correlated with an important reduction of mechanical properties of the muscle such as twitch force and maximal tetanic absolute force, which were accompanied by a featured phenotype with slow kinetics (longer time to peak, half time to peak and relaxation time).

Nevertheless, calcium, a secondary messenger that intervenes in a number of physiological processes, and in particular in muscle it underlies excitation contraction coupling and therefore force generation had not been investigated in relation to mTOR complexes and muscle function and in this context it should be mentioned that mishandling of calcium homeostasis is an important factor that compromises muscle performance and leads to several neuromuscular diseases (MacLennan, 2000; Treves et al., 2005).

Many of the degenerated muscle phenotype features caused by suppressing the mTORC1 signaling pathway and its downstream targets, might alter not only metabolism, protein synthesis and muscle performance but also affect directly the calcium dynamics through the molecular machinery that operates the excitation contraction (EC) process. This aspect was investigated during my PhD and we provide evidence (results section manuscript 1) that mTORC1 inactivation by ablation of its regulatory protein RAPTOR, affects the macromolecular EC coupling integrity and therefore the calcium homeostasis in skeletal muscle.

## ***An overview to skeletal muscle physiology***

### Structural organization of skeletal muscle

Muscle, the tissue responsible for all the movement in organisms, is composed of elongated thin fused multinucleated cells called fibers. A muscle unit is composed of several elongated fibers lying parallel to each other and held together in bundles by connective tissue. They have a finely organized architecture that enables them to rapidly undergo significant changes in shape and size, which is then translated into motion. Motion is a highly dynamic process due to the shortening and elongation of the fiber size, a process referred to as contraction and relaxation respectively.

A remarkable feature of muscle fibers is the presence of multiple nuclei formed by the fusion of myoblasts (premature muscle cells) at the embryonic stage and the presence of many mitochondria, the power generating organelle that supplies the energy required by muscle cells (Hill, 2012).

Fibers are equipped with numerous myofibrils, a cylindrical structure of about 1-2  $\mu\text{m}$  in diameter, extending along the fiber. They constitute the contractile elements made up of cytoskeletal microfilaments that, when observed under the microscope, display distinguishable repeated dark and light bands called A band and I band, respectively.

An A band is composed of set of thick filaments that overlap on both ends with thin filaments. The central region of the band A, where thin filaments are not present, is called the H zone and at its center it is divided by the M line. The I band is composed by thin filaments that do not project to the A band and are connected by the Z line at the center. Thick filaments are made up myosin chains that extend perpendicularly from the M line towards the Z line, whereas thin filaments are made up primarily of the protein actin, that on the contrary, extend from the Z line towards the band M. The smallest functional contractile unit in muscle, the sarcomere, is defined as the section between two consecutive Z line. A detailed scheme of the structural organization of a myofibril is shown on Figure 2.

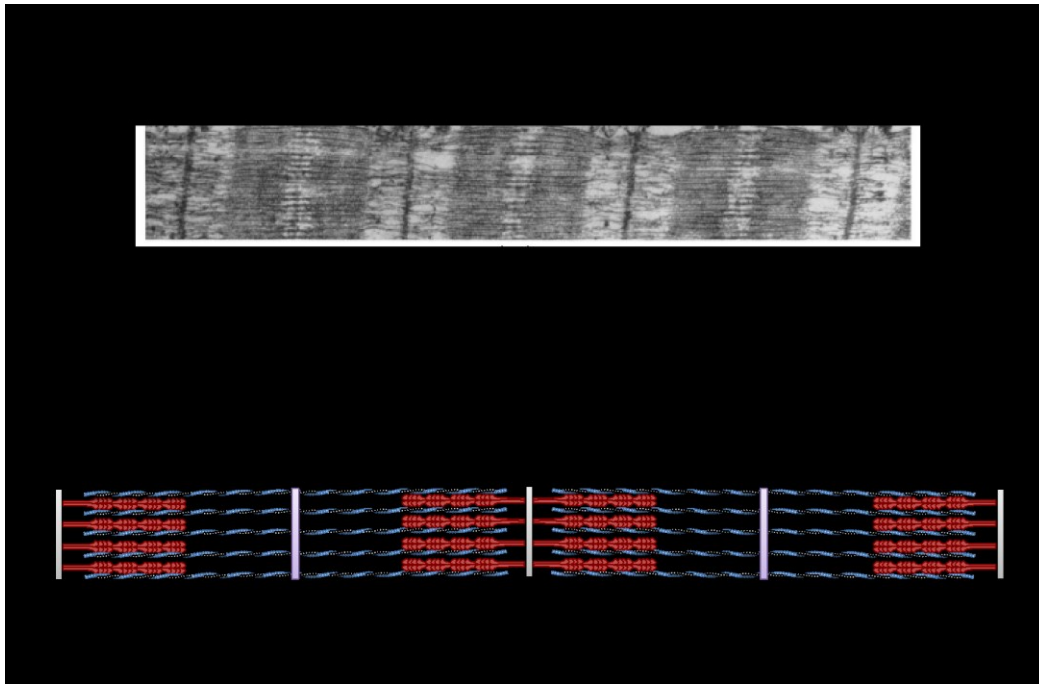


Figure 2. Structural organization of a skeletal muscle sarcomere. A An electron microscope (EM) micrograph of the organization of myofibrils from rabbit psoas muscle (magnification 60000x) taken from pioneer structural work of Hugh Huxley on the determination of the myofilaments array (Huxley, 1957). B schematic representation of myofilaments organized in a sarcomere. The blue and grey threads represent the thin filaments and the red threads represent the thick filaments.

This arrangement of the contractile proteins is specific and necessary in order to allow force generation in the muscle by the shortening of the sarcomere, a mechanism known as “cross-bridge” or sliding-filaments (Podolsky, 1961). This mechanism consists in shortening the distance between two adjacent Z lines through the sliding of the thick filaments (myosin) and thin filaments (actin) passed one another by mechanical interaction (Huxley, 1969). This is an energy dependent process that involves the regulatory proteins troponin and tropomyosin forming a molecular complex together with the actin filaments that are in motion (active) only in the presence of calcium (Ebashi, 1972; Hayashi, 1952; Weber and Winicur, 1961).

### Muscle fiber type

Skeletal muscles can be divided in different subgroups that have adapted to perform special functions e.g. from long lasting, continuous and low-intensity activities to fast, explosive and high- intensity activities.

Although the contractile properties, calcium kinetics, molecular composition, histochemical and biochemical features have helped to identify at least four different muscle fiber types known as slow type I and fast types IIA, IIX/D and IIB (Bottinelli and Reggiani, 2000; Calderon et al., 2010; Schiaffino and Reggiani, 2011), for reasons of simplicity we will use an old conventional classification of two muscle types: the fast-twitch muscles, characterized by glycolytic metabolism and specialized for phasic activity, generally identified as white muscles, and the slow-twitch muscles, rich in myoglobin and oxidative enzymes and specialized for more continuous activity, also called red muscles (Cassens and Cooper, 1971).

### EC coupling

The generation of force requires a sophisticated mechanism of signal communication that initiates contractile proteins activity and consecutively terminates it. This signal starts in the neurons innervating the muscle fiber and is transmitted through chemical and physical communication in a space denominated the neuromuscular junction: the edge between a terminal axon from a motor neuron and the sarcolemma of a muscle fiber (Del Castillo and Katz, 1954). When a motor neuron generates an action potential, a fast and sudden transient change in the membrane potential triggers the exocytosis of neurotransmitters including acetylcholine (Augustine and Kasai, 2007; Fatt and Katz, 1951). The surface of the muscle fiber membrane is equipped with acetylcholine receptors able to sense this signal and translate it into an action potential within the whole sarcolemma, the cellular membrane of the muscle fiber. Similar to what occurs in neurons, in muscle fibers the action potential is an electrical signal that is detected by antenna proteins able to translate this information into a chemical signal. The L-type voltage-dependent calcium channel referred to as dihydropyridine receptor or Cav1.1 is a voltage sensor that acts as a physical-chemical translator of this signal. It is located at the T-tubules (Fosset et al., 1983): invaginations of the sarcolemma that extend radially in an intricate network into the center of the fibers and is tightly connected with the muscle sarcoplasmic reticulum (SR) cisternae (Catterall, 1991; Nelson and Benson, 1963; Porter and Palade, 1957). The SR constitutes an extended calcium store organelle formed by a longitudinal section and another section disposed in close contact with the T-tubule called terminal cisternae (Costello et al., 1986; Meissner, 1975). The structure formed by a T-tubule with two adjacent terminal cisternae is referred to as triad and contains the functional unit of electrical and mechanical coupling (Franzini-Armstrong,

1980). In this membrane junction formed by the T-tubule and the SR several proteins have been identified aside the Cav1.1 channel, including the calcium release channel of the SR or ryanodine receptor (RyR) (Kawamoto et al., 1986), a large homotetrameric protein of about 560 KDa (Zucchi and Ronca-Testoni, 1997).

This protein assembles in clusters of four units (tetrads) forming what is considered to be the “feet” that bridge the SR and the T-tubule. Each tetrad in the SR is associated with four aligned Cav1.1 of the sarcolemma in alternate positions so that they form a coupled checkerboard structure (Block et al., 1988). In other words, the Cav1.1 is associated with the tetrads forming a coupled unit every 2 tetrads. This can be better visualized as shown in Figure 3.

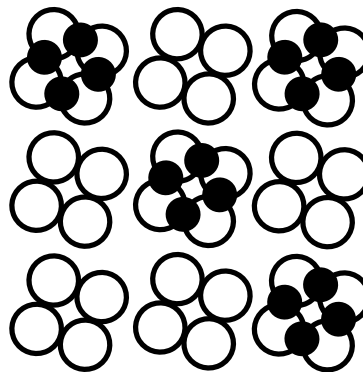


Figure 3. Tetrad organization in the SR-T-tubule junction. The empty circles forming a tetrad represent the uncoupled RyR, whereas the filled circles are the Cav1.1, aligned with the RyR forming a coupled tetras in an alternated pattern. From the model of Block and colleagues 1988.

Such an arrangement seems to be important for the controlled opening of the RyR by the voltage sensor Cav1.1, since experimental evidence have shown that artificially uncoupling the RyR-Cav1.1 communication leads to elementary calcium release events called sparks (Apostol et al., 2009), and the presence of sparks can indicate a deleterious signal of impaired calcium homeostasis in some myopathies (Franzini-Armstrong et al., 1991; Wang et al., 2005).

Thus, when an action potential reaches the sarcolemma, it produces structural conformational changes of the Cav1.1 that are physically connected with RyR, which once activated leads to a massive and transient calcium release from the SR to the cytosol. Free cytosolic calcium is



the trigger signal that allows the cross-bridge formation of the contractile proteins myosin and actin to generate contraction.

The sequence of events in the muscle initiated by an electrical signal transformed in a contractile response is referred to as excitation-contraction coupling (EC coupling). This concept was first introduced by Alexander Sandow more than sixty years ago (Sandow, 1952) and much has been discovered since concerning the molecular mechanism involved in EC coupling. The termination of this event is conducted by a decrease of the cytosolic calcium concentration of the fiber to resting levels leading to muscle relaxation.

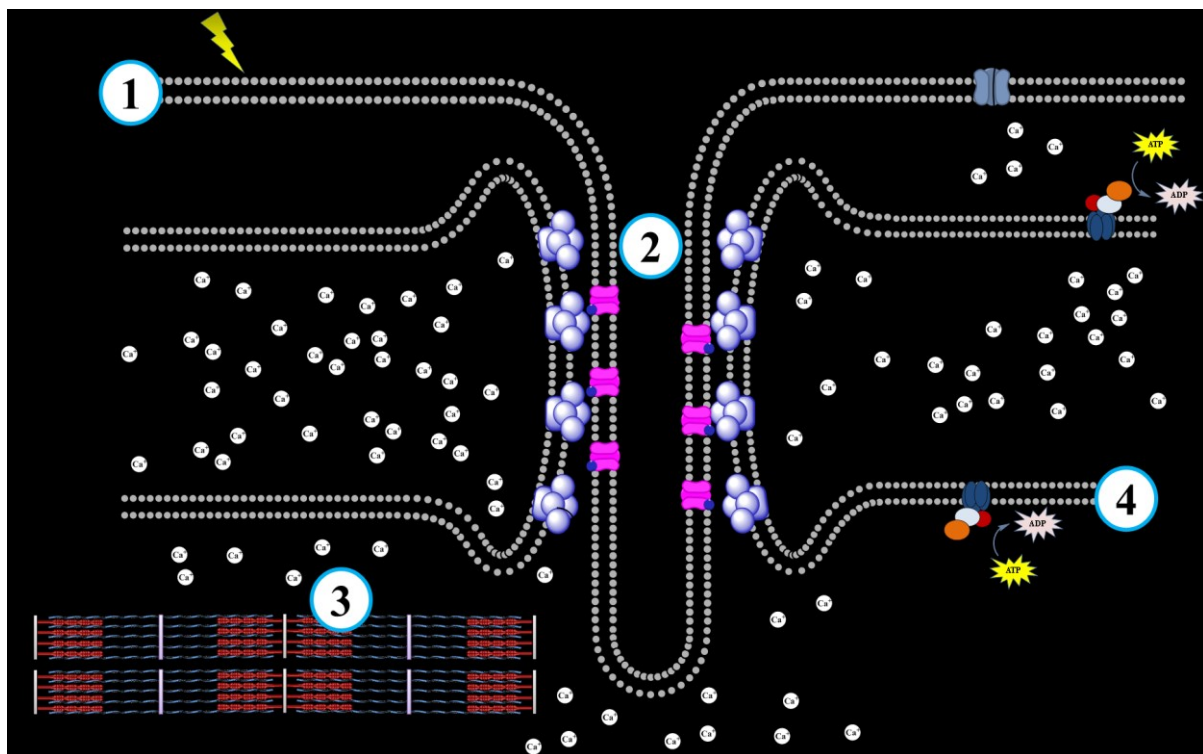


Figure 4. Sequence of events that take place during the EC coupling in a muscle fiber. Contraction is initiated by an electrical signal that propagated along the sarcolemma (1). The signal is received by the voltage sensor Cav1.1 and transmitted to a coupled RyR channel to trigger calcium release (2). The cytosolic calcium content increases dramatically and activates the contractile proteins (3). The cytosolic calcium level is restored to resting level and therefore the relaxation by reuptaking calcium to the SR of through the SERCA calcium pump activity or ejected out of the cell by the NCX (4).

To allow this to occur, the cell uses an energy-dependent mechanism to diminish the cytosolic calcium content to its resting level by the active extrusion of the cytosolic calcium through the sarcoplasmic/endoplasmic calcium ATPase (SERCA) that reuptakes the calcium

from the cytosol and translocates it back into the SR (Inesi, 1985). The sodium-calcium exchanger (NCX) located at the sarcolemmal membrane also contributes though to a lesser extent in skeletal muscle, to restoring the calcium concentration back to resting levels by transporting calcium into the extracellular space (Gonzalez-Serratos et al., 1996).

A representation of the sequence of events that occurs in a muscle fiber from the reception of an action potential till the generation of contraction is shown in Figure 4. Although, the process that comprise the initiation of the contraction triggered by an action potential until the restoration of the calcium levels is broadly understood, the role of many additional molecular components that are present in T-tubules and in the SR junctional face as well as in the SR lumen are still under investigation and their role in regulating and fine tuning the EC coupling machinery not completely understood.

### ***Major proteins involved in skeletal muscle EC coupling***

The SR contains a set of proteins that are directly or indirectly involved in the EC coupling process. Many of these proteins relay important information and are involved in the calcium handling, whereas other proteins are still being discovered and their roles are under investigation (Barone et al., 2015; Treves et al., 2009).

Some of the major molecular components of the EC coupling machinery are displayed in Figure 4. Some of these proteins and others not shown in the cartoon will be described in more detail below.

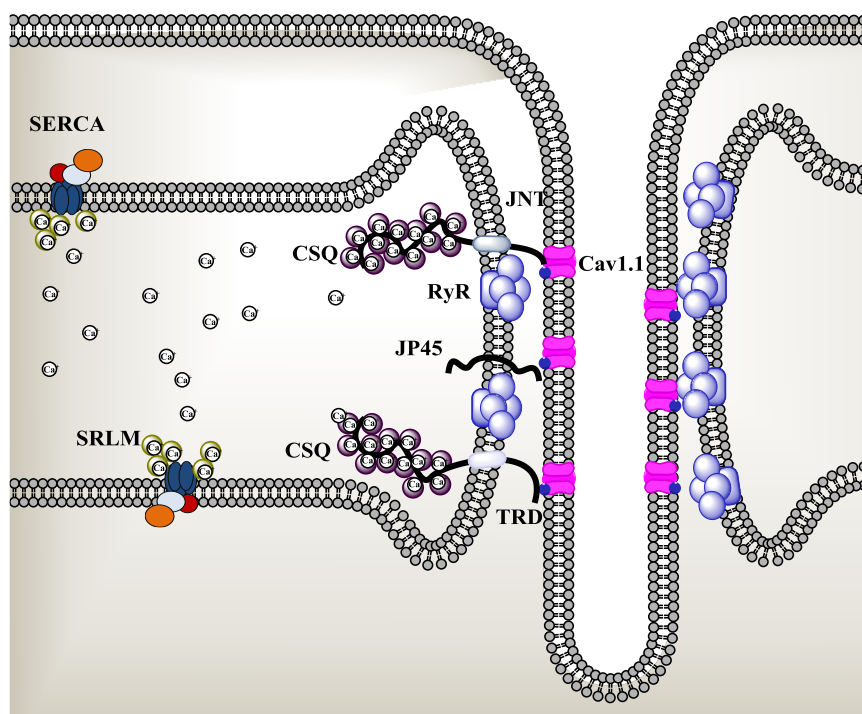


Figure 5. Some proteins in the EC coupling located in the SR and T-Tubule membrane system. Major proteins participating in the EC coupling are represented here (RyR, Cav1.1 and SERCA), as well as others minor proteins with buffer or structural organization properties. Cav1.1, Skeletal isoform of Type L voltage calcium channel; CSQ, Calsequestrin, JNT, Junctin; JP-45, Junctional Protein of 45 kDa; SERCA, Sarco/Endoplasmic reticulum  $\text{Ca}^{2+}$  ATPase; SRLM, Sarcalumenin; TRD, Triadin; RyR, Ryanodine receptor.

## RyR

The RyR is a calcium channel located on the SR or endoplasmic reticulum in many excitable and nonexcitable cells (Giannini et al., 1995; Ledbetter et al., 1994). Three isoforms have been identified in mammals referred to as RyR1 RyR2 and RyR3. RyR1 is expressed mainly in skeletal muscle and RyR2 is present in cardiac muscle while RyR3 is associated with the nervous system particularly the brain (Mackrill et al., 1997). Smooth muscle cells are heterogeneous and express all three isoforms (Fritz et al., 2007; Neylon et al., 1995). RyR1 and RyR2 have been more extensively investigated because of their crucial role in EC coupling in skeletal and cardiac muscle, respectively. In humans the gene that encodes for RyR1 is located on chromosome 19q13.2 and spans 106 exons, which translates into a polypeptide chain of 5038 residues (Gillies et al., 2015). A number of mutations have an important impact on RyR1 function and have been associated with several musculoskeletal diseases including Malignant Hyperthermia (MH), central core disease (CCD) and multiminicore diseases (MmD) (Treves et al., 2005; Treves et al., 2009).

In skeletal muscle RyR1 assembles into a homotetrameric structure of about 2 MDa where each subunit has a molecular weight of approximately 560 kDa, with the shape of a square around the central pore. Recent structural data predict that each RyR1 contains 6 transmembrane domains arranged with the amino and carboxy terminal tails located at the cytosolic face of the SR membrane (Zalk et al., 2015). The C-terminus region forms the channel, whereas the large N-terminal domain serves as a scaffold, which interacts with other regulatory proteins modulating the pore opening. A detailed representation of the architecture of the Ryanodine receptor can be visualized in the Figure 6.

Although RyR1 activity is largely controlled by the calcium channel, voltage sensing Cav1.1 (Rios and Brum, 1987) by allosteric interaction (Kugler et al., 2004; Proenza et al., 2002; Sheridan et al., 2006), other protein such as calmodulin, FKBP12, triadin, junctin, calsequestrin also interact with RyR1 (Lanner et al., 2010; Zalk et al., 2007). Additionally, and not less importantly small molecules such as ATP, calcium and magnesium serve as positive or negative regulators of RyR1 activity (Laver et al., 2001; Meissner et al., 1986; Meissner et al., 1997).

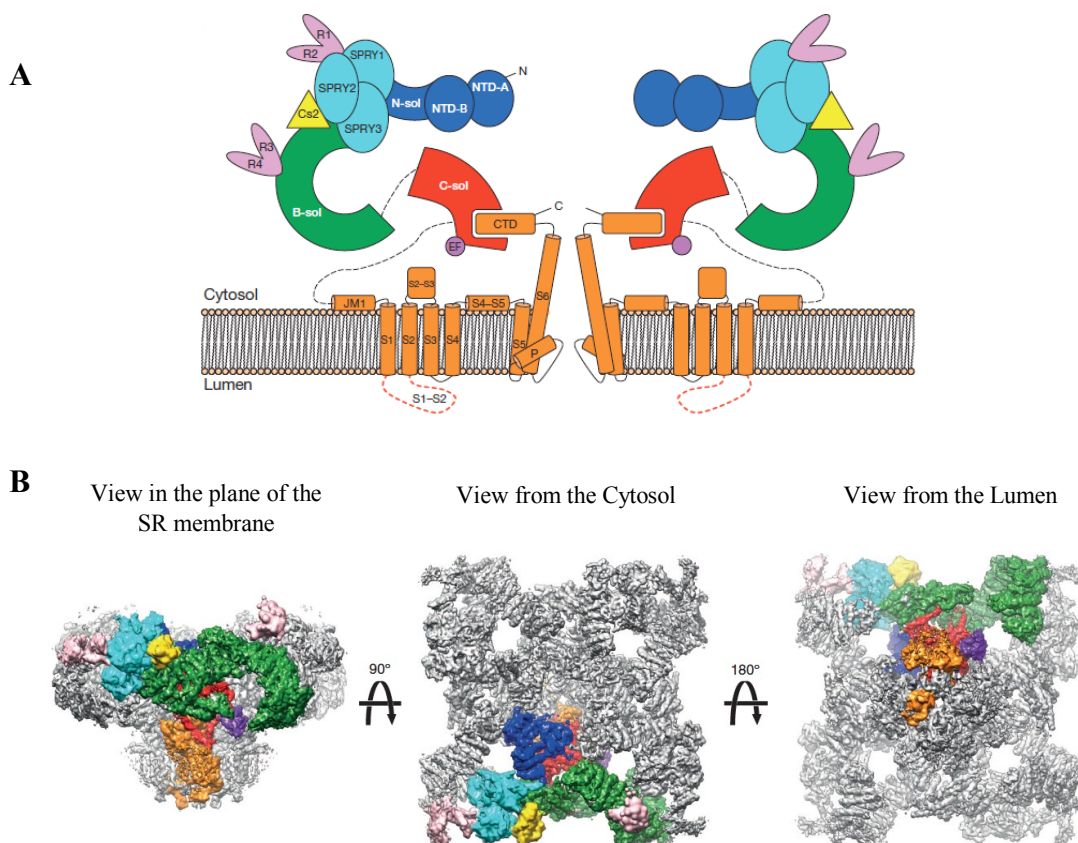


Figure 6. Architecture of the Ryanodine receptor. **A**, color-code schematic representation of the RyR. **B**, Predicted structure of the RyR tetramer displayed at different perspectives. B-sol, bridge solenoid; C-sol, core solenoid; N-sol, N-terminus solenoid. Coloured as follows: blue, N-terminal domain; cyan, SPRY1, SPRY2 and SPRY3; salmon, clamp region (RY12 repeats), and phosphorylation domain (RY34 repeats); yellow, FKBP12; green, the bridge solenoid scaffold; red, the core solenoid; and orange, transmembrane and C-terminal domains; purple, putative  $\text{Ca}^{2+}$ -binding domain (EF).

### *RyR1 function and Malignant Hyperthermia*

Unbalance of calcium dynamics caused by dysfunctional RyR1 has been associated with several human neuromuscular diseases (see for example reviews by (Hwang et al., 2012; Treves et al., 2008)). Dominant and recessive mutations identified in the *RyR1*, the gene encoding RyR1 have been linked to disorders including central core disease (CCD) (Wu et al., 2006), centronuclear myopathy (CNM) (Wilmshurst et al., 2010), multiminicore disease (MmD) (Ferreiro et al., 2002), congenital fiber type disproportion (Clarke et al., 2010), heat/exercise induced rhabdomyolysis (Capacchione et al., 2010) and malignant hyperthermia (MH) (MacLennan et al., 1990; McCarthy et al., 1990). MH is an autosomal dominant disease, in which genetically predisposed individuals react to inhalation anesthetics (e.g.,

halothane) and depolarizing muscle relaxants (e.g., succinylcholine) or exercise/heat, by undergoing a hypermetabolic reaction which is potentially fatal if not treated promptly (Denborough, 1998; Rosenberg et al., 2015). The mechanism underlying this pathology implicates an uncontrolled rise in the cytosolic calcium concentration due to release from the SR mediated by RyR1 after the predisposed individual comes into contact with a trigger agent. The elevated cytosolic calcium induces generalized muscle contractures, activates glycogenolysis and metabolism resulting in the generation of heat and excess lactate production (Jurkat-Rott et al., 2000). The most notable clinical symptoms include metabolic acidosis, hypercapnia, rhabdomyolysis, generalized muscle rigidity, hyperthermia and tachycardia.

When recognized early, treatments of the MH crisis can be implemented by methods for lowering the body temperature such as immersion in an as ice bath and rapid administration of the antidote dantrolene. This drug normalizes the cellular resting calcium level by blocking calcium release driven by RyR1 hyperactivation (Krause et al., 2004; Paul-Pletzer et al., 2002; Zhao et al., 2001).

Although the incidence of this disorder ranges from 1:10,000 and 1:250,000 general anesthetics, it is estimated that the prevalence of *RYR1* causative mutations of MH predisposition in the population might be much higher (1:3000 to 1:8500) (Rosenberg et al., 2007). However, the true number of individuals with MHS is difficult to estimate, principally due the fact that in the majority of MH susceptible individuals do not present any physical symptoms of muscle dysfunction until they come into contact with a trigger agent in surgery or when exposed to high temperatures or stress (Hopkins et al., 1991). Investigations into the genetic background and family history of individuals can lead to the identification of this disorder that can then be properly investigated either by molecular tools (genetic diagnosis) or functionally (*in vitro* contracture test). In this way, when a potential MH susceptible individual is found, and the diagnosis ascertained (including identification of mutations in *RYR1* or other genes (Gillies et al., 2015; Gonsalves et al., 2013; Hwang et al., 2012) alternative anesthetics can be safely administered. In the absence of a genetic diagnosis individuals undergo the *in vitro* contracture test (IVCT) in which the force generated by a fresh muscle biopsy is challenged with increasing concentrations of the trigger agent halothane or caffeine and the force generated and thresholds values to the stimulants are determined and compared to those of normal, non susceptible individuals (Hopkins et al., 2015).

---

Although, the European Malignant Hyperthermia Group (EMHG) has reported 35 causative mutations in the *RyR1* for the diagnosis of MHs, 240 mutations seem to be linked to the clinical or molecular MH phenotype among the more than 600 variants reported in the databank (European Malignant Hyperthermia, 2016; Rosenberg et al., 2003). Additionally, two mutations in the gene that encode the  $\alpha 1S$  subunit of the Cav1.1 (*CACNA1S*) have also been identified as a MHs causative.

Interestingly, channelopathies associated with *RyR1* mutations do not cause the same phenotype at functional level (Treves et al., 2008). Depending on the effect on RyR1 function, mutations are classified as causing 1) Hypersensitive channels: higher probability of electrical or chemical activation, 2) Leaky channels:  $Ca^{2+}$  dysregulation leading to depletion of SR stores, 3) Voltage sensor uncoupled channels: inability of the Cav1.1 to correctly mediate activation of RyR1 and finally 4) Low RyR1 expression level. Most of the *RyR1* mutations associated with MH principally belong to the first and second categories.

Experimental data have revealed that MH-related mutations in *RyR1* knocked-in in mouse cause an enhanced muscle contractility in response to pharmacological agents (halothane, caffeine) and heat (Chelu et al., 2006; Gallant and Lentz, 1992); enhanced voltage-dependent stimulation (Dietze et al., 2000), decreased sensitivity to inactivation by  $Mg^{2+}$  and  $Ca^{2+}$  (Owen et al., 1997).

## DHPR

The Cav1.1 also called dihydropyridine (DHPR) receptor is a voltage-gated calcium channel belonging to the family of transmembrane channel proteins that includes voltage-gate sodium and potassium channels (Catterall, 1995). Based on its homology, biophysical and pharmacological properties, the voltage gate calcium channel comprises a family of at least ten members (Cav1.1-1.4; Cav2.1-2.3; Cav3.1-3.3, where Cav1.1 and Cav1.2 are referred to as the skeletal and the cardiac form respectively because of their initial identification and distribution in such tissues (Curtis and Catterall, 1984; Glossmann et al., 1984).

The DHPR is a ~430 kDa heteropentamer composed of different subunits:  $\alpha_1$ ,  $\alpha_2$ ,  $\beta$ ,  $\delta$  and  $\gamma$ . The  $\alpha_1$  subunit (Cav1.1) (190 kDa) encompasses both the voltage sensor and the pore, thus conferring the major biophysical and functional properties to the channel; whereas the  $\alpha_2\delta$ ,  $\beta$  and  $\gamma$  subunits control channel expression, membrane incorporation, drug binding and gating characteristics of the pore subunit (Buraei and Yang, 2013; Dolphin, 2012; Triggle, 2006).

The  $\alpha 1$  subunit is a protein of about 2000 amino acid residues organized in 4 repeated domains (I-IV), each one containing six transmembrane segments (S1-S6) and both amino- and carboxi terminus ends are oriented towards the cytosolic space. The loop between domains II-III of the of the  $\alpha 1$  subunit are critical for the mechanical communication with the RyR1 (Grabner et al., 1999; Lu et al., 1994; Tanabe et al., 1990), however other domains of the  $\alpha 1$  subunit appear to interact with the RyR1 as well (Slavik et al., 1997).

The  $\beta$  subunit has a molecular weight of about 55 KDa and its distribution is confined to the cytoplasmic face of the channel. It has two important functions: 1) it regulates the transport/insertion of the  $\alpha 1$  subunit into the sarcolemma (Beurg et al., 1999a; Beurg et al., 1999b; Gregg et al., 1996) and 2) it acts as a scaffolding protein that stabilizes the communication between the  $\alpha 1$  subunit of the DHPR.1 and the RyR1 (Neuhuber et al., 1998; Schredelseker et al., 2005).

Regarding the other subunits ( $\alpha 2$ ,  $\delta$  and  $\gamma$ ), not much is known about their contribution to the DHPR channel function/regulation (Obermair et al., 2008).

## SERCA

SERCAs are 110 KDa transmembrane proteins located in the terminal cisternae and the longitudinal SR, where there are particularly abundant representing approximately 80 percent of the total protein content (Costello et al., 1986; Meissner, 1975; Zorzato et al., 1986). They play two important functions in muscle calcium homeostasis: 1) removal of the cytosolic free calcium thus contributing to the relaxation process and 2) refilling the calcium store after contraction by taking up the cytosolic calcium and pumping it back the SR in a ATP-dependent way.

SERCAs are monomeric integral membrane proteins composed of a large cytosolic segment “headpiece” connected to a transmembrane domain (M) by a short stalk segment. The cytosolic segment consists of 3 separated domains: A, N and P. The A domain may work as an actuator or anchor for Domain N, which binds nucleotide. The phosphorylation site is contained within domain P which is connected to the transmembrane domain (M) the last domain (A) that acts as a actuator or anchor for the domain N, connecting the transmembrane domain (M); the latter is made up of ten transmembrane helices (M1-M10) anchoring the protein to the SR. (Toyoshima et al., 2000). Mammalian cells express three different genes (*ATP2A1-3*) encoding for five different SERCA isoforms: SERCA1a,b, SERCA2a-c, SERCA3a-f. In skeletal muscle SERCA1a is principally expressed in adult fast-twitch fibers,



while SERCA2a is present in slow-twitch fibers and cardiac muscle (Damiani et al., 1981; DeFoor et al., 1980; Jorgensen et al., 1988; Jorgensen and Jones, 1986; Zubrzycka-Gaarn et al., 1984). SERCA2b and SERCA3 are ubiquitously expressed in different tissues (Burk et al., 1989; Genteski-Hamblin et al., 1988; Lytton et al., 1989)

As other ATPase pumps, SERCA utilizes the energy obtained from the hydrolysis of ATP to maintain a calcium concentration gradient of about 4 orders of magnitude between the lumen of the SR (millimolar) and the cytosol (sub-micromolar). The kinetic mechanism is such that two calcium ions are transported into the SR lumen for each molecule of ATP hydrolyzed in exchange of two or three protons ( $H^+$ ) (Hasselbach, 1980; Olesen et al., 2007; Yu et al., 1993).

SERCA pump activity is regulated by the proteins phospholamban and sarcolipin in a tissue specific fashion (Periasamy and Kalyanasundaram, 2007). In cardiac SR, phospholamban binds to and regulates the activity of SERCA2a depending on its phosphorylation state (MacLennan and Kranias, 2003). In its dephosphorylated form, phospholamban is an inhibitor of SERCA2a, but, when phosphorylated by PKA (or  $Ca^{2+}$ /CaM kinase), phospholamban dissociates from SERCA2a, activating this  $Ca^{2+}$  pump.

On the other hand sarcolipin, a smaller homologue of phospholamban lacking the phosphorylation site (Mascioni et al., 2002), is almost exclusively expressed in fast-twitch muscles associated with SERCA1. Sarcolipin modulates SERCA1 activity by decreasing its calcium affinity at low calcium concentrations, whereas at high calcium concentrations it enhance SERCA1a activity by increasing the  $V_{max}$  (Odermatt et al., 1998).

A number of others factors including calcium ion concentration, ATP levels, pH, and ADP and inorganic phosphate levels also influence SERCA pump activity.

### Calsequestrin

The calcium binding protein calsequestrin is the main protein component of the lumen of the terminal cisternae in striated muscles (Costello et al., 1986; Saito et al., 1984). Although it is a soluble protein, it is almost entirely located in the terminal cisternae of the SR (Franzini-Armstrong et al., 1987; Wagenknecht et al., 2002), where it is anchored to the junctional face through its interaction with the SR membrane proteins triadin (95 KDa), junctin (20 KDa) and JP45 (Beard et al., 2004; Beard et al., 2009; Zhang et al., 1997). This quaternary complex serves to buffer calcium near the site of calcium release and additionally it communicates the

---

calcium store level to the RyR, thereby regulating internally the activity of the RyR channel (Beard et al., 2005; Beard et al., 2009; Ikemoto et al., 1989; Qin et al., 2009). Calsequestrin has a high capacity (40-50 mol of  $\text{Ca}^{2+} \times \text{mol}^{-1}$  of protein) and low affinity (dissociation constant  $K_D = 1 \text{ mM}$ )  $\text{Ca}^{2+}$  binding properties (MacLennan and Wong, 1971), thus it acts as a calcium buffer and a calcium storage reservoir in the SR. When the luminal calcium concentration is high ( $\sim 1 \text{ mM}$ ) calsequestrin aggregates to form a linear polymer thereby increasing its calcium binding capacity (He et al., 1993). The monomeric structure of calsequestrin is composed of three similarly folded domains (DI-III) where each domain exposes acidic amino acid residues to the exterior increasing cation binding (Wang et al., 1998).

Calsequestrin is present in mammalian cells in two isoforms: the “skeletal” form Calsequestrin 1 (migrating with an apparent mol mass of 63 KDa) and the “cardiac” form calsequestrin 2 (migrating with an apparent molecular mass of 55 KDa), encoded by two different genes *CASQ1* and *CASQ2*, respectively (Fliegel et al., 1990; Scott et al., 1988). Calsequestrin 1 is expressed in fast- and slow-twitch skeletal muscles, whereas the cardiac isoform is expressed in both cardiac muscle and slow-twitch skeletal muscles (Biral et al., 1992; Damiani and Margreth, 1994; Damiani et al., 1990; Scott et al., 1988). Calsequestrin has also been reported to be present in other tissues including smooth muscle cells and cerebellum (Damiani et al., 1988; Novak and Soukup, 2011; Volpe et al., 1990; Volpe et al., 1994).

### Calreticulin

Calreticulin is a 46 KDa calcium binding protein present in the luminal space of the endoplasmic reticulum (ER) or SR and is expressed in a wide range of tissues (Michalak et al., 1999). Similar to calsequestrin, calreticulin can bind calcium with high capacity and relatively low affinity (25 mol of  $\text{Ca}^{2+} \times \text{mol}^{-1}$  of calreticulin). The protein consists of three functional domains: N-, P- and C-. The N- and the P domains are implicated in its chaperone function, whereas the C-domain highly rich in negatively charged amino acids is responsible for its calcium binding properties (Michalak et al., 1999; Nakamura et al., 2001; Prins and Michalak, 2011; Treves et al., 1990).

Calreticulin also plays an important role as a chaperone and together with calnexin (an ER integral membrane chaperone) and ERp57 (Protein disulfide-isomerase A3, resident in the

ER) contributes to the quality control and folding of newly-synthesized (glyco)proteins (Trombetta, 2003). Recent studies suggest that calreticulin influence SERCA expression and activity in heart, thus acting possibly not only as calcium buffer but also as a calcium reuptake regulator (Jiao et al., 2012; Shimura et al., 2008)

### Sarcalumenin

Sarcalumenin is another calcium binding protein of the SR lumen present in striated muscle (Rossi and Dirksen, 2006; Treves et al., 2009). It is predominantly found in the longitudinal SR localized together with SERCA (Leberer et al., 1990).

Two isoforms of sarcalumenin exist, a 160 kDa and a 35 kDa glycoprotein that are formed as alternative spliced products of a primary transcript encoded by the *SAR* gene. This protein exhibits a high capacity and moderated affinity for calcium (35 mol of  $\text{Ca}^{2+} \times \text{mol}^{-1}$  of sarcalumenin;  $K_D = 0.6 \text{ mM}$ ) (Leberer et al., 1990).. Although sarcalumenin is not crucial for muscle function, its absence in mouse leads to poor calcium re-uptake into the SR, thus revealing its important role in calcium handling (Manring et al., 2014; Yoshida et al., 2005).

### Albumin

Albumin is a globular 66.5 KDa protein present in serum involved in the transport of proteins, cations ( $\text{Na}^+$ ,  $\text{Ca}^{2+}$  and  $\text{K}^+$ ), fatty acids, hormones, bilirubin and drugs, but whose main function is to regulate the colloidal osmotic pressure of blood (Merlot et al., 2014). Although albumin is widely distributed in the extracellular environment, some is also present within the cell. Studies have demonstrated that albumin can interact with different proteins including calreticulin (Fritzsche et al., 2004). Interesting, albumin seems to have additional functions in skeletal muscle particularly in the t-tubular membrane, where it constitutes around 7 % of the total proteins content (Knudson and Campbell, 1989). Thus, this protein has been used as an important marker of tubule integrity and composition in skeletal muscle. (Knudson and Campbell, 1989; Muller and Heizmann, 1982),

### SR protein of 35 KDa (SRP-35)

SRP-35 is a recently identified protein of the SR membrane complex of skeletal muscle. This protein has a molecular weight of 35 KDa (hence its name) and is a transmembranal protein of the SR with its N- terminus embedded in the SR membrane and a C- terminal catalytic domain orientated towards the myoplasm (Treves et al., 2012). SRP-35 belongs to the trans-all retinol dehydrogenase family of proteins, which catalytic function is the conversion of all-*trans*-retinol to retinaldehyde by reducing the cofactor NAD<sup>+</sup> to NADH (Liden and Eriksson, 2006).

The retinoic acid signaling pathway is involved in the transcription of several genes, including some involved in growth, development, differentiation, cytokine production and metabolism (Napoli, 1996; Theodosiou et al., 2010). SRP35 is expressed in different tissues which are actively involved in metabolism including adipocyte, liver and skeletal muscle (Treves et al., 2012). In muscle the retinoic acid pathway promotes the activation of transcription factors involved in myogenesis and muscle differentiation (Halevy and Lerman, 1993; Muscat et al., 1994), however its specific role in skeletal muscle as a potential regulator of metabolism is currently being investigated.

### JP-45

This protein of 45 KDa (JP-45) is located on the junctional face membrane of skeletal muscle SR. It was discovered as a minor constituent of the membrane proteins associated with the SR (Treves et al., 2009; Zorzato et al., 2000). Initial characterization of JP-45 showed that it consists of a single pass transmembrane domain with the C- terminus orientated towards the lumen of the SR and the N- terminus facing the cytosolic space (Zorzato et al., 2000). Its expression is exclusively confined to skeletal muscle where it is highly enriched in the SR of both fast and slow twitch fibers. JP-45 acts as a signaling switch between calsequestrin and Cav1.1 (Anderson et al., 2003). This interaction seems to be important for the appropriate control of Cav1.1 activity (Mosca et al., 2013). In summary, the role of JP-45 in EC coupling can be described as an important maintainer of the functional integrity of Cav1.1 since ablation of JP-45 in mouse decreases the functional expression of Cav1.1 in t-tubules, which is translated as a loss of muscle strength (Delbono et al., 2007). Additionally, genetic variants

of JP-45 can influence the functional characteristics of Cav1.1 in MH susceptible individuals (Yasuda et al., 2013).

## ***Calcium Homeostasis***

Calcium is a universal second messenger that functions in a variety of signaling systems ranging from secretion, to transcriptional regulation, proliferation, fertilization and metabolism (Berridge et al., 2003). Because of its important function, cells have evolved a sophisticated mechanism to regulate its intracellular levels. As mentioned in a previous section, in muscle, calcium plays a decisive role as a trigger signal for the activation of the contractile proteins.

Quantal calcium release unit: The Elementary Calcium Release Event (ECRE) as a fundamental calcium signal

In muscle, a calcium transient is a transient and massive calcium release event that occurs in the cytoplasmic space as a response to a trigger signal. From a physiological point of view, the rapid and large calcium transient observed in EDL fibers, or the repetitive and slow cytosolic calcium changes observed in some smooth muscle cells, are both due to the activation of multiple microdomains of calcium release units. Such microdomains were initially identified in cardiac myocytes and called calcium sparks (Cheng et al., 1993), sparks were shown to play an important role in the activation of neighboring clusters of RyR to activate more calcium release propagating the calcium signal, a process called calcium induced calcium release (CICR) (Fabiato, 1983).

Localized calcium release events of similar nature have also been observed in other cells and were given different names, depending on their kinetics, subcellular localization or channels involved (Berridge, 2006; Cheng and Lederer, 2008; Niggli and Shirokova, 2007). Thus, microdomains of calcium release can be defined in general as “elementary calcium release events” (ECREs), and represent the minimum quantity of calcium released from one or a few release units (calcium channel) that combined give rise to the global calcium transient (Collier et al., 1999; Inoue and Bridge, 2003).

Although discrete calcium release events have been identified in the ER due to the opening of inositol triphosphate receptors (InsP3R) (Yao et al., 1995; Yao and Parker, 1994), the RyR in its different isoforms, is the main calcium channel involved in the generation of calcium sparks.

Applying advanced microscopy techniques together with computational tools, the RyR-dependent calcium ECREs have been the subject of extensive investigations and our understanding of their biophysical properties and regulation have greatly advanced (Bankhead et al., 2011; Csernoch et al., 2004; Demuro and Parker, 2008; Jiang et al., 1999; Picht et al., 2007).

#### Initiation and termination of ECREs in muscle

The activation and termination of ECREs activity might be due to several factors including intrinsic activity of the RyR channel, depolarization of the membrane, the presence of physiological or non-physiological ligands, cytosolic and SR calcium levels and phosphorylation of RyR among others (Lukyanenko and Gyorke, 1999; Satoh et al., 1997; Zhou et al., 2004). Studies in cardiac muscle cells suggest that spontaneous ECREs activity might be due to the intrinsic stochastic activity of RyR in the resting state (Cheng et al., 1993). In skeletal muscle, this is markedly different, since spontaneous ECREs activity has not been observed in adult skeletal fibers under normal physiological conditions (Shirokova et al., 1998). This is due to the fact that the organization of the calcium release-coupling units (RyR-Cav1.1) in skeletal and cardiac muscle are fundamentally different. In particular, in skeletal muscle the Cav1.1 controls RyR activity by physical contact and specific spatial arrangement, while in cardiac muscle this control is only partial or lacking (Block et al., 1988; Franzini-Armstrong, 1980). Nevertheless, ECREs can be induced in skeletal muscle fibers by artificially disrupting the RyR-Cav1.1 communication by osmotic shock, chemical permeabilization or mechanical removal of the sarcolemma (Apostol et al., 2009; Kirsch et al., 2001; Weisleder et al., 2012).

Though the mechanisms governing calcium release are quite clear, this is not so for those controlling its termination and many mechanisms have been proposed to explain this process. At least five different models have been put forward to explain what terminates the ECRE. These mechanisms can be listed as follow:

- 1) *Local calcium depletion*: this hypothesizes that a local reduction of calcium content in the SR reduces RyR activity (Launikonis et al., 2006);
- 2) *Coupled gating*: involves two or more physically associated RyRs that influence each others gating behavior through mechanical contact (Marx et al., 1998);

- 3) *Voltage sensor deactivation*: consist in the deactivation of the voltage sensor in skeletal muscle cells (Cav1.1) that enforces early termination of an ongoing spark (Lacampagne et al., 2000);
- 4) *Stochastic attrition*: requires the random closure of independently gated channels that confers a finite probability for all channels in a cluster to close at once (Stern, 1992);
- 5) *Channel inactivation*: this is a state in which the RyR calcium channel closes and no longer responds to stimuli that usually open it (Cheng and Lederer, 2008).

#### ECRE as a physiological signal for normal EC coupling integrity

Interestingly, ECREs behavior has been used as an important tool to study normal and pathological conditions in muscle. In fact in skeletal muscle spontaneous ECREs are not normally observed, and the occurrence of such events has been found to correlate with special or pathological conditions including stress, aging, mouse models knocked out for certain SR proteins or certain neuromuscular disorders (Ward and Lederer, 2005; Weisleder and Ma, 2006). For instance, in the mouse model of Duchenne muscular dystrophy (*mdx*), which lacks the structural protein dystrophin, osmotic stress or strenuous exercise conditions have been associated with impaired membrane organization that disrupts the interaction between the RyR-Cav1.1 proteins leading to the appearance of ECREs activity (Wang et al., 2005).

Additionally, during aging substantial changes of ECREs activity have been identified in skeletal muscle in response to hypertonic shock. As opposed to the dystrophic *mdx* mouse model however, aged skeletal muscles exhibit diminished osmotic-induced ECREs activity (Weisleder et al., 2006). This change was also accompanied by a full set of other changes including fragmentation of the SR membrane system, loss of EC coupling proteins components such as Cav1.1 (Delbono et al., 1995), calsequestrin (Margreth et al., 1999) SERCA (Schoneich et al., 1999) and a change in the RyR/Cav1.1 ratio (Renganathan et al., 1997) that altogether maintain the appropriate organization, function and performance of the EC coupling machinery.



## ***Overview of vascular smooth muscle cell physiology***

### Vascular smooth muscle cell function and organization

Smooth muscle cells are present in the tissues of several hollow organ including gastrointestinal and urinary tracts, respiratory airways, reproductive organs. Additionally, smooth muscle cells are the principal constituents responsible for maintaining the arterial tone in the circulatory system within vertebrates. Due to their diverse distribution within many systems, they are largely different in function and structure. However, smooth muscles can be roughly classified according to their contractile properties or their electrical coupling (Hill et al., 2012). As far as their contractile properties are concerned, they can be divided into *tonic* and *phasic*. Tonic smooth muscle cells can maintain force for long periods of time, while phasic smooth muscle cells can produce rhythmic or intermittent force activity. On the other hand, when smooth muscle cells are electrically coupled to each other by gap junctions, they function as a single entity called *single-unit smooth muscle*; on the other hand *multi-unit smooth muscle* lacks this feature working as independent units and individual cells are under more direct neural control than single-unit smooth muscles. Nevertheless many smooth muscle types do not fit in this classification and present a more mixed and heterogeneous contractile features (Hill, 2012). Not surprisingly, variability is also present within the smooth muscle cell populations present in the vascular system in small and large arteries. Smooth muscle cells present in large arteries are characterize by their tonic phenotype, while smooth muscle cells of the small resistance arteries typically exhibit phasic contractions (Reho et al., 2014).

The dilation and contractile properties of blood vessels allows an adequate blood flow to the different organs throughout the body. The majority of blood vessels (except capillaries) are formed by three different layers: intima, media and adventitia and are shown in Figure 7.

The inner layer, the intima, is a single layer of endothelial cells facing the lumen of the blood vessels in direct contact with the blood. It is separated from the next layer, the media by the basal lamina. The media is principally made up by smooth muscle cells disposed so that their contraction reduces the vessel diameters. An extracellular matrix of collagen, elastin and other glycoproteins not only surround and embed the smooth muscle cells but also provide elasticity to the blood vessel. Finally the adventitia is the outer layer and is composed of

collagen and fibroblasts and larger vessels may contain small blood vessels (*vasa vasorum*, which supply blood to the wall of large blood vessels), lymphatic vessels and autonomic nervous from the sympathetic system principally.

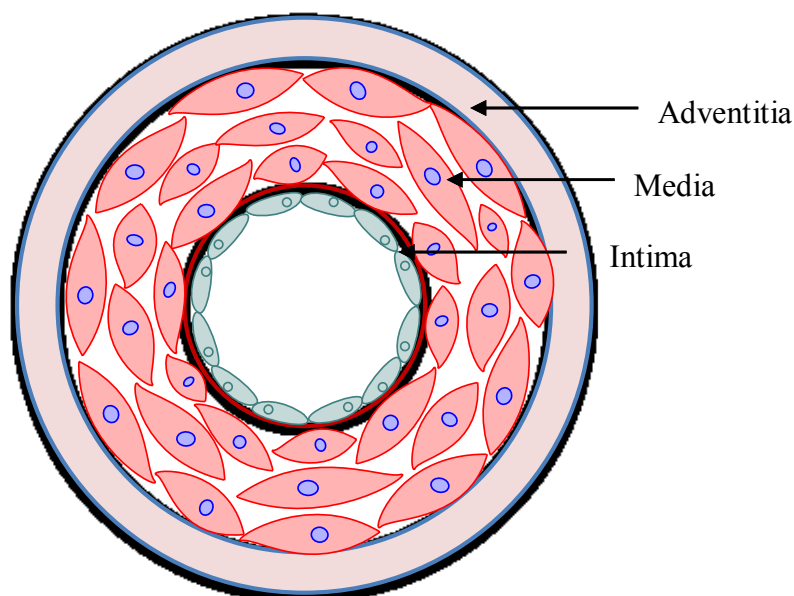


Figure 7. Blood vessel layers composition. Except capillaries, blood vessels are composed of three distinguished layers named adventitia, media and intima as indicated by the arrows. The intima contains a single layer of endothelial cells. The media is equipped with a multilayer of smooth muscle cells that confers contractile properties to the vessels. The adventitia provides support and elasticity to the blood vessels and receives external signals from the autonomous nervous system and other cells (not shown).

#### Vascular smooth muscle cell structure

Smooth muscle cells are elongated and spindle shaped, typically from 5 to 10  $\mu\text{m}$  in width and from 40 to 300  $\mu\text{m}$  in length that are arranged in sheets. In addition to their small size and mononuclear structure, they do not contain T-tubules, are not striated and their SR is considerably less organized compared to skeletal or cardiac muscle cells. In smooth muscle tropomyosin is present but the regulatory protein troponin is lacking. However, the protein caldesmon that has an analogous regulatory function as the troponin-tropomyosin system is expressed (Gusev, 2001).

Similar to skeletal and cardiac muscle, smooth muscles use actin and myosin to generate force, however they are not organized in the repeated band pattern found in striated muscles

since they do not form myofibrils and do not have a sarcomeric structure. Instead, smooth muscle contains structures called dense bodies within the cell and dense bands located closed to the sarcolemma that have a similar protein composition as the Z-lines, which function as anchoring centers for the contractile proteins. The actin filaments are attached to the dense bodies, and instead of being disposed in parallel along the cell as in skeletal and cardiac muscle, they are oriented slightly diagonally within the cell. On the other hand, each myosin filament is surrounded by several actin filaments and arranged so that the cross bridges are present along the whole filament length. Thus, the thick and thin contractile filament units form a dynamic cross-bridge lattice shape within the cell (Figure 8). Additionally, smooth muscle cells also contain intermediate filaments that are also anchored to the dense bodies, which do not participate directly in the contraction process but contribute to maintain the organization of the cytoskeleton and cell shape.

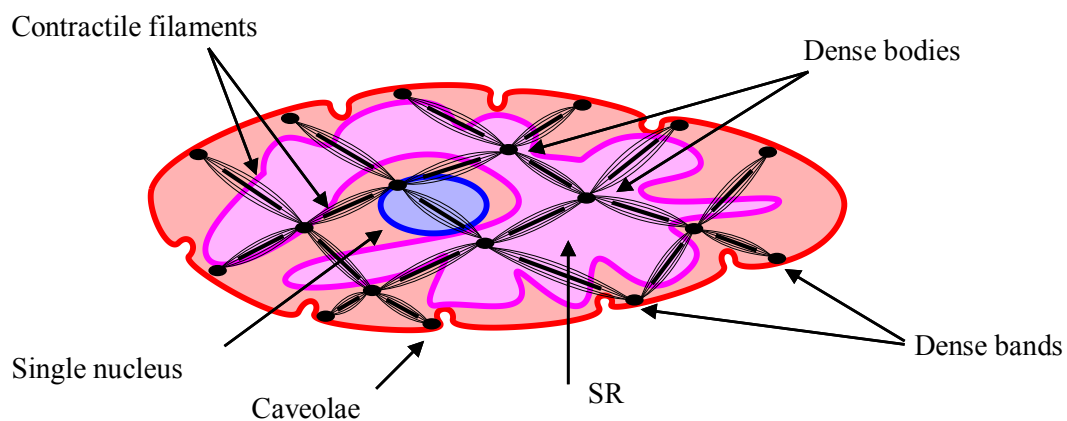


Figure 8. Organization of a vascular smooth muscle cell. Major cellular structures (contractile filaments, dense bodies and bands, caveolae, SR and nucleus) are indicated by arrows. The actin and myosin contractile proteins form a lattice shape structure within the whole cell interconnected through the dense bodies and dense bands.

#### Excitation contraction coupling in smooth muscle cells

In resting conditions, vascular smooth muscle cells maintain low cytosolic calcium levels but a rise of the cytosolic calcium level will lead to the activation of the contractile apparatus (the actin and myosin system). As opposed to skeletal muscles however, the mechanisms underlying the activation and regulation of contraction are considerably different. Stimuli from different sources including sympathetic adrenergic nerves, circulating hormones,

substances released by endothelial cells or substances released by the tissue surrounding the vessels, can influence the vascular tone. At the same time, vascular smooth muscle cell contraction can be initiated by electrical, chemical or mechanical stimuli (Bolton, 1979; Gollasch and Nelson, 1997; Nakayama and Tanaka, 1994; Rembold, 1992). The summation of all inputs will determine the cytosolic calcium levels and therefore the contractile or relaxed state of the cell. Electrical depolarization of the sarcolemma elicits contraction primarily by opening the voltage activated calcium channel Cav1.2 (Clapp et al., 1987; Gollasch and Nelson, 1997; Vivaudou et al., 1988). Calcium influx via Cav1.2 can also occur by membrane depolarization activated by receptor operated channels (Large, 2002). Many different chemical stimuli (norepinephrine, epinephrine, angiotensin II, vasopressin, endothelin-1, and thromboxane A<sub>2</sub>) activate signal transduction pathways that ultimately lead to an increase of cytoplasmic calcium, producing contraction. High levels of cytosolic free calcium triggered by any of the mechanism mentioned above will bind to the calcium binding protein calmodulin, a protein structurally similar to troponin (Ikura, 1996). The calcium-calmodulin complex binds to and activates the myosin light chain kinase that successively phosphorylates the myosin light chain in the presence of ATP. Myosin light chain phosphorylation permits the cross-bridge formation between the head of the myosin heavy chain and actin, leading to contraction. Since smooth muscles lack the troponin complex, the above mentioned proteins are the main regulators of contraction. Dephosphorylation of myosin light chains by the enzyme myosin light chain phosphatase provide the signals leading to termination of muscle contraction (Hirano et al., 2004).

The SR/ER serves as a calcium store that can release calcium into the cytosol by activation of the inositol triphosphate receptors (InsP<sub>3</sub> receptor) (Sasaguri et al., 1985; Somlyo et al., 1985; Suematsu et al., 1984). RyR calcium channels are also present in the smooth muscle SR, however they participate to the excitation contraction coupling mechanism in a different way. As opposed to InsP<sub>3</sub> receptors, localized calcium release via RyR channel activate calcium dependent potassium channels located at the sarcolemma, which, once activated, leads to spontaneous transient outward currents (STOCs) (Benham and Bolton, 1986; Ganitkevich and Isenberg, 1990). Activation of STOCs shifts the membrane potential to more negative values (hyperpolarized) and prevent calcium entrance via Cav1.2 (Jaggar et al., 1998; Nelson et al., 1995; Perez et al., 1999), therefore inducing smooth muscle cell relaxation. In this context, since calcium has a dual role in smooth muscle cells, the spatial and temporal characteristics of the calcium transients are a critical determinant in whether the cells contract or relax.

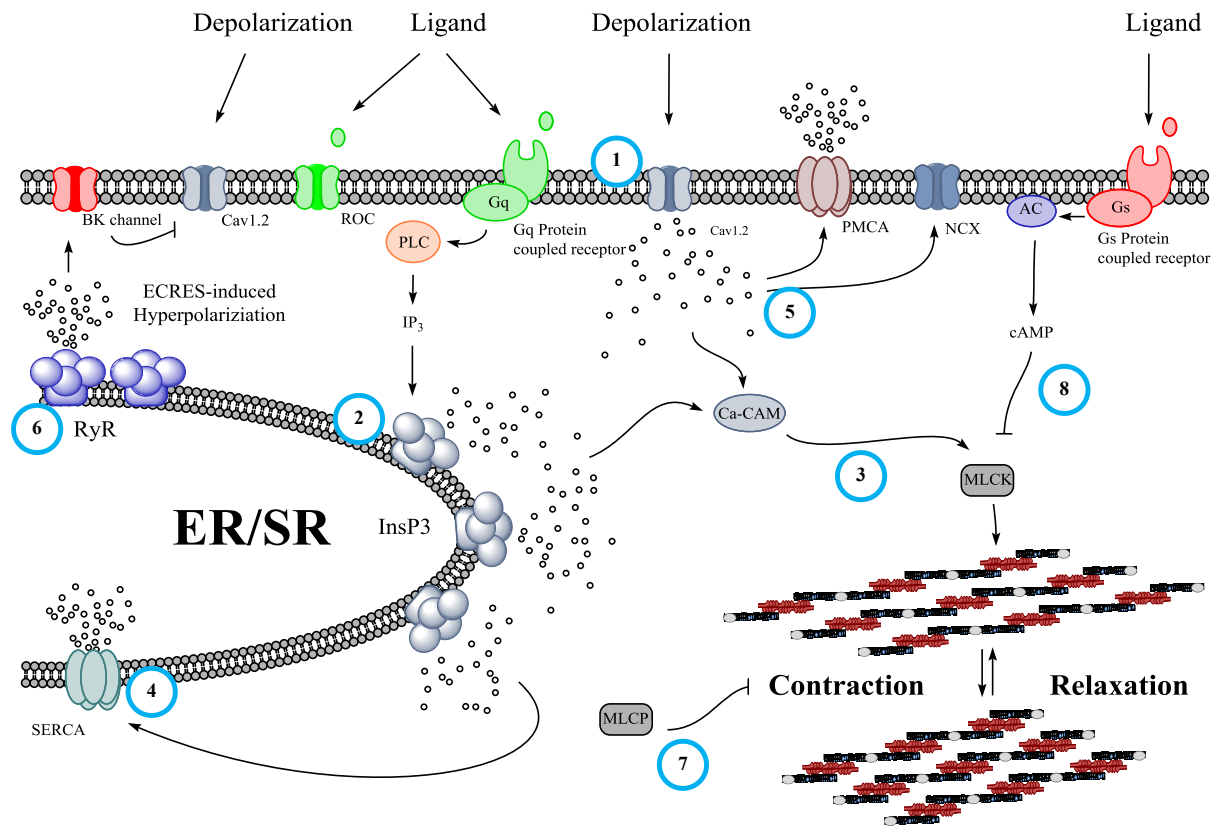


Figure 9. EC coupling mechanism in vascular smooth muscle cells. Depolarization of the plasma membrane by an action potential or by activation of receptor operated channel (ROC) cause a calcium influx via the voltage sensor calcium channel (Cav1.2) (1). Chemical stimuli can also increase cytosolic calcium via signal transduction of Gq protein-coupled receptors that ultimately activate InsP3 receptors and mobilize calcium from the SR (2). Increased free cytosolic calcium binds to calmodulin and activates the myosin light chain kinase to initiate contraction (3). Decreased cytosolic calcium initiates the relaxation. Calcium is removed from the cytosol by re-uptaking into the SR through SERCA activity (4) or by extrusion to the extracellular space via the PMCA or the NCX (5). On the other hand relaxation can also be promoted by elementary calcium release (ECRE) activity through activation of RyR, which trigger STOCs from the calcium dependent potassium channels (BK) and hyperpolarize the sarcolemma preventing calcium influx from Cav1.2 (6). Dephosphorylation of myosin light chain via MLCP (7) or inhibition of MLCK (8) via cAMP production through activation of Gs protein-coupled receptors inhibit contraction. Ca-CAM: calcium-calmodulin complex; PLC: phospholipase C; AC: adenylyl cyclase; MLCK: myosin light chain kinase; MLCP: myosin light chain kinase; STOCs: Spontaneous transient Outward Current(s).

Similar to skeletal muscle, relaxation in smooth muscle cells is also accompanied by mechanisms that decrease the free cytosolic calcium concentration to resting levels. The main mechanisms involved in lowering the calcium concentration include 1) reuptake of calcium

to the SR via SERCA2 activity, 2) calcium extrusion to the extracellular space via PMCA (Cartwright et al., 2011; Floyd and Wray, 2007; Wray and Burdyga, 2010) or via the sodium calcium exchanger (NCX) (Nazer and van Breemen, 1998; Zhu et al., 1994) and to a lesser extent by the mitochondrial calcium uniporter (MCU) (McCarron et al., 2013).

It should be mentioned that modulation of calcium homeostasis and therefor the vascular tone is greatly dependent on several signal transduction mechanisms. These mechanisms can be summarized as follows: 1) the inositol three phosphate (IP3) pathway via activation of Gq-protein-coupled receptors (Wu et al., 1992) leading to SR calcium release (contraction); 2) inhibition of the myosin light chain kinase (relaxation) by cyclic adenosine monophosphate (cAMP) via activation of Gs-protein-coupled receptors (Takuwa, 1996) and 3) inhibition of the Cav1.2 calcium channel and the InsP3 receptor (relaxation) by protein kinase G (PKG) via endothelial nitric oxide (NO) production and formation of cyclic guanosine monophosphate (cGMP) (Zhao et al., 2015).

Figure 9 summarizes the main mechanisms leading to calcium mobilization in vascular smooth muscle during EC coupling.

---

## ***Hemostasis and bleeding disorders associated to impaired vascular response***

Hemostasis comprises the physiological response activated to arrest blood loss from an injured vessel (Colman, 2006). This complex process depends on the activation of different pathways within the vasculature, platelets and coagulation factors. The cascade of events taking place to stop the bleeding can be summarized as indicated below:

1) Primary hemostasis: in this step two important events occur to prevent further blood loss: a local vascular contraction and platelet plug formation. The first event is a local vascular contraction also referred to as vascular spasm, which is caused by contraction of the smooth muscle cells lining the blood vessels and limits blood flow to the injured site. This vascular response is triggered by endothelins, small peptides released by cells lining the vessel and pain receptor in response to vessel injury (Loscalzo, 1995). Immediately following the vascular response, platelets that normally flow freely in the blood, encounter and adhere to the area of vessel injury due to the exposure of connective tissue and collagen fibers on the luminal face of the vessel (Broos et al., 2011). At this point platelets release their cytoplasmic granules containing chemicals that promote the recruitment and adhesion of more platelets to the site of injury and also maintain vasoconstriction. Thus a temporary plug is formed in the vessel wall that seals the injured vessel and serves as an initial defense against blood loss.

2) Secondary hemostasis: in this step a more sophisticated and durable repair sequence of events occurs leading to the formation of the blood clot (or coagulation). Damage of the endothelium results in exposure of membrane-bound pro-coagulant factors (Tissue Factor) that act in conjunction with secreted platelet factors to activate the coagulation cascade: a series of enzymatic reactions that culminate in thrombin activation (Versteeg et al., 2013). The result is the formation of a gelatinous but robust clot made up of mesh of fibrin, an insoluble fibrous protein derived from fibrinogen in which platelets and blood cells are trapped.

3) Fibrinolysis. As the vessel heals the normal blood flow is restored and the clot is removed. Fibrinolysis is the process by which the fibrin clot is broken down (Chapin and Hajjar, 2015). During this process a series of enzymatic reactions take place whereby plasminogen is converted into the active form plasmin, which gradually degrades the fibrin mesh within the clot. Additionally, vasodilatory substances are released allowing relaxation of the smooth muscle cells thereby helping to restore the normal circulation (de Maat et al., 2014).

---

Alterations on any of the components of this delicate balance will result in thrombosis or hemorrhagic disorders. A number of pathological conditions leading to hemorrhage have been well characterized and the most severe forms generally affect platelets function or coagulation factors (Czarnecki, 2008). However, bleeding disorders associated with impaired vessel contraction have been described. As far as the vascular system is concerned, bleeding may result from different deficiencies in different factors including deficiency of connective tissue function (e.g Ehlers-Danlos syndrome (Malfait and De Paepe, 2014)), arteriovenous malformation (e.g. hereditary hemorrhagic telangiectasia (Dittus et al., 2015)) vessel infiltration with amyloid (Mumford et al., 2000) or inflammatory processes caused by some infections (Chetty et al., 2000; Pulido-Perez et al., 2012).

Nevertheless, the mechanism underlying many bleeding disorders are still uncertain, and such disorders are difficult to diagnosis (Quiroga and Mezzano, 2012; Toso et al., 2013). We hypothesized that impaired calcium homeostasis in smooth cells may be responsible for alterations of the primary vasoconstriction response and thus may be at the basis of mild bleeding disorders of undefined causes. Indeed though arterial smooth muscle cells play an important role in primary hemostasis, few studies have connected smooth muscle calcium homeostasis with bleeding abnormalities. In the next section (results, manuscript two) we present evidence that these two processes: namely smooth muscle  $\text{Ca}^{2+}$  homeostasis and bleeding physiology are importantly associated in order to maintain the appropriate balance of primary hemostasis.



## RESULTS

### **Manuscript I: mTORC1 signaling on EC coupling and Ca<sup>2+</sup> homeostasis of skeletal muscle**

#### *Summary of publication 1*

This study was undertaken following the observations of Bentzinger and colleagues (2008) in their RAPTOR KO muscle specific mouse model and the similar findings by Risson and coworkers (2009) in their muscle specific mTOR KO mouse model. These studies showed that mTOR plays an important role in skeletal muscle. Indeed, lack of this complex causes a dystrophic phenotype, fibers with centralized nuclei, presence or core-like structures, decreased muscle mass, reduced twitch force and maximal tetanic absolute force accompanied by a slow kinetics as well as changes in metabolism intracellular signaling. We decided to study in detail whether the molecular machinery of EC coupling is directly responsible for the deleterious changes observed on muscle performance and Ca<sup>2+</sup> homeostasis. By immunoblotting we investigate the protein content of total SR preparations from skeletal muscles of RAPTOR KO (RamKO) and their WT littermates with commercial antibodies reacting against some of the main proteins participating in EC coupling (SERCA1, SERCA 2, calsequestrin, calreticulin, sarcalumenin, RyR1, DHPR $\alpha$ 1, DHPR  $\beta$ 1, albumin, SRP-35 or anti-JP-45). We also investigate by ligand binding the content of RyR1 and Cav1.1 proteins. Additionally, we investigated glycogen phosphorylase content and activity of total SR preparations. Finally we studied the Ca<sup>2+</sup> homeostasis of enzymatically isolated single skeletal muscle fibers (EDL and soleus) by measuring the resting Ca<sup>2+</sup> level, electrically elicited Ca<sup>2+</sup> transient and Elementary calcium Release Events (ECREs) after osmotic shock. The results coming from this biochemical and functional characterization extend the role of mTORC1 signaling and implicate its function in maintaining the integrity of the molecular components of the EC coupling of skeletal muscles.

## Raptor ablation in skeletal muscle decreases Cav1.1 expression and affects the function of the excitation–contraction coupling supramolecular complex<sup>¶</sup>

<sup>¶</sup>Note: manuscript published and available online at *The Biochemical Journal* 2015 Feb 15; 466(1):123-35. doi: 10.1042/BJ20140935.

Rubén J. Lopez\*, Barbara Mosca\*<sup>†</sup>, Susan Treves\*<sup>†</sup>, Marcin Maj\*, Leda Bergamelli<sup>†</sup>, Juan C. Calderon<sup>‡</sup>, C. Florian Bentzinger<sup>§</sup>, Klaas Romanino<sup>§</sup>, Michael N. Hall<sup>§</sup>, Markus A. Rüegg<sup>§</sup>, Osvaldo Delbono<sup>#</sup>, Carlo Caputo<sup>‡</sup> and Francesco Zorzato\*<sup>†1</sup>

\*Departments of Anesthesia and of Biomedicine, Basel University Hospital, Hebelstrasse 20, 4031 Basel, Switzerland

<sup>†</sup>Department of Life Sciences, General Pathology section, University of Ferrara, Via Borsari 46, 44100 Ferrara, Italy

<sup>‡</sup>Laboratorio de Fisiología Celular, Centro de Biofísica y Bioquímica, Instituto Venezolano de Investigaciones Científicas (IVIC), Apartado 20632, 1020A Caracas, Venezuela

<sup>§</sup>Biozentrum, University of Basel, CH-4056 Basel, Switzerland

<sup>#</sup>Department of Internal Medicine, Section on Gerontology and Geriatric Medicine, Wake Forest University School of Medicine, Winston-Salem, NC 27157, U.S.A.

<sup>1</sup> To whom correspondence should be addressed (email [zor@unife.it](mailto:zor@unife.it))

### Abstract

The protein mammalian target of rapamycin (mTOR) is a serine/threonine kinase regulating a number of biochemical pathways controlling cell growth. mTOR exists in two complexes termed mTORC1 and mTORC2. Regulatory associated protein of mTOR (raptor) is associated with mTORC1 and is essential for its function. Ablation of raptor in skeletal muscle results in several phenotypic changes including decreased life expectancy, increased glycogen deposits and alterations of the twitch kinetics of slow fibres. In the present paper,

we show that in muscle-specific raptor knockout (RamKO), the bulk of glycogen phosphorylase (GP) is mainly associated in its cAMP-non-stimulated form with sarcoplasmic reticulum (SR) membranes. In addition, 3[H]–ryanodine and 3[H]–PN200-110 equilibrium binding show a ryanodine to dihydropyridine receptors (DHPRs) ratio of 0.79 and 1.35 for wild-type (WT) and raptor KO skeletal muscle membranes respectively. Peak amplitude and time to peak of the global calcium transients evoked by supramaximal field stimulation were not different between WT and raptor KO. However, the increase in the voltage sensor-uncoupled RyRs leads to an increase of both frequency and mass of elementary calcium release events (ECRE) induced by hyper-osmotic shock in flexor digitorum brevis (FDB) fibres from raptor KO. The present study shows that the protein composition and function of the molecular machinery involved in skeletal muscle excitation–contraction (E–C) coupling is affected by mTORC1 signalling.

#### Key words

Dihydropyridine receptor (DHPR), excitation–contraction (E–C) coupling, mammalian target of rapamycin (mTOR), ryanodine receptor (RyR), skeletal muscle sarcoplasmic reticulum (SR).

Abbreviations: Ab, antibody; AM, acetoxymethylester; BTS, N-benzyl-p-toluensulfonamide; CR, calreticulin; CSA, cross-sectional area; DHPR, dihydropyridine receptor; DMEM, Dulbecco's Modified Eagle's medium; E–C, excitation–contraction; ECRE, elementary calcium release events; EDL, extensor digitorum longus; FDB, flexor digitorum brevis; FDHM, full duration at half-maximum amplitude; FKBP12, FK506-binding protein; FWHM, full width at half-maximum amplitude; GP, glycogen phosphorylase; HEK, human embryonic kidney; KO, knockout; mLST8, mammalian lethal with SEC13 protein 8; mTOR, mammalian target of rapamycin; NR, normal Ringer; RamKO, muscle-specific raptor knockout; raptor, regulatory associated protein of mTOR; RyR, ryanodine receptor; SERCA, sarcoplasmic reticulum calcium pump; SR, sarcoplasmic reticulum; SRP-35, SR protein of 35 kDa; WT, wild-type.

## Introduction

The mammalian target of rapamycin (mTOR) is a serine/threonine kinase controlling different biochemical pathways activated in response to growth factors and nutrient availability, including protein synthesis, ribosome biogenesis, nutrient transport, lipid synthesis and autophagy, thus playing a central role in metabolism, growth and aging [1–5]. Two different mTOR complexes possessing different roles within the cell have been identified: mTORC1 and mTORC2. The immunosuppressant drug rapamycin is an allosteric inhibitor of mTORC1, a complex playing a role in nutrient sensing and controlling protein synthesis, lipid synthesis and glycolysis [6]. After forming a complex with its cytoplasmic receptor FKBP12 (FK506-binding protein), rapamycin binds mTORC1 and induces its destabilization, resulting in the inability of mTOR to phosphorylate target proteins [6]. mTORC1 complex is made up of mTOR, regulatory associated protein of mTOR (raptor), mammalian lethal with SEC13 protein 8/G-protein  $\beta$ -subunit like protein (mLST8/G $\beta$ L) and proline-rich Akt substrate of 40 kDa (PRAS40) [7,8]. Its kinase activity is regulated through a dynamic interaction between mTOR and raptor, the latter being a conserved 150 kDa protein, which besides mTOR, also interacts with S6K1 (ribosomal protein S6 kinase 1) and 4E-BP1 (eukaryotic translation initiator factor 4E-binding protein 1). mTORC2 on the other hand, is largely insensitive to rapamycin, is active in growing cells and regulates the actin cytoskeleton, cell survival and apoptosis. It forms a complex with rictor, mSIN1 (target of rapamycin complex 2 subunit Mitogen-activated protein kinase 2-associated protein 1), mLST8 and mTOR [9].

During the past decade, research on the role of mTOR has revealed that this kinase is implicated in a variety of diseases, including cancer, neurodegeneration and metabolic disorders [9]. Furthermore mTOR activity has been shown to be involved in the control of muscle mass and indeed rapamycin treatment delays recovery of skeletal muscle from atrophy whereas activation of the mTOR's upstream components induces muscle hypertrophy [10]. It has been shown that skeletal muscle-specific mTOR inactivation increases the glycogen content of muscle fibres, an effect linked to the down-regulation of glycogen phosphorylase (GP) and of other enzymes involved in the glycogenolytic pathway [11]. Similar results were also obtained by Bentzinger et al. [12] who investigated the role of the mTORC1 signalling pathway in skeletal muscle, by generating muscle-specific raptor knockout mice (RamKO). Skeletal muscles of RamKO mice became progressively atrophic,

had increased glycogen content and showed a transition of the metabolic signature from oxidative to glycolytic, despite slow twitch fibre-type predominance [12]. Although RamKO mice have poor in vivo oxidative muscle performance on the running wheel, in vitro tetanic stimulation shows that isolated extensor digitorum longus (EDL) and soleus from RamKO mice are more resistant to fatigue. The reduction in absolute force development is accounted for by the decrease in muscle mass, since after normalization for cross-sectional area (CSA) there is no significant difference in maximal tetanic force between control and RamKO mice. Nevertheless the twitch kinetics of the soleus from RamKO mice is dramatically affected: there is an increased time to peak and almost doubling of the half relaxation time. Because of these changes and because mTORC1 inhibition is a common therapeutic strategy in humans, we investigated in more detail the functional changes of ablation of mTORC1 in skeletal muscle by examining excitation–contraction (E–C) coupling in RamKO mice. E–C coupling involves the conversion of an electrical signal into a transient increase in the intracellular  $[Ca^{2+}]$  and is initiated by conformational changes at the level of the L-type voltage-dependent calcium channel [dihydropyridine receptor (DHPR),  $Ca_v1.1$ ] localized in the membrane of the transverse tubules [13,14]. Activation of  $Ca^{2+}$  release from terminal cisternae is due to the transmission of a conformational change occurring on the DHPR to the ryanodine receptor (RyR) 1 via direct protein–protein interaction [15–17]. The resulting increase in the intracellular  $[Ca^{2+}]$  is due to the opening of the RyR1 and this is followed by  $Ca^{2+}$  removal, which depends mostly on the activity of sarcoplasmic reticulum (SR) calcium pumps (SERCA) localized in the longitudinal SR and, to a lesser extent, on the sarcolemmal  $Na^+ /Ca^{2+}$  exchanger and plas-malemma  $Ca^{2+}$  pump [18]. Mutations in the two  $Ca^{2+}$  channels (RyR1 and DHPR  $\alpha 1$  subunit) directly involved in E–C coupling are the underlying feature of a group of several disorders including core myopathies in which the underlying histological feature is the presence of cores and fibre type I pre-dominance (for review see [19]). Interestingly, the muscles of RamKO mice also exhibit core-like structures and slow fibre-type predominance [12].

In the present study, we investigated the functional and biochemical properties of the SR membranes from RamKO mice. We found that the inactivation of mTORC1 is associated with the compartmentalization of GP to SR membranes. In addition, we found an increase in the: (i) half-time of the decay of the calcium transient in soleus fibres; (ii) ryanodine to DHPRs ratio; (iii) frequency and mass of elementary calcium release events (ECRE) induced by hyperosmotic shock in FDB fibres. Altogether our data suggest that protein composition

and function of the membrane compartments involved in E–C coupling is affected by mTORC1 signalling.

## Materials and Methods

### RamKO mice

Details of the targeting strategy and initial characterization of RamKO mice are previously described [12]. KO mice were identified by PCR amplification of genomic DNA. All experiments were conducted on male mice in accordance with local Kantonal guidelines and regulations (Kantonales Veterinäramt Basel Stadt).

### RNA extraction, reverse transcription and PCR reactions

Total RNA was extracted from mouse leg muscles using Tri-reagent following the manufacturer's recommendations (Molecular Research Centre). Total RNA was converted into cDNA using SuperScript™ II Reverse Transcriptase (Invitrogen) as previously described [20]. PCR reactions were carried out using the following primer sets: mouse  $\beta$ -actin forward: 5'-GGACCTGACAGACTACCTCA-3' and reverse 5'-GCAGTAATCTCCTTCTGCAT-3'; DHPR $\alpha$ 1 (Ca<sub>v</sub>1.1) forward 5'-CATTAGGTAGAGCCGTGCACCTG-3' and reverse 5'-GCCTGTTGTCATGACGAAGTTAGC-3'. Amplification conditions were 5 min at 95°C followed by 35 cycles of 30 s denaturation at 92°C, 40 s annealing at the recommended temperature for each primer pair and 40 s extension at 72°C followed by a final extension for 5 min at 72°C using the 2.5× Master Mix Taq polymerase from Eppendorf. The products of the PCR reaction were separated on a 1% agarose gel and the DNA bands were visualized by Ethidium Bromide staining.

### SR isolation, Western blotting and biochemical assays

Total SR was prepared as previously described from mouse skeletal muscle [20]; vesicles enriched in terminal cisteranae, longitudinal SR and plasmalemma were prepared as

described by Saito et al. [21] and stored in liquid nitrogen until used. C<sub>2</sub>C<sub>12</sub> myotubes were treated for 16 h with 20  $\mu$ M rapamycin or left untreated; cells were then washed twice with PBS, harvested, and the heavy SR protein fraction was obtained by differential centrifugation. For Western blotting, proteins were separated by SDS/PAGE, blotted on to nitrocellulose and probed with commercial antibodies (Abs) against SR proteins [SERCA1, SERCA 2, calsequestrin, calreticulin (CR), sarcalumenin, RyR1, DHPR $\alpha$ 1, DHPR  $\beta$ 1, albumin, SRP- 35 (SR protein of 35 kDa) or anti-JP-45 Abs; 20] followed by peroxidase-conjugated secondary Abs. The immunopositive bands were visualized by chemiluminescence as previously described [22]. To accurately quantify DHPR and RyR content in the SR and the Ca<sup>2+</sup> dependency of [<sup>3</sup>H]-ryanodine binding, radioligand-binding experiments using [<sup>3</sup>H]-PN200-110 (DHPR expression) and [<sup>3</sup>H]-ryanodine were performed as described [23]. The different free [Ca<sup>2+</sup>] (750 pM, 9.1 nM, 95 nM, 1.1  $\mu$ M, 9  $\mu$ M, 104  $\mu$ M, 1 mM) were obtained by the addition of different amounts of CaCl<sub>2</sub> as described by Fabiato [24]. The amount of bound [<sup>3</sup>H] ligand was measured by liquid scintillation counting.

#### In vitro muscle strength assessment

To test force *in vitro*, EDL and soleus muscles were dissected and mounted into a muscle-testing setup (Heidelberg Scientific Instruments). Muscles were stimulated with 15-V pulses for 0.5 ms and force was digitized at 4 kHz by using an AD instruments converter. EDL tetanus was recorded in response to a 400 ms train of pulses delivered at 10–120 Hz; soleus tetanus was recorded in response to an 1100 ms train of pulses delivered at 10–150 Hz. Specific force was normalized to the muscle CSA per wet weight (mg)/length (mm) per 1.06 (density mg/mm<sup>3</sup>) as previously described [23].

#### Isolation of extensor digitorum longus and soleus muscle fibres

Single muscle fibres were obtained from 6–8 week old mouse hindlimbs by enzymatic dissociation, as previously described [25]. Briefly, muscles were dissected and pinned via the tendons to a Sylgard-lined dissecting chamber. The outer connective tissue was removed and the muscles were incubated in Tyrode's solution containing 0.22% type I collagenase (Sigma) at 37°C for 1h followed by rinsing in 10% fetal bovine serum (FBS) in DMEM (Dulbecco's Modified Eagle's medium). To release single fibres, muscles were triturated

gently in serum-free DMEM, then plated on glass coverslips pre-treated for 2 h with 1.5  $\mu$ l of natural mouse laminin (Invitrogen) diluted with distilled water. Fibres were then incubated in DMEM, 10% FBS, 1% penicillin/streptomycin, 5% CO<sub>2</sub> at 37°C overnight. FDB fibres were isolated as previously described [23].

### Calcium measurements

The resting [Ca<sup>2+</sup>]<sub>i</sub> was monitored in isolated fibres from RamKO mice and control littermates with the ratiometric fluorescent Ca<sup>2+</sup>-indicator indo-1/AM (acetoxymethylester); changes in the [Ca<sup>2+</sup>]<sub>i</sub> induced by electrical depolarization were monitored in EDL and soleus fibres loaded with mag-fluo-4/AM in Tyrode's buffer. All experiments were carried out at room temperature (20°C–22°C) in the presence of 50  $\mu$ M N-benzyl-p-toluensulfonamide (BTS; Tocris) to minimize movement artefacts. Measurements were carried out with a Nikon ECLIPSE TE2000-U inverted fluorescent microscope equipped with a 20 $\times$  PH1 DL magnification objective. The light signals from a spot of 1 mm diameter of the magnified image of flexor digitorum brevis (FDB) fibres, were converted into electrical signals by a photomultiplier connected to a Nikon Photometer P101 amplifier. Calcium transients were collected by custom made (RCS AUTOLAB) software and analysed by PowerLab Chart5 and Origin.6 programs. Changes in fluorescence were calculated as  $\Delta F/F = (F_{\max} - F_{\text{rest}}) / (F_{\text{rest}})$ .

FDB fibres were isolated, kept for 4 h in a 37°C, 5%CO<sub>2</sub> cell incubator, placed on a laminin-coated coverslip and loaded for 20 min at room temperature with 10  $\mu$ M fluo-4 AM Ca<sup>2+</sup> indicator (fluo-4/AM, Molecular Probes). All experiments were performed at room temperature. ECREs were measured using a Nikon A1R laser scanning confocal microscope (Nikon Instruments Inc.) with a 60 $\times$  oil immersion Plan Apo VC Nikon objective, numerical aperture 1.4. (Nikon Instruments Inc.). Five-second-duration linescan images (x,t) were acquired in resonant mode at 7680 lps with 512 pixels (0.05  $\mu$ m/pixel) in the x- and 39936 pixels (0.126 ms/pixel) in the t-direction using a pinhole size of 72.27  $\mu$ m. Fifteen images were taken at different positions across each cell. The Ca<sup>2+</sup> indicator was excited with a laser at 487 nm and the fluorescence emitted at 525  $\pm$  25 nm was recorded. To minimize photo damage, the laser intensity was set at 3%–4% of the maximal power. The viability of fibres after osmotic shock was assessed by monitoring single calcium transient evoked by supramaximal field stimulation pulses. Fibres were first perfused with isotonic (~290 mOsm)



normal Ringer (NR) (in mM, 140 NaCl; 2 MgCl<sub>2</sub>; 2.5 CaCl<sub>2</sub>; 10 HEPES; 5 KCl; pH adjusted to 7.4) using a Minipuls 2 peristaltic pump (Gilson Medical Electronics). To induce ECREs, cells were perfused with a hypertonic solution (~420 mOsm) by increasing the [Ca<sup>2+</sup>] to 50 mM (in mM, 140 NaCl; 2 MgCl<sub>2</sub>; 50 CaCl<sub>2</sub>; 10 HEPES; 5 KCl; pH adjusted to 7.4) [26,27]. Osmolarity of the solution was assessed with a Vogel 801 Osmometer (Vogel GmbH). All solution contained 10 μM BTS.

### ECRE analysis

ECREs morphology [amplitude,  $\Delta F/F_0$ ; full width at half-maximum amplitude (FWHM); full duration at half-maximum amplitude (FDHM)] were determined from linescan images using the open source image analyser software Fiji [28]. After images were binned by average 4× at the t-axis, they were processed using the automated spark detection plugin Sparkmaster [29]. Because of the heterogeneity of the ECREs duration, events were split in two groups: the short lasting events with <50 ms of FWHM and the long lasting events ECREs with >50 ms of FWHM duration [30]. Frequency was calculated for each group by counting the number of events occurring per image. The mass was determined by the following formula  $mass = 1.206 \cdot \Delta F/F_0 \cdot FWHM^3$  [31]. Statistical analysis was performed using the program OriginPro® version 8.6.0. ECRE derived from 25 and 26 fibres obtained from five wild-type (WT) and RamKO mice respectively. Data are expressed as mean ± S.E.M.; values were considered statistically significant if  $P < 0.05$  using the Student's t-test.

### Glycogen phosphorylase activity measurement

GP activity was measured as described [32–34]. Reactions were initiated by adding 30–60 μg of SR to a 500 μl of reaction buffer containing 50 mM imidazole pH 7.0, 20 mM K<sub>2</sub>HPO<sub>4</sub>, 1.25 mM MgCl<sub>2</sub>, 5 μM glucose 1,6-diphosphate, 0.5 mM DTT, 3 μg/ml phosphoglucomutase, 0.25% BSA, 10 mg/ml AMP-free glycogen. For measurement of total activity (forms 'a' and 'b' of GP) AMP was added to obtain a final concentration of 3 mmol/l. The reaction was carried out at 30°C for 30 min (total activity) or for 60 min (to determine the amount of form 'a') and terminated by the addition of 60 μl of 0.5 M HCl. Aliquots of 50 or 100 μl (for total and form 'a' measurement respectively) of primary reaction mixture were added to 1 ml of a glucose- 6-phosphate dehydrogenase reaction buffer containing 50 mM Tris/HCl, pH 8.0, 1

mM EDTA, 250  $\mu$ M NADP and 0.5  $\mu$ g/ml glucose-6-phosphate dehydrogenase. This reaction was allowed to proceed for 10 min at room temperature and the absorbance of the samples at 340 nm was determined spectrophotometrically to quantify the degree of conversion of NADP into NADPH (which is proportional to the content of glucose 6-phosphate formed in the first reaction). GP activity is expressed in micromoles per minute per milligram protein (unit/mg).

#### Luciferase reporter assay

The constructs containing DHPR $\alpha$ 1.1 promoter region fragments (Luc7P-724, Luc/P756) were cloned in frame in pGL3-basic expression vector (Promega) [35]. C<sub>2</sub>C<sub>12</sub> myoblasts (2  $\times$  10<sup>4</sup> cells per dish) were plated on gelatin-coated 35 mm cell culture dishes and allowed to grow in DMEM plus Glutamax, 4.5 g/l glucose, 20% FBS, 50 units/ml penicillin, 50  $\mu$ g/ml streptomycin until 50% confluent. Two microgram of each construct and 200 ng of the control vector pRL-TK were used for transfection using the FuGENE6 transfection reagent (Roche). Twenty-four hours after transfection, cells were induced to differentiate by changing the medium to DMEM plus Glutamax, 4.5 g/l glucose, 5% horse serum and penicillin/streptomycin. After 4–6 days, when cells had visibly fused into myotubes, 20  $\mu$ M rapamycin (Sigma) was added as described [36,37]. Cells were then washed twice with PBS and lysed using Passive Lysis Buffer (Promega). Firefly luciferase and renilla activity were measured with Victor<sup>2</sup> Luminometer (PerkinElmer). Firefly luciferase activity was normalized to renilla activity and expressed as mean ( $\pm$  S.E.M.) enzymatic activity units.

## Results

Mechanical properties of isolated fibres and content of proteins involved in excitation–contraction coupling in skeletal muscles of RamKO mice

Ablation of raptor induces changes in the mechanical properties of fast and slow twitch muscles [12]; Figure 1 shows representative traces of twitch and tetanic force of EDL and soleus from control and RamKO mice [12]. Although tetanic-specific force in EDL and

soleus muscles do not vary between control and RamKO [12] mice, the twitch kinetics in RamKO soleus show a remarkable prolongation of the half relaxation time at lower peak force. The changes of the mechanical properties of the twitch in EDL and soleus muscles could be due (i) to fibre-type switching induced by ablation of raptor, (ii) to an effect on the contractile protein machinery, (iii) to alterations of the E–C coupling mechanism or (iv) to a combination of two or more of these mechanisms.

#### Protein composition of skeletal muscle sarcoplasmic reticulum from RamKO mice

Analysis of the main protein components of total SR membranes from RamKO mice and control littermates revealed no significant changes in the content of SERCA1, SERCA2, JP-45, calsequestrin and CR. In addition, there was a small but significant decrease in sarcalumenin (Figure 2), a modulator of SERCA activity [38]. We also found a decrease in SRP-35, a newly identified membrane-bound retinol dehydrogenase of sarcotubular membranes [22].

#### RamKO ablation affects the excitation–contraction coupling macromolecular complex

To study in greater detail the effect of raptor ablation, we determined the membrane density of the two core components of the E–C coupling machinery, namely the  $Ca_v1.1$  ( $\alpha 1.1$  of the DHPR) and RyR1 by performing quantitative Western blot analysis and equilibrium ligand binding on the crude microsomal preparation isolated from skeletal muscle of RamKO and control littermates. The most interesting results of the present study are that the content of  $Ca_v1.1$  in RamKO mice was reduced by almost 50% compared with control littermates (Figure 3A). Equilibrium binding of the  $Ca_v1.1$  ligand PN200-100 to crude SR membranes shows that the maximal binding capacity ( $B_{max}$ ) for PN200-100 binding was  $0.68 \pm 0.05$  and  $1.25 \pm 0.13$  pmol/mg protein in RamKO and control littermates respectively with no significant changes of its dissociation constant ( $K_D = 0.96 \pm 0.16$  compared with  $1.35 \pm 0.32$  nM, mean  $\pm$  S.E.M.,  $n=6$  for RamKO and control littermates respectively). The reduced expression of  $Ca_v1.1$  is, surprisingly, accompanied by a 3.5-fold increase in the content of the  $Ca_v\beta 1$  subunit (Figures 3B and 3C). On the other hand, the decrease in the total amount of  $Ca_v1.1$  was not due to a reduction in the relative amount in T-tubule membranes in the total sarcotubular membrane fraction, as the content of albumin, a marker for T-tubules [39] was

unchanged (Figures 3B, 3C and 4B). mTORC1 regulates protein expression by affecting translation via S6K1 and 4E-BP [5] and/or by controlling the transcription of several additional genes [40]. To determine if the decrease in Ca<sub>v</sub>1.1 in the muscles of RamKO mice was due to alterations in transcription we performed semi-quantitative PCR experiments. As shown in Figure 4(A), there were no significant changes in Ca<sub>v</sub>1.1 mRNA content in RamKO mice. We next evaluated the activity of the Ca<sub>v</sub>1.1 promoter in C<sub>2</sub>C<sub>12</sub> myotubes and human embryonic kidney (HEK)293 cells transfected with a luciferase reporter construct containing the 5' flanking region of the Ca<sub>v</sub>1.1 gene. Figure 4(C) shows that the Ca<sub>v</sub>1.1 promoter is active in C<sub>2</sub>C<sub>12</sub> myotubes but not in HEK293 cells. Since FKBP12 is a ubiquitously expressed protein, including in C<sub>2</sub>C<sub>12</sub> myotubes [41], we next tested the effect of rapamycin, a drug which pharmacologically mimics the effect of knocking out raptor, on the activity of the Ca<sub>v</sub>1.1 promoter. Incubation of C<sub>2</sub>C<sub>12</sub> myotubes for 2 and 16 h with 20 μM rapamycin abolished the phosphorylation of the mTORC1 downstream target S6 ribosomal protein (Figure 4D), without influencing the activity of the Ca<sub>v</sub>1.1 promoter (Figure 4C). Nevertheless, rapamycin treatment of C<sub>2</sub>C<sub>12</sub> myotubes causes a decrease in the immunoreactive band corresponding to the Ca<sub>v</sub>1.1 (Figure 4E) without effecting CR content, an extrinsic protein of the SR membrane. Our data clearly show that, even in the presence of a partial inhibition of the mTORC1 complex [42], the phenotype of rapamycin-treated C<sub>2</sub>C<sub>12</sub> cells recapitulates the effect of Ca<sub>v</sub>1.1 expression observed in RamKO mature skeletal muscle fibres. In particular, it appears that functional ablation of mTORC1 affects the synthesis and/or the stability of Ca<sub>v</sub>1.1. A great deal of data show that rapamycin dissociates FKBP12 from the RyR complex, leading to leaky RyRs [43]. It is unlikely that the decrease in the Ca<sub>v</sub>1.1 expression results from the acute appearance of leaky RyR in C<sub>2</sub>C<sub>12</sub> cells, since chronic dysregulation of intracellular calcium concentration in muscle fibres expressing leaky RyR1 mutation do not display a decrease in Ca<sub>v</sub>1.1 current density [44]. The decrease in the total sarcotubular membrane density of Ca<sub>v</sub>1.1 was apparently also not paralleled by a decrease in the SR RyR1 calcium release channels, as we found no change in the B<sub>max</sub> of equilibrium [<sup>3</sup>H]ryanodine binding to the total SR membrane fraction (0.99 ± 0.10 compared with 0.92 ± 0.07 pmol/mg protein for WT and RamKO respectively) (Figure 5) from RamKO and control littermates.

Glycogen phosphorylase is targeted to sarcoplasmic reticulum membrane in skeletal muscle from RamKO mice

Skeletal muscles from RamKO and control littermates were homogenized and fractionated by differential centrifugation. Comparison with the protein profile of total homogenates shows a decrease in a band of 97 kDa in the total homogenate of skeletal muscle from RamKO mice compared with that from control littermates (Figure 6A,\*). It was previously shown that skeletal-muscle-specific mTORC1 inactivation reduces the content of GP, a result consistent with glycogen accumulation in RamKO muscle fibres [11,12]. Nevertheless, SDS gel electrophoresis of isolated SR membrane fractions revealed that the band with an apparent molecular mass of 97 kDa was enriched in the total SR of RamKO mice (Figure 6A, \*\*). MS identified the 97 kDa SR protein band as the GP. This finding was further confirmed by staining a Western blot of total SR membrane proteins with specific anti-GP Abs (Figure 6D). Quantification showed that ablation of raptor led to a 2.9-fold increase in GP associated with the total SR membrane fraction (Figure 6B). Sub-fractionation of SR membranes by sucrose density centrifugation revealed that GP was enriched in the light R1 fraction (Figure 6C; white arrowheads), which is made up of membranes derived from longitudinal SR, sarcolemma and T-tubules. GP activity is regulated in several ways including (i) substrate availability, (ii) interconversion (phosphorylation/dephosphorylation), and (iii) allosteric modification, with AMP being a key activator [45,46]. We assessed whether the cAMP-stimulated (GP-a) or cAMP non-stimulated (GP-b) forms of the enzyme are enriched in the muscle from RamKO mice. As shown in Figure 6(E), there was a similar increase in GP-total and GP-b activity, suggesting that the cyclic AMP-non-stimulated form of GP is enriched in the SR membranes of RamKO mice [47]. Hirata et al. reported that GP is a negative regulator of RyR since it decreases mastoparan-induced calcium release [48] and thus may affect the twitch kinetics. To explore this possibility, we studied  $\text{Ca}^{2+}$  homeostasis in enzymatically-dissociated single EDL and soleus fibres.

Calcium transients on isolated EDL and soleus fibres

To assess the resting calcium concentration, we loaded EDL and soleus fibres with the ratiometric fluorescent  $\text{Ca}^{2+}$  indicator Indo-1. In both WT and RamKO mice, the resting  $[\text{Ca}^{2+}]$  in EDL fibres from control mice is slightly higher compared with that in soleus fibres. On

the other hand, EDL and soleus fibres from RamKO mice exhibited a small but significant decrease in the resting  $[Ca^{2+}]$  compared with control littermates (Table 1). Mag-fluo-4, a low affinity calcium indicator, was used to monitor rapid  $Ca^{2+}$  transients (Figure 7) elicited by an action potential in single EDL and soleus fibres excited by supramaximal field stimulation [49]. The results we obtained are summarized in Table 1. The  $\Delta F/F$  peak  $Ca^{2+}$  transient amplitude in EDL from WT ( $0.46 \pm 0.04$ , mean  $\pm$  S.E.M.  $n=29$  fibres) mice was 18% and 22% higher compared with that of soleus muscles from WT ( $0.38 \pm 0.02$ , mean  $\pm$  S.E.M.,  $n=22$  fibres) and RamKO ( $0.36 \pm 0.02$ , mean  $\pm$  S.E.M.  $n=5$  fibres) mice respectively. Surprisingly, the peak amplitude and the 10%–90% rise time of the calcium transients were not different between RamKO mice and control littermates both in EDL and in soleus. The 10%–90% fall time of the calcium transients in soleus from RamKO mice is increased compared with that of WT ( $120.2 \pm 15.7$ ,  $n=25$  compared with  $66.2 \pm 7.4$ ,  $n=22$  fibres respectively; values are mean  $\pm$  S.E.M.;  $P < 0.05$  Mann Whitney test). The 10%–90% fall time of the calcium transients reflects the removal of calcium from the cytosol leading to muscle relaxation. Slow fibres are distinct from fast fibres since they typically display a lower relaxation rate compared with fast fibres [50]. In addition, peak calcium release induced by an action potential is lower in slow fibres compared with fast fibres [51]. The increase in 10%–90% fall time and the decrease in  $\Delta F/F$  peak  $Ca^{2+}$  transient are consistent with the observation that almost 100% of the fibres of the soleus from RamKO mice are of type 1 [12]. EDL fibres from RamKO mice exhibited a small and non-significant increase in 10%–90% fall time of the calcium transients. Similar results were also obtained with enzymatically-dissociated FDB fibres (result not shown).

The lack of a decrease in the peak amplitude calcium transients evoked by an action potential in RamKO EDL and soleus fibres is apparently inconsistent with the decrease in density of  $Ca_v1.1$  in the T-tubular membrane. A number of possibilities may account for this discrepancy. For example, the 50% decrease in  $Ca_v1.1$  in RamKO fibres ought to be accompanied by a larger fraction of voltage-sensor uncoupled RyR1. It has been proposed that (i) the interaction of  $Ca_v1.1$  with RyR1 inhibits the appearance of ECRE in mammalian adult muscle fibres [26,50,52] and that (ii) the global calcium transients supporting E–C coupling in skeletal muscle fibres may result from the summation of ECRE [30]. Equilibrium binding on total microsomes shows that in RamKO there are five/six uncoupled RyRs per voltage-sensor coupled RyR, whereas in WT there is one/two uncoupled RyR per voltage-sensor-coupled RyR. On the basis of the equilibrium ligand-binding data, we reasoned that the doubling of the voltage-sensor-uncoupled RyRs may affect ECRE. If this were so, the

---

release of calcium from voltage-coupled RyRs in RamKO fibres might propagate to adjacent voltage-sensor-uncoupled RyRs triggering a larger number of ECRE, which together contribute to the global amplitude of the peak calcium transients in muscle fibres from RamKO. In the next set of experiments, we set out to test this idea by measuring the ECRE properties in FDB fibres from WT and RamKO mice induced by hyperosmotic shock [26,27], a treatment that weakens the inhibitory activity of  $\text{Ca}_v1.1$  on the RyR1 and thus unmasks the spontaneous activity of RyR1.

#### Elementary calcium release events in WT and RamKO FDB fibres

Intact single FDB fibres from WT and RamKO mice were first perfused with NR solution and then they were exposed to hyperosmotic Ringer solution containing 50 mM  $\text{CaCl}_2$  [26,27]. After exposure to hyperosmotic solution, the FDB fibres were rinsed with NR and their viability was confirmed by their ability to respond with a robust global calcium transient upon the delivery of an action potential by supramaximal field stimulation (Supplementary Figure S1). The perfusion of FDB fibres from WT and RamKO with NR solution did not cause the appearance of spontaneous ECRE (Figures 8A, 8C, 8D and 8F left panels). Exposure to hyperosmotic Ringer solution containing 50 mM  $\text{CaCl}_2$  [26,27], induced localized increase in fluo-4 fluorescence signals, which were mostly distributed under the inner leaflet of the sarcolemma (Figures 8B and 8E, Supplementary videos). Reperfusion of FDB fibres with NR abolished the appearance of local transient increases in fluo-4 fluorescence (Figures 8C and 8F). Figures 8(H) and 8(I) show  $x,t$  line scan images of fibre exposed to hyperosmotic solution. As can be seen, hyperosmotic treatment causes a transient increase in the fluorescence and, on the basis of the criteria proposed by Kirsch et al. [30], we refer to the local increase in fluo-4 fluorescence as ECRE. ECRE analysis was performed with Sparkmaster plug-in and ECRE were divided into two groups: short-lasting (sparks-like) events having a FDHM lower than 50 ms and long-lasting (ember-like) events with FDHM higher than 50 ms [29]. Analysis of 1923 and 2547 short-lasting ECRE from WT and RamKO fibres revealed significant differences of the morphological parameters of ECRE (Table 2). Although the amplitude of short-lasting ECRE was not different between WT and RamKO FDB fibres, the latter fibres exhibited a 10% increase in both FWHM ( $0.89 \pm 0.01$  compared with  $0.98 \pm 0.01$   $\mu\text{m}$  for WT and RamKO FDB fibres respectively;  $P < 0.05$ ) and FDHM ( $13.31 \pm 0.26$  compared with  $14.11 \pm 0.24$  ms for WT and RamKO FDB fibres

respectively;  $P < 0.05$ ). The estimated ECRE mass at peak time of the  $\Delta F/F$  was 37% increased in RamKO FDB fibres ( $0.62 \pm 0.02$  compared with  $0.85 \pm 0.03 \mu\text{m}^3$  for WT and RamKO FDB fibres respectively;  $P < 0.05$ ). The increase in estimated ECRE mass was paralleled by a 30% increase in the frequency of short lasting ECRE events in RamKO fibre ( $6.81 \pm 0.36$  compared with  $8.83 \pm 0.40$  sparks/image for WT and RamKO FDB fibres respectively;  $P < 0.05$ ). The appearance of ECRE in both WT and RamKO fibres dropped to zero upon pre-incubation of the fibres with RyR, indicating that the calcium source flux of ECRE are the RyR calcium release channels (Figures 8J and 8K).

## Discussion

In the present study, we investigated the structural and functional properties of the membrane compartment involved in E–C coupling of skeletal muscle from WT and raptor KO mice. Our results show that muscle-specific ablation of raptor, and the consequent down-regulation of the mTORC1 complex, causes a 1.70-fold increase in the RyR1 to DHPRs ratio in total sarcotubular membranes. This event increases both the frequency and the width of ECRE induced by exposure of FDB fibres to hyperosmotic shock. In addition, in RamKO skeletal muscles, the cAMP non-stimulated form b of GP is mostly associated with the sarcotubular membrane fraction. We propose that mTORC1 signalling affects the structure and function of the membrane compartments involved in E–C and excitation–glycogen metabolism coupling.

### Ca<sub>v</sub>1.1 content in RamKO mice

The transmission of the signal from the T-tubular membrane to the SR is performed by a supramolecular complex in the contact region between the two membrane systems. The core components of such a complex are the  $\alpha 1$ -subunit (Ca<sub>v</sub>1.1) of the L-type Ca<sup>2+</sup> channel DHPR, the RyR and calsequestrin which serve as voltage sensor, SR Ca<sup>2+</sup> release channel and calcium storage protein respectively [13]. The decrease in the membrane density of DHPR is not accompanied by a decrease in the membrane density of the RyR1 whereby the ryanodine to DHPRs ratio of RamKO mice is higher compared with that of WT mice. The lower membrane density of the DHPR is neither due to mis-localization of the protein to a different membrane compartment as the total amount of Ca<sub>v</sub>1.1 was also reduced in the total muscle



homogenate, nor to decreased levels of specific transcript. A similar decrease in the membrane density of DHPR was previously reported by Avila and Dirksen [37] upon acute treatment of cultured myotubes with 20  $\mu$ M rapamycin and confirmed in the present study in C<sub>2</sub>C<sub>12</sub> cells treated in culture with rapamycin. However, it seems that the functional effect caused by the decreased membrane density of DHPR depends on the maturation stage of muscle cells, namely in myotubes [37] it causes a substantial decrease in the voltage-dependent calcium release, whereas in mature RamKO FDB fibres (in the present work) calcium release evoked by action potential is not affected. The decrease in DHPR content may be caused by increased degradation via ubiquitination and indeed it has been shown that rapamycin treatment induces protein ubiquitination in rat myocardium and mTOR inhibition induces autophagy [53,54]. Interestingly, the ratio of DHPR to RyR1 in slow fibres is lower compared with that in fast fibres, leading to a higher content of uncoupled RyR1 in soleus compared with fast twitch muscles [55]. Thus, our equilibrium binding results are consistent with the fast to slow fibre transition in RamKO muscles [12], in particular more than 90% of soleus's fibres from RamKO are of type 1. Importantly, however, although this reduction in voltage sensor does not seem to be directly responsible for changes in E-C coupling, it may trigger some of the structural variations seen in biopsied muscles, particularly the presence of smaller fibres containing core-like structures such as those described in the mouse RamKO muscles [12]. Indeed, immunofluorescence analysis of skeletal muscle biopsies from some patients with recessive RYR1 mutations show that mis-alignment of RyR1 and DHPR is a feature of some patients with core myopathies [56]. A decrease in the DHPR calcium channels has also been reported in myotubular/centronuclear myopathy [57,58]. Razidlo et al. [59] proposed that the lack of myotubularin inhibits Akt signalling to mTORC1 leading to down-regulation of the signalling pathways mediated by the mTORC1 complex.

#### RyR/Ca<sub>v</sub>1.1 ratio in skeletal muscle of RamKO mice

High resolution EM has demonstrated that Ca<sub>v</sub>1.1 are organized in groups made up of four units regularly oriented in the T-tubular membrane to form structures referred to as tetrads, which correspond to the position of every other RyR localized in the opposite SR terminal cisternae membrane [14]. Equilibrium binding with total sarcotubular membrane fractions shows a ryanodine to DHPR ratio of 0.79 and 1.35 for WT and RamKO skeletal muscle respectively. The RyR/DHPR ratio we found in WT is consistent with that found by others in

total rabbit skeletal muscle homogenates and total microsomal fraction [60–62]. Assuming that there are four PN200-110 binding sites per tetrad and one ryanodine-binding site per RyR, these results imply that in sarcotubular membranes from RamKO mice there is one tetrad-coupled RyR every five/six RyRs, whereas in WT sarcotubular membranes there is one tetrad-coupled RyR every 2–3 RyRs. The ryanodine to DHPR ratio of skeletal muscle from RamKO mice is more similar to that of cardiac [60] and or amphibian [61] skeletal muscles than to that of mature mammalian skeletal muscle. Thus, at this time, it is difficult to reconcile the functional behaviour of such a large fraction of uncoupled RyR in RamKO fibres with that of uncoupled RyR present in WT skeletal muscle having canonical ryanodine to DHPR ratios. Although a great deal of data do not support the notion that in mammalian skeletal muscle fibres, uncoupled RyR are activated by the calcium released from voltage-sensor coupled RyRs via calcium-induced calcium release [63–65], we cannot exclude the possibility that the large ‘cardiac-like’ fraction of voltage-sensor uncoupled RyR in RamKO fibres might have distinct functional behaviour.

#### Global calcium signals and elementary calcium release events in WT and RamKO fibres

Measurements of global calcium in single EDL, soleus and FDB show no differences in the peak amplitude of depolarization-induced  $\text{Ca}^{2+}$  release between WT and RamKO. Such a result was unexpected because of the significant decrease in the membrane density of DHPR and is not consistent with the general idea that the DHPR drives the voltage-dependent activation of RyR1. Nevertheless, it may be possible that a large fraction of uncoupled RyRs are sensitive to regulation by physiological modulators and the activation of the uncoupled RyRs might compensate for the lower content of voltage sensors in RamKO muscles. This line of reasoning is supported by our finding of the modification of the morphology of ECRE induced by osmotic shock, a manoeuvre which weakens the control of the DHPR over the RyR1 and may thus unmask a distinct regulatory mechanism of uncoupled RyR1 in RamKO fibres. ECRE in RamKO fibres are spatially wider and this apparently does not correlate with the changes of the amplitude of ECRE between WT and RamKO fibres. A larger FWHM of ECRE in FDB fibres from raptor KO mice may be caused by a decrease in the removal of calcium at the source site by SERCA and/or by cytosolic calcium-binding proteins. A decrease in removal of calcium is probably not due to the changes in the membrane density of the  $\text{Ca}^{2+}$  pump, since staining of Western blots with either SERCA1 or SERCA2 Ab did

not reveal differences in their protein level in crude SR membrane preparations. The wider ECRE in RamKO fibres may result from the recruitment of the larger fraction of RyRs which are not directly coupled to DHPRs, as described in frog skeletal muscles [65], a tissue with a ryanodine to DHPRs ratio higher than that of mammalian skeletal muscle fibres [61]. If such a distinct functional behaviour is also operating in RamKO skeletal muscle fibres under physiological condition, it is possible that during an action potential voltage-operated RyR1 channels open and the calcium released by the voltage-operated RyR1s propagates to neighbouring uncoupled RyR1 channels. The latter channels release calcium by a calcium-induced calcium release mechanism and ultimately contribute to the calcium transient.

#### Compartmentalization of glycogen phosphorylase to SR membrane

In skeletal muscle, glycogen forms a dense network of granules which are mostly localized on the myoplasmic surface of terminal cisternae and along the membrane of the fenestrated collar [66]. Excitation of skeletal muscle is associated by a rapid (seconds) glycogen breakdown via activation of GP, the enzyme responsible for the release of glucose-1-phosphate from glycogen particles, which ultimately supports muscle metabolism during exercise. It has been demonstrated that excitation–glycolysis coupling occurs without an increase in the myoplasmic concentration of cAMP and without the subsequent conversion of GP-b into GP-a by the cAMP-dependent activity of phosphorylase kinase [67]. GP-b can be allosterically activated by AMP; this cAMP-non-stimulated activity is thought to be predominant during the early phases of skeletal muscle contraction [68]. In resting conditions, the intracellular concentration of AMP is not sufficient to activate GP-b, thus GP-b is thought to be inactive in resting muscles [69]. During strenuous muscle activity however, the intracellular AMP concentration increases, signalling a demand in energy requirement. AMP is the product of the activity myokinase, an enzyme which utilizes as a substrate the ADP generated by the activity of the SR calcium ATPase (CaATPase), Na<sup>+</sup>/K<sup>+</sup>-ATPase and myosin-ATPase. In resting conditions, the average myoplasmic concentration of AMP is 0.2 μM and it increases 10-fold during intense muscle activity [70,71]. However, in regions of high ATP consumption, such as in domains where the SERCA enzyme pumps calcium back into the SR, a greater amount of ATP is required and this may be made available by the allosteric activation of GP-b by AMP. Interestingly, lower glycogen content and an increase in its degradation have been linked to a fast decay of calcium transients and force during

tetanic stimulation [72,73]. The cAMP-dependent active form of GP-a inhibits the activation of the RyR1 by caffeine [48]. Thus, the presence of GP-b associated with the SR membrane is consistent with the concept that the increase in fatigue resistance described in RamKO [11] mice correlates with sustained calcium release, thanks to the compartmentalization to the SR of an energy supplying system made up of glycogen and GP-b.

Overall these results indicate that the muscle phenotype of RamKO mice is complex and due to the interaction of multiple biochemical pathways governed by the mTORC1 signalling complex. The present study shows that an adequate mTORC1 activity is required to maintain the structure and the function of the membrane compartments involved in E–C coupling.

## Figures, Legends and Tables

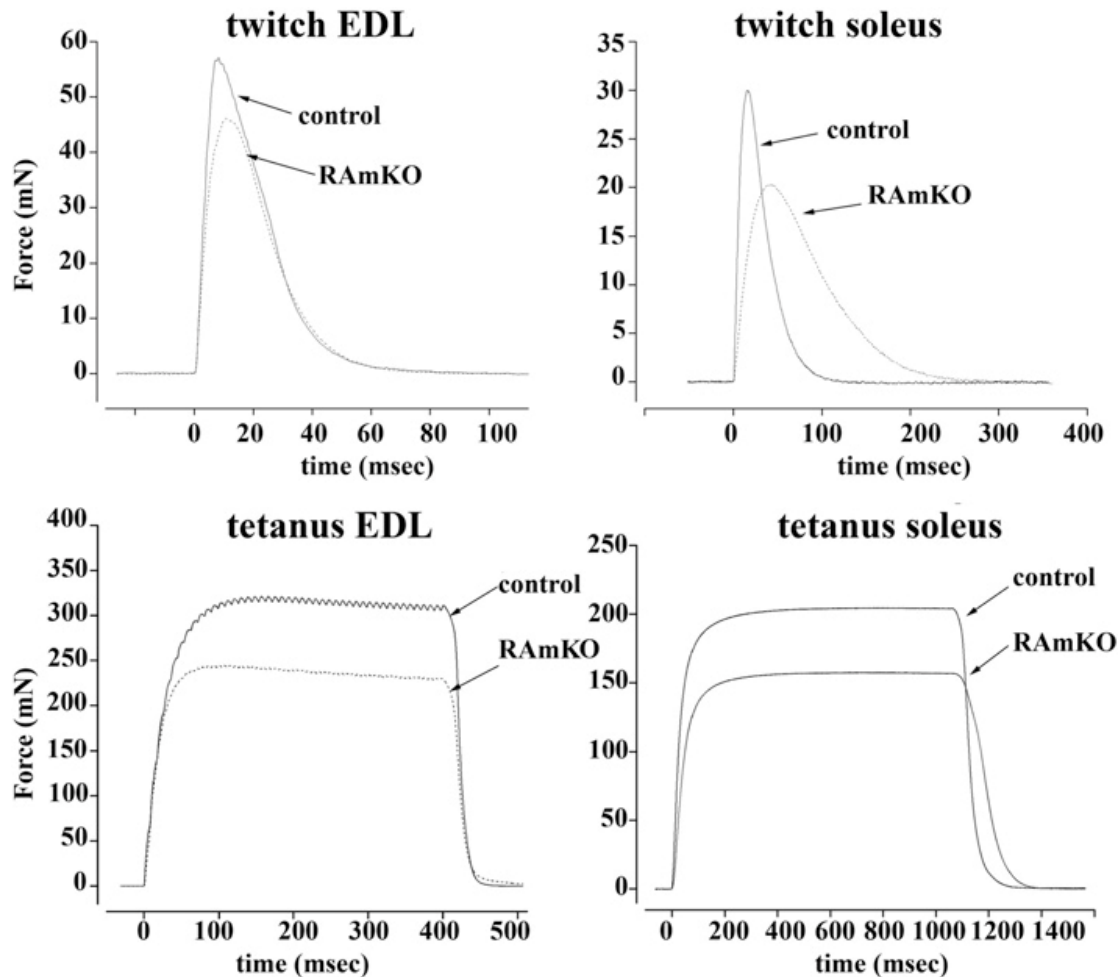


Figure 1. Mechanical properties of isolated EDL and soleus muscles from RamKO and control littermates

Isolated muscles from 8-week-old mice were electrically stimulated as described in the ‘Materials and Methods’ section. Top panels show single twitches, bottom panels maximal tetanus force. Dotted line RamKO mice, continuous line control littermates. Note that the muscles from RamKO mice developed approximately 20% less force than controls. Slow twitch muscles also showed a significant decrease in the half relaxation time. Traces are representative of experiments carried out by Bentzinger et al. [12] on at least three/four different muscle preparations.

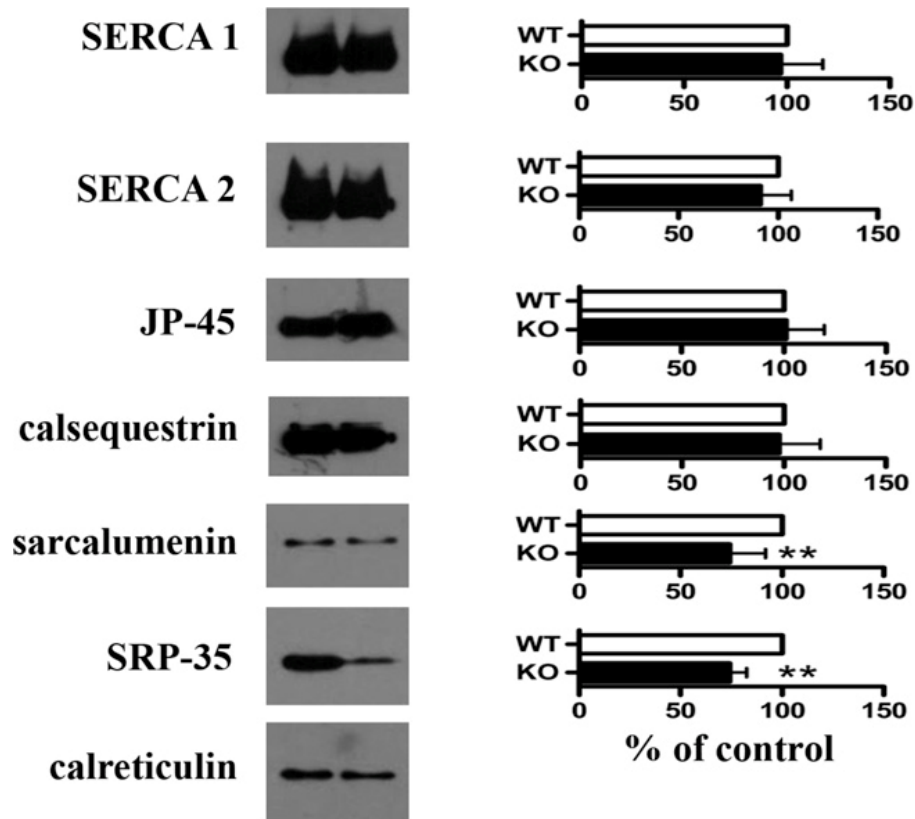


Figure 2. Biochemical characterization of SR proteins from RamKO mice

Left panels show representative Western blots with specified Abs; right panels, mean band intensity ( $\pm$  S.D.) of 6–9 determinations from three different SR preparations. Values were normalized with respect to intensity values obtained from control littermates. White bars, controls; black bars, RamKO. \*\* $P < 0.002$ .

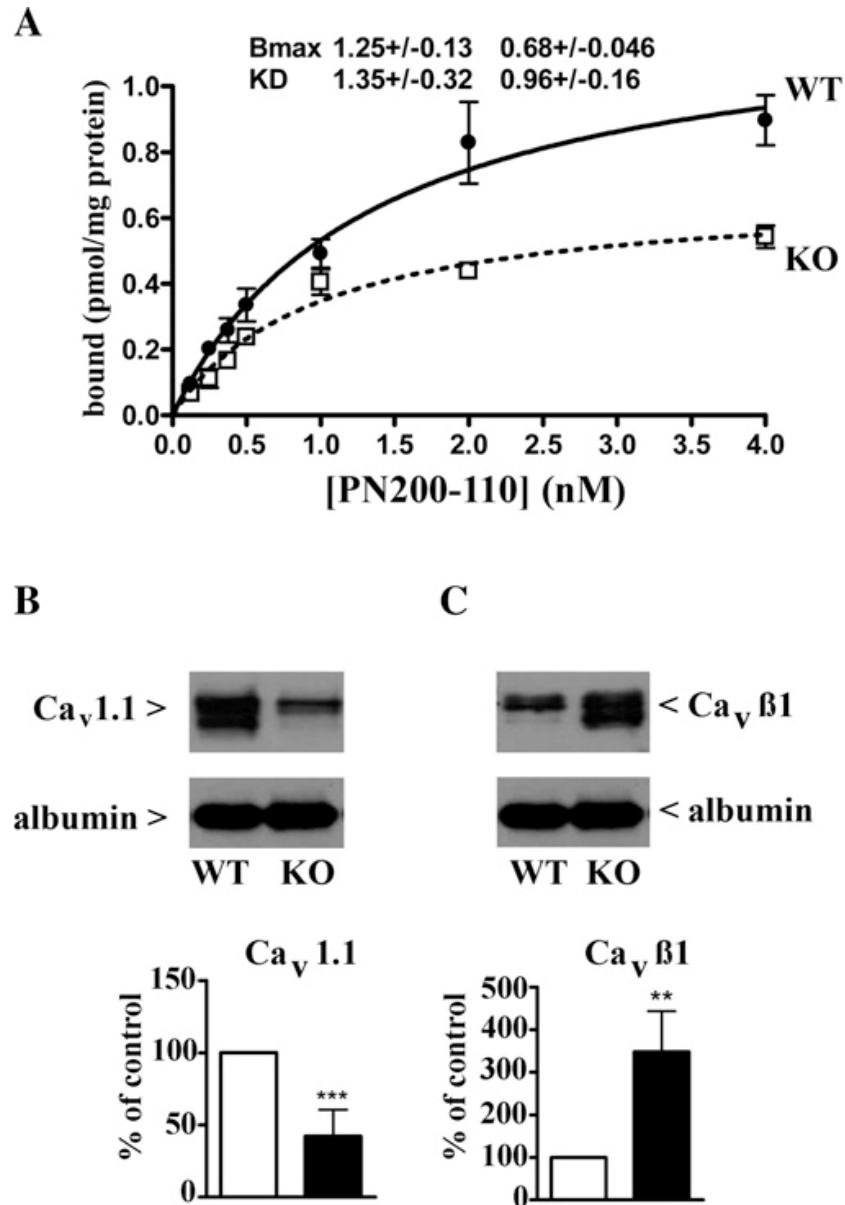


Figure 3. Ca<sub>v</sub>1.1 is decreased in RamKO mice

(A) Equilibrium binding of PN200-110 to skeletal muscle SR of control (filled circle) and RamKO (empty boxes) mice. Data points represent mean ( $\pm$  S.E.M.) of six determinations carried out in two different SR preparations. (B and C) Western blots of Ca<sub>v</sub>1.1 and Ca<sub>v</sub> β1 in SR of control (empty bars) and RamKO (filled bars) mice; the mean band intensity of 5–7 determinations from three different SR preparations.

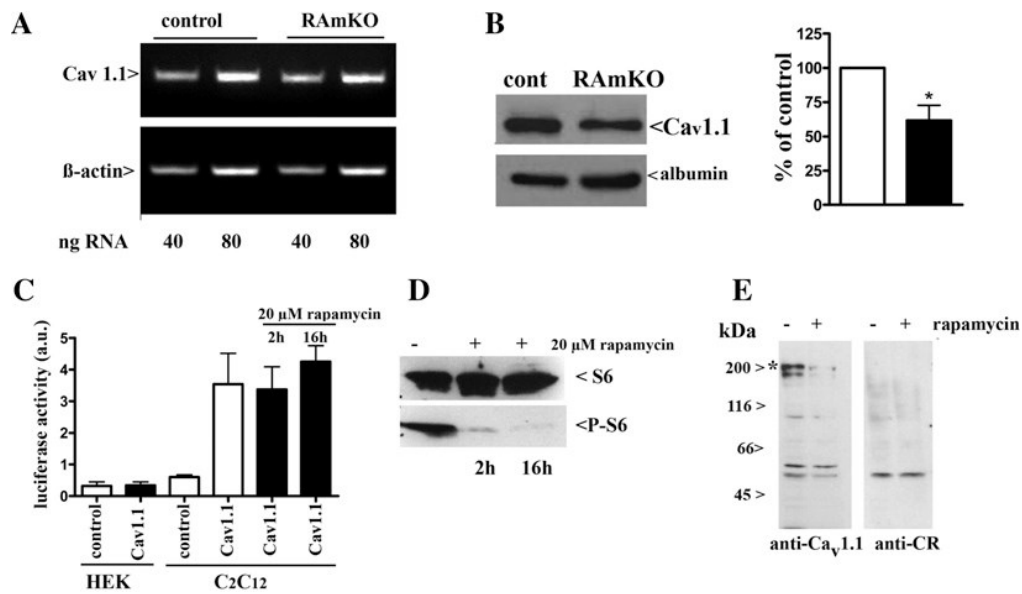


Figure 4.  $Ca_v1.1$  decrease in RamKO mice is not due to a decrease in transcription of  $Ca_v1.1$  mRNA

(A) Semi-quantitative RT-PCR of  $Ca_v1.1$ . The Figure represents results obtained in four different experiments with RNA extracted from two muscle preparations. (B) Western blot of total muscle homogenate with anti- $Ca_v1.1$  and anti-albumin, a marker for transverse tubule content. The bar histogram shows mean ( $\pm$  S.E.M.) band intensity of six determinations from four different muscle preparations; band intensity from the RamKO mice are normalized to that obtained in control littermates. (C) The  $Ca_v1.1$  promoter is not affected by treatment with 20  $\mu$ M rapamycin as determined by luciferase activity. No activity was seen upon transfection of cells with either a control plasmid (white bars) or upon transfection of HEK293 with the luciferase reporter (black bars).  $C_2C_{12}$  cells transfected with a control plasmid showed no luciferase activity, whereas transfection with the luciferase reporter resulted in strong activity which was not affected by 2 or 16 h incubation with rapamycin (black bars). (D) Rapamycin treatment of  $C_2C_{12}$  cells was effective as it resulted in the decrease in phosphorylation of S6 after 2 and 16 h. (E) Rapamycin treatment of differentiated  $C_2C_{12}$  causes a decrease in  $Ca_v1.1$  as determined by Western blotting. Cells were treated with 20  $\mu$ M rapamycin for 16 h and 25  $\mu$ g of microsomes were loaded on SDS/7.5% PAGE and blotted on to nitrocellulose. The blot was probed with anti- $Ca_v1.1$ , stripped and re-probed with anti-CR Ab as a loading control; \*band corresponding to the  $Ca_v1.1$  protein.



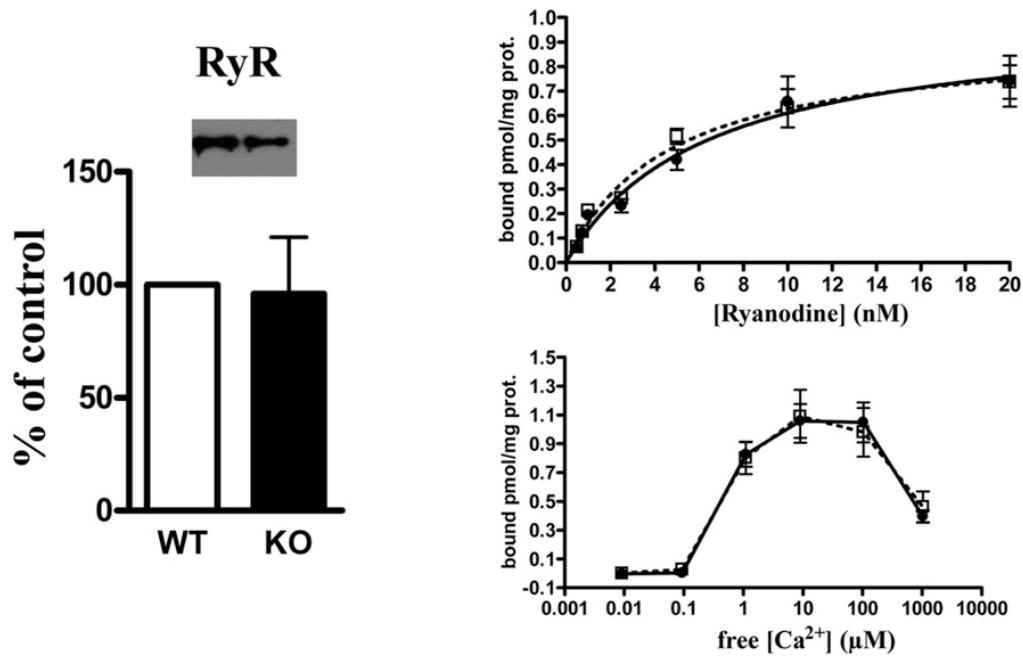


Figure 5. RyR content and functional characteristics are not changed in RamKO mice

Left panel: Representative Western blot of total SR and mean band intensities ( $\pm$  S.D.) of eight determinations from three different SR preparations. Top right: [<sup>3</sup>H]ryanodine binding to SR preparations from control (filled circles) and RamKO (open boxes) mice were performed as described in the ‘Materials and Methods’. Data points represent the mean ( $\pm$  S.E.M.) of 12 determinations from three different SR preparations. No significant change in the Bmax or apparent  $K_D$  was found. Bottom right: Ca<sup>2+</sup>-dependent [<sup>3</sup>H]ryanodine binding to SR preparations from control (filled circles) and RamKO (open boxes) mice. Data points represent mean ( $\pm$  S.E.M.) of six determinations on two different SR preparations.

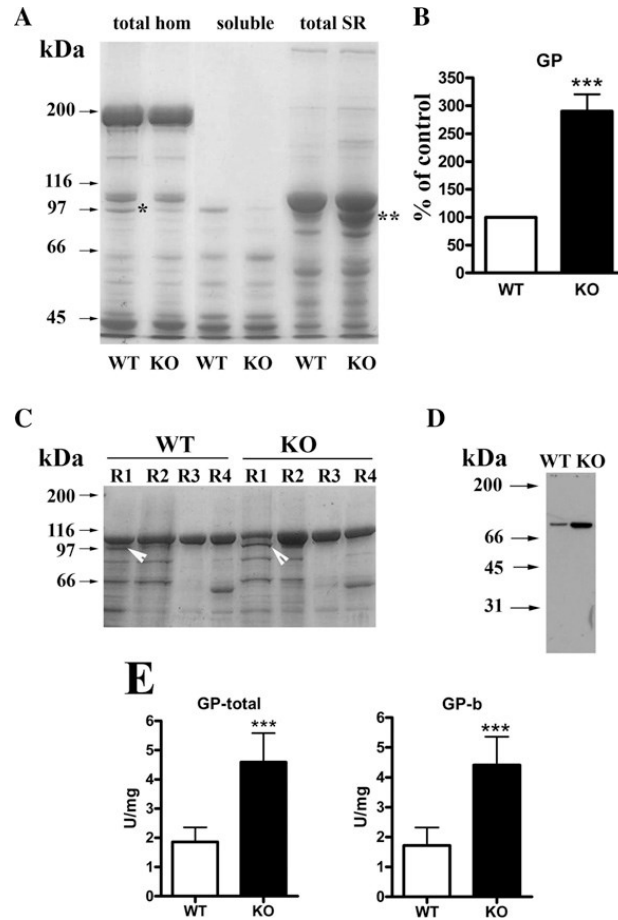


Figure 6. GP is accumulated in the SR of RamKO mice and represents mainly the enzymatically-inactive form

(A) Ten  $\mu$ g of protein from total skeletal muscle homogenate, myoplasm or SR fraction was separated on a SDS/7.5% PAGE and stained with SimplyBlue Safe Stain. \*Represents a band present in the total homogenate from WT muscle but not in RamKO muscle; \*\*represents a band present in the SR fraction of RamKO mice but not in WT mice. (B) Densitometric analysis of GP band in total SR of control (white bars) and RamKO (black bar) mice. (C) SR was fractioned into light SR (R1), longitudinal SR (R2) and terminal cisternae (R4). Fifteen  $\mu$ g of protein from each fraction was loaded on a SDS/7.5% PAGE and stained with SimplyBlue Safe Stain or (D) blotted on to nitrocellulose and stained with anti-GP Abs. White arrows in C indicate GP, which is enriched in the light SR fraction R1. (E) Total (left bar histogram) and inactive form (right bar histogram) GP enzymatic activity in SR from control (white bars) and RamKO (black bars) mice. Values represent the mean (+ S.D.) of 11 determinations from three different SR preparations. \*\*\* $P < 0.05$ .

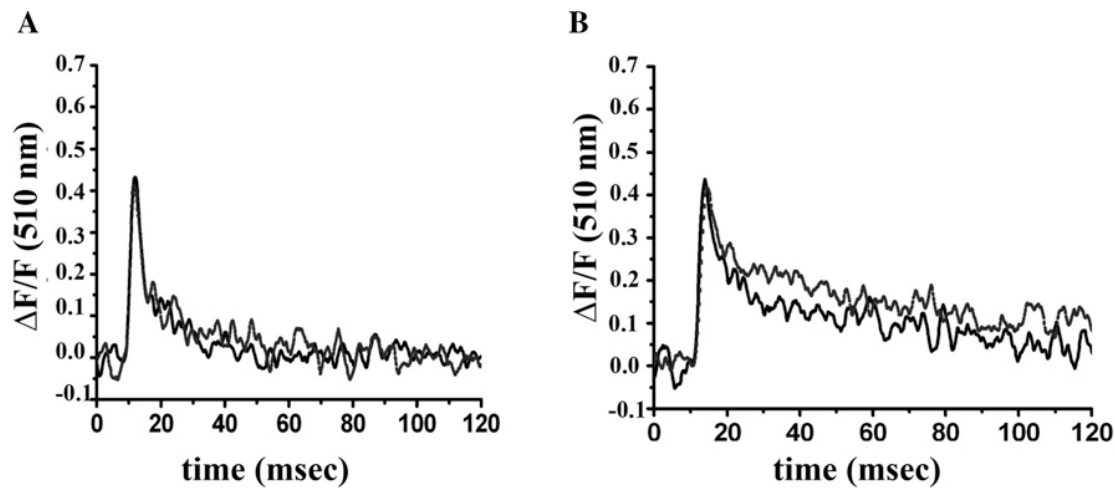


Figure 7. Changes in the myoplasmic  $[Ca^{2+}]$  of individual, enzymatically dissociated EDL and soleus fibres

Control and RamKO fibres were loaded with 10  $\mu M$  mag-fluo-4AM in Tyrode's solution for 10–15 min at 20°C. This solution was replaced and acquisitions were made during continuous perfusion with Tyrode's buffer plus 50  $\mu M$  BTS. Calcium transients were elicited by single pulses of 1 ms duration, through a platinum electrode inside a glass pipette placed near the fibre surface. The representative traces from EDL (A) and soleus (B) show no differences in the peaks and velocities of the  $Ca^{2+}$  transients; there is a significant increase in the half relaxation time in soleus fibres from RamKO mice. See Table 1 for a thorough analysis of the kinetic parameters.

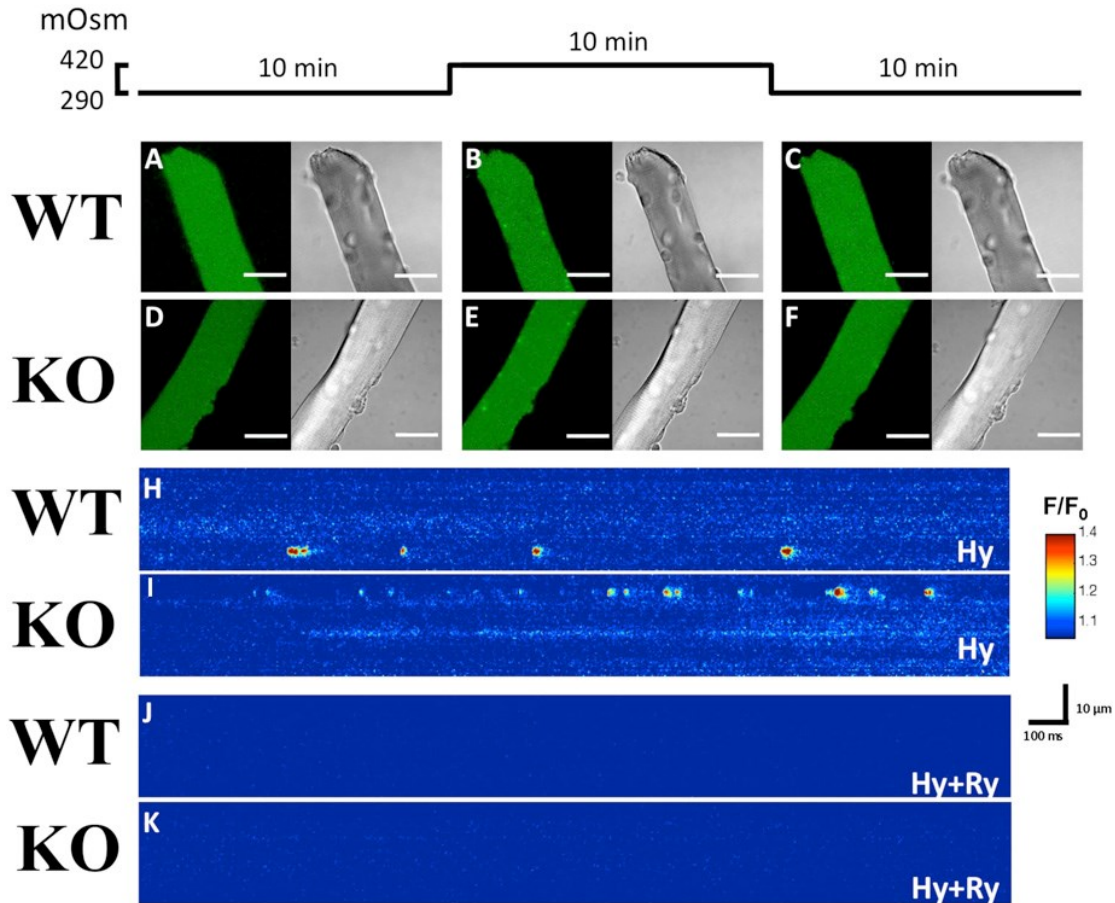


Figure 8. Osmotic-shock triggered ECRE are more frequent in FDB fibres from RamKO than WT mice

ECREs were triggered by exposure of FDB fibres to a hyperosmotic solution. (A–F) Left images show fluo-4 fluorescence and right images bright-field images of the same FDB fibre. Scales bars = 30  $\mu$ m. (A and D) show ( $xy$ ) images of the calcium fluorescence (AU) in WT and RamKO fibres in NR, (B and E) show images of the same fibres after hyperosmotic shock treatment and (C and F) show images of the fibres after 10 min re-perfusion with a normo-osmotic Ringer solution; as shown after removal of the hyperosmotic medium ECRE are no longer visible. (H and I) are pseudocoloured linescan images ( $xt$ ) showing in detail the ECREs shape in WT and RamKO fibres when bathed with hypertonic solution (Hy). (J and K) show that ECREs are due to the opening of RyRs as they are abolished by a 30 min pre-incubation with 10  $\mu$ M. Scale bar (H–K): horizontal: 100 ms, vertical: 10  $\mu$ m.

Table 1. Kinetic properties of calcium transients of isolated EDL and soleus fibres from control and RamKO mice

Values are mean + S.E.M.; n, number of fibres from six WT and RamKO mice.

	Resting Ca <sup>2+</sup> [nM]†	Peak amplitude‡ (ΔF/F)	Time to peak (ms)	Rise time 10%– 90% (ms)	Fall time 10%–90% (ms)
EDL control	141.0±0.35 (n=23)	0.46±0.04 (n=29)	2.9±0.1 (n=29)	1.7±0.05 (n=29)	34.1±4.3 (n=29)
EDL RamKO	115.5±4.8* (n=21)	0.43±0.02 (n=27)	3±0.1 (n=27)	1.8±0.06 (n=27)	39.4±5.4 (n=27)
Soleus control	117±3.6 (n=26)	0.38±0.02 (n=22)	3.4±0.2 (n=22)	2.1±0.2 (n=22)	66.2±7.4 (n=22)
Soleus RamKO	93.8±4.26* (n=8)	0.36±0.02 (n=25)	3.4±0.1 (n=25)	2.1±0.1 z(n=25)	120.3±15.7* (n=25)

\* P < 0.05 Mann Whitney U test.  
†† Calcium measurements performed with the ratiometric indicator indo-1.  
‡ Calcium measurements performed with mag-fluo-4.

Table 2. Morphology of ECREs in skeletal muscle fibres

Values are expressed as mean ± S.E.M.

		Amplitude (ΔF/F <sub>0</sub> )	FWHM (μm)	FDHM (ms)	Mass	Freq* (Sparks/imag)	N†
<50 ms ECREs	WT	0.38±0.00	0.89±0.01	13.31±0.26	0.62±0.02	6.81±0.36	1923
	RamKO	0.38±0.00	0.98±0.01‡	14.11±0.24‡	0.85±0.03‡	8.83±0.40‡	2547
>50 ms ECREs	WT	0.56±0.01	1.32±0.02	143.36±3.32	2.51±0.17	2.51±0.17	538
	RamKO	0.60±0.01‡	1.45±0.02‡	138.49±2.80	3.56±0.18‡	3.56±0.18‡	731

\*WT 168 images, RamKO 162 images.  
† Number of ECREs analysed in 25 fibres and 26 fibres from five WT and RamKO five mice respectively.  
‡ p < 0.005 Student t test.

Supplementary Material

This work contains 1 Supplementary Figure and 6 Supplementary videos.

Supplementary Figure

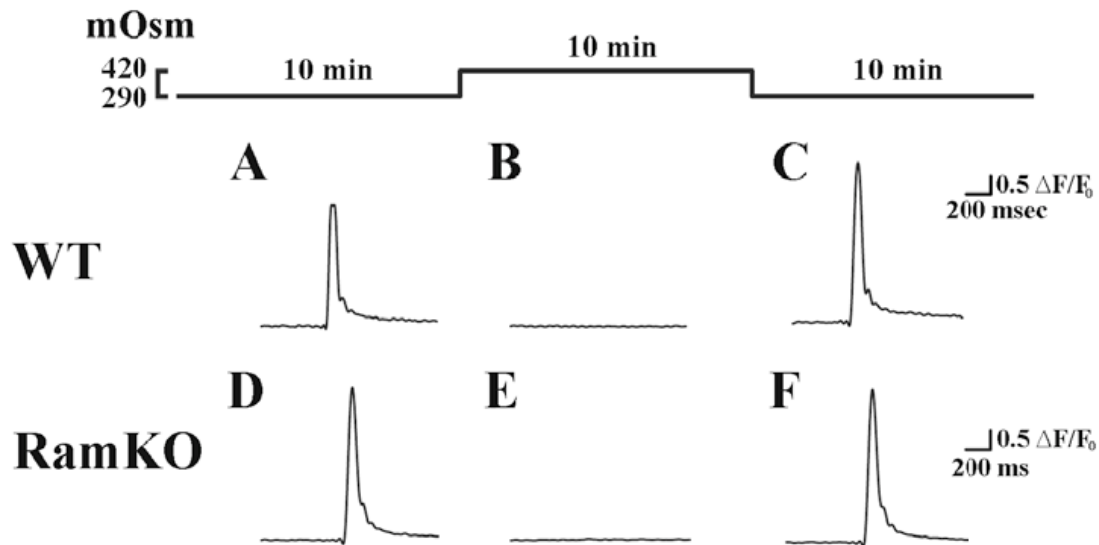


Figure S1. Global  $\text{Ca}^{2+}$  transients in mouse FDB fibers isolated from WT and RamKO littermates elicited before and after hyperosmotic stress-induced-ECREs.

FDB fibers were loaded with Fluo4 and electrically stimulated to check their viability before, during and after application of the hypertonic solution. Panels A and D display representative traces of  $\text{Ca}^{2+}$  transient triggered by an electrical pulse (4ms, 30-40 V) in WT (panel A) and RamKO (panel B) fibers respectively. Cells lose the ability to contract after a 10 min exposure to the hyperosmotic solution (B, E). Panels C and F show that the  $\text{Ca}^{2+}$  transients recover after 10 min of washing with NR (290 mOsm).

## Supplementary Videos

The supplementary videos 1, 2 and 3 show simultaneously white field and the fluorescence calcium changes of a single WT FDB fiber electrically stimulated when perfused when exposed to isotonic, hyperosmotic and return to isotonic medium respectively as indicated in the Supplementary Figure 2-9. Similarly the videos 4, 5 and 6 show FDB fibers from RamKO mice under the same protocol followed before (isosmotic, hyperosmotic and isotonic restitution respectively). To get access to the videos refer to the links indicated below.

### Supplementary video 1

File name: ***WT Single twitch Pre-HyperOsm.avi***

<https://www.dropbox.com/s/0d5gvkas4h0rce6/WT%20Single%20twitch%20Pre-HyperOsm.avi?dl=0>

### Supplementary video 2

File name: ***WT Single twitch HyperOsm.avi***

<https://www.dropbox.com/s/mvhe8pq2r2m2hix/WT%20Single%20twitch%20HyperOsm.avi?dl=0>

### Supplementary video 3

File name: ***WT Single twitch Post-HyperOsm.avi***

<https://www.dropbox.com/s/unvaxpc7dnljmlld/WT%20Single%20twitch%20Post-HyperOsm.avi?dl=0>

### Supplementary video 4

File name: ***RamKO Single twitch Pre-HyperOsm.avi***

<https://www.dropbox.com/s/8xas03dqyq9xt5a/RamKO%20Single%20twitch%20Pre-HyperOsm.avi?dl=0>

### Supplementary video 5

File name: ***RamKO Single twitch HyperOsm.avi***

<https://www.dropbox.com/s/6z9by7rytppslof/RamKO%20Single%20twitch%20HyperOsm.a vi?dl=0>

### Supplementary video 6

File name: ***RamKO Single twitch Post-HyperOsm.avi***

<https://www.dropbox.com/s/cmw3tchbs2mkycl/RamKO%20Single%20twitch%20Post-HyperOsm.avi?dl=0>

## Author Contribution

Ruben Lopez, Marcin Maj, Barbara Mosca, Leda Bergamelli and Susan Treves performed the experiments, analysed the data and drafted the article. Juan Calderon and Carlo Caputo critically revised the manuscript for important intellectual content. Osvaldo Delbono provided the plasmid with the Ca<sub>v</sub>1.1 promoter. Florian Bentzinger, Klaas Romanino, Michael Hall and Markus Rüegg provided the muscle-specific Raptor knockout mouse. Francesco Zorzato designed and performed experiments, collection, analysis and interpretation of data and drafted the article.

## Aknowledgements

We gratefully acknowledge Anne-Sylvie Monnet's technical support.

## Funding

This work was supported by the Department of Anesthesia, Basel University Hospital, Telethon, Italy [grant number GGP14003].

## References

- [1]. De Virgilio, C. and Loewith, R. (2006) The TOR signalling network from yeast to man. *Int. J. Biochem. Cell. Biol.* **38**, 1476-1481.
- [2]. Wullschleger, S., Loewith, R. and Hall, M.N. (2006) TOR signaling in growth and metabolism. *Cell* **124**, 471-484.



- [3]. Guertin, D.A. and Sabatini, D.M. (2007) Defining the role of mTOR in cancer. *Cancer. Cell.* **12**, 9-22.
- [4]. Yang, Q. and Guan, K.L. (2007) Expanding mTOR signaling. *Cell. Res.* **17**, 666-681.
- [5]. Hay, N. and Sonenberg, N. (2004) Upstream and downstream of mTOR. *Genes. Dev.* **18**, 1926-1945.
- [6]. Banaszynski, L.A., Liu, C.W. and Wandless, T.J. (2006) Characterization of the FKBP.rapamycin.FRB ternary complex. *J. Am. Chem. Soc.* **127**, 4715-4721.
- [7]. Kim, D.H., Sarbassov, D.D., Ali, S.M., King, J.E., Latek, R.R., Erdjument-Bromage, H., Tempst, P. and Sabatini, D.M. (2002) mTOR interacts with raptor to form a nutrient-sensitive complex that signals to the cell growth machinery. *Cell* **110**,163-175.
- [8]. Kim, D.H., Sarbassov, D.D., Ali, S.M., Latek, R.R., Guntur, K.V., Erdjument-Bromage, H., Tempst, P. and Sabatini, D.M. (2003) GbetaL, a positive regulator of the rapamycin-sensitive pathway required for the nutrient-sensitive interaction between raptor and mTOR. *Mol. Cell.* **11**, 895-904.
- [9]. Dazert, E. and Hall, M.N. (2011) mTOR signalling in disease. *Curr. Opin. Cell Biol.* **23**, 705-706.
- [10]. Bodine, S.C., Stitt, T.N., Gonzalez, M., Kline, W.O., Stover, G.L., Bauerlein, R., Zlotchenko, E., Scrimgeour, A., Lawrence, J.C., Glass, D.J. and Yancopoulos, G.D. (2001) Akt/mTOR pathway is a crucial regulator of skeletal muscle hypertrophy and can prevent muscle atrophy in vivo. *Nat. Cell. Biol.* **3**, 1009-1013.
- [11]. Risson V1, Mazelin L, Roceri M, Sanchez H, Moncollin V, Corneloup C, Richard-Bulteau H, Vignaud A, Baas D, Defour A, Freyssenet D, Tanti JF, Le-Marchand-Brustel Y, Ferrier B, Conjard-Duplany A, Romanino K, Bauché S, Hantaï D, Mueller M, Kozma SC, Thomas G, Rüegg MA, Ferry A, Pende M, Bigard X, Koulmann N, Schaeffer L, Gangloff YG (2009) Muscle inactivation of mTOR causes metabolic and dystrophin defects leading to severe myopathy *J. Cell Biol.* **187**: 859-874
- [12]. Bentzinger, C.F., Romanino, K., Cloetta, D., Lin, S., Mascarenhas, J.B., Oliveri, F., Xia, J., Casanova, E., Costa, C.F., Brink, M., Zorzato, F., Hall, M.N. and Rüegg, M.A. (2008) Skeletal muscle-specific ablation of raptor, but not of rictor, causes metabolic changes and results in muscle dystrophy. *Cell. Metab.* **8**, 411-424.

- [13]. Rios, E. and Pizarro, G. (1991) Voltage sensor of excitation-contraction coupling in skeletal muscle. *Physiol. Rev.* **71**, 849-908.
- [14]. Franzini-Armstrong, C. and Jorgensen, A.O. (1994) Structure and development of E-C coupling units in skeletal muscle. *Annu. Rev. Physiol.* **56**, 509-534.
- [15]. Beam, K.G., Tanabe, T. and Numa, S. (1989) Structure, function, and regulation of the skeletal muscle dihydropyridine receptor. *Ann. N. Y. Acad. Sci.* **560**, 127-137.
- [16]. Schneider, M.F. and Chandler, W.K. (1972) Voltage dependent charge movement of skeletal muscle: a possible step in excitation-contraction coupling. *Nature* **242**, 244-246.
- [17]. Melzer, W., Hermann-Frank, A. and Lüttgau, H.C. (1995). The role of Ca<sup>2+</sup> ions in excitation-contraction coupling of skeletal muscle fibres. *Biochim. Biophys. Acta* **1241**, 59-116.
- [18]. Fleischer, S. and Inui, M. (1989) Biochemistry and biophysics of excitation-contraction coupling. *Annu. Rev. Biophys. Biophys. Chem.* **18**, 333-364.
- [19]. Treves, S., Jungbluth, H., Muntoni, F. and Zorzato, F. (2008) Congenital muscle disorders with cores: the ryanodine receptor calcium channel paradigm. *Curr. Opin. Pharmacol.* **8**, 319-326.
- [20]. Anderson, A.A., Treves, S., Biral, D., Betto, R., Sandonà, D., Ronjat, M. and Zorzato, F. (2003) The novel skeletal muscle sarcoplasmic reticulum JP-45 protein: molecular cloning, tissue distribution, developmental expression and interaction with  $\alpha_1$  subunit of the voltage gated calcium channel. *J. Biol.Chem.* **278**: 39987-39992.
- [21]. Saito, A., Seiler, S. Chu, A. and Fleischer, S. (1984) Preparation and morphology of sarcoplasmic reticulum terminal cisternae from rabbit skeletal muscle. *J. Cell. Biol.* **99**, 875-885.
- [22]. Treves, S., Thurnheer, R., Mosca, B., Vukcevic, M., Bergamelli, L., Voltan, R., Oberhauser, V., Ronjat, M., Csernoch, L., Szentesi, P. and Zorzato, F. (2012) SRP-35, a newly identified protein of the skeletal muscle sarcoplasmic reticulum, is a retinol dehydrogenase. *Biochem. J.* **44**, 731-741.
- [23]. Delbono, O., Xia, J., Treves, S., Wang, Z.M., Jimenez-Moreno, R., Payne, A.M., Messi, M.L., Briguet, A., Schaerer, F., Nishi, M., Takeshima, H. and Zorzato, F. (2007) Loss of skeletal muscle strength by ablation of the sarcoplasmic reticulum protein JP45. *Proc. Natl. Acad. Sci. U.S.A.* **104**, 20108-20113.

- [24]. Fabiato, A. (1988) Computer programs for calculating total from specified free or free from specified total ionic concentrations in aqueous solutions containing multiple metals and ligands. *Methods. Enzymol.* **157**, 378-417.
- [25]. Calderon, J.C., Bolanos, P. and Caputo, C. (2010) Myosin heavy chain isoform composition and Ca<sup>2+</sup> transients in fibres from enzymatically dissociated murine soleus and extensor digitorum longus muscles. *J. Physiol.* **588**, 267-279.
- [26]. Wang, X., Weisleder, N., Collet, C., Zhou, J., Chu, Y., Hirata, Y., Zhao, X., Pan, Z., Brotto, M., Cheng, H. and Ma, J. (2005) Uncontrolled calcium sparks act as a dystrophic signal for mammalian skeletal muscle. *Nat Cell Biol.* **7**, 525-530.
- [27]. Apostol, S., Ursu, D., Lehmann-Horn, F. and Melzer, W. (2009) Local calcium signals induced by hyper-osmotic stress in mammalian skeletal muscle cells. *J. Muscle Res. Cell. Motil.* **30**, 97-109.
- [28]. Schindelin J., Arganda-Carreras, I., Frise, E., Kaynig, V., Longair, M., Pietzsch, T., Preibisch, S., Rueden, C., Saalfeld, S., Schmid, B., Tinevez, J.Y., White, D.J., Hartenstein, V., Eliceiri, K., Tomancak, P. and Cardona, A. (2001) Fiji: an open-source platform for biological-image analysis. *Nature Methods* **9**, 676-682.
- [29]. Picht, E., Zima, A.V., Blatter, L.A. and Bers, D.M. 2007. SparkMaster: automated calcium spark analysis with ImageJ. *Am. J. Physiol. Cell. Physiol.* **293**, C1073-C1081.
- [30]. Kirsch, W.G., Uttenweiler, D. and Fink, R.H. (2001) Spark- and ember-like elementary Ca<sup>2+</sup> release events in skinned fibres of adult mammalian skeletal muscle. *J. Physiol.* **537**, 379-89
- [31]. Hollingworth, S., Peet, J., Chandler, W.K. and Baylor, S.M. (2001) Calcium sparks in intact skeletal muscle fibers of the frog. *J Gen Physiol.* **118**, 653-678.
- [32]. Danforth, W.H., Helmreich, E. and Coric, F. (1962) The effect of contraction and of epinephrine on the phosphorylase activity of frog sartorius muscle. *Proc. Natl. Acad. Sci. U.S.A.* **48**, 1191-1199.
- [33]. Chasiotis, D., Brandt, R., Harris, R.C. and Hultman, E. (1983) Effects of beta-blockade on glycogen metabolism in human subjects during exercise. *Am. J. Physiol.* **245**, E166-170.
- [34]. Rush, J.W. and Spriet, L.L. (2001). Skeletal muscle glycogen phosphorylase a kinetics: effects of adenine nucleotides and caffeine. *J. Appl. Physiol.* **91**, 2071-2078.

- [35]. Zheng, Z., Wang, Z.M. and Delbono, O. (2002) Charge movement and transcription regulation of L-type calcium channel  $\alpha(1S)$  in skeletal muscle cells. *J. Physiol.* **540**, 397-409.
- [36]. Lamb, G.D. and Stephenson, D.G. (1996) Effects of FK506 and rapamycin on excitation-contraction coupling in skeletal muscle fibres of the rat. *J. Physiol.* **494**,569-576.
- [37]. Avila, G. and Dirksen, R.T. (2005) Rapamycin and FK506 reduce skeletal muscle voltage sensor expression and function. *Cell Calcium* **38**, 35-44.
- [38]. Yoshida, M., Minamisawa, S., Shimura, M., Komazak, S., Kume, H., Zhang, M., Matsumura, K., Nishi, M., Saito, M., Saeki, Y., Ishikawa, Y., Yanagisawa, T. and Takeshima, H. (2005) Impaired  $Ca^{2+}$  store functions in skeletal and cardiac muscle from sarcoplumenin-deficient mice. *J. Biol. Chem.* **280**, 3500-3506.
- [39]. Knudson, C.M. and Campbell, K.P. (1989) Albumin is a major protein component of transverse tubule vesicles isolated from skeletal muscle. *J. Biol. Chem.* **264**, 10795-10798.
- [40]. Peng, T., Golub, T.R. and Sabatini, D.M. (2002) The immunosuppressant rapamycin mimics a starvation-like signal distinct from amino acid and glucose deprivation. *Mol. Cell. Biol.* **22**, 5575-5584.
- [41]. Shin, D.W., Pan, Z., Bandyopadhyay, A., Bhat, M.B., Kim, D.H., Ma, J. (2002)  $Ca^{2+}$ -dependent interaction between FKBP12 and calcineurin regulates activity of the  $Ca^{2+}$  release channel in skeletal muscle *Biophys J.* **83**: 2539-25492.
- [42]. Nyfeler, B., Bergman, P., Triantafellow, E., Wilson, C.J., Zhu ,Y., Radetich, B., Finan, P.M., Klionsky, D.J., Murphy, L.O. (2011) Relieving autophagy and 4EBP1 from rapamycin resistance *Mol Cell Biol* **31**: 2867-2876.
- [43]. Andersson, D.C., Betzenhauser, M.J., Reiken, S., Meli, A.C., Umanskaya, A., Xie, W., Shiomi, T., Zalk, R., Lacampagne, A., Marks, A.R. (2011) Ryanodine receptor oxidation causes intracellular calcium leak and muscle weakness in aging *Cell Metab.* **14**:196-207
- [44]. Durham WJ, Aracena-Parks P, Long C, Rossi AE, Goonasekera SA, Boncompagni S, Galvan DL, Gilman CP, Baker MR, Shirokova N, Protasi F, Dirksen R, Hamilton SL. (2008) RyR1 S-nitrosylation underlies environmental heat stroke and sudden death in Y522S RyR1 knockin mice *Cell.* **133**:53-65.
- [45]. Cuenda, A., Henao, F., Nogues, M. and Gutierrez-Merino, C. (1994) Quantification and removal of glycogen phosphorylase and other enzymes associated with

- sarcoplasmic reticulum membrane preparations. *Biochim. Biophys. Acta.* **1194**, 35-43.
- [46]. Johnson LN (1992) Glycogen phosphorylase: control by phosphorylation and allosteric effectors. *FASEB J.* **6**, 2274–2282.
- [47]. Cuenda, A., Nogues, M., Henao, F. and Gutierrez-Merino, C. (1995). Interaction between glycogen phosphorylase and sarcoplasmic reticulum membranes and its functional implications. *J. Biol. Chem.* **270**, 11998-12004.
- [48]. Hirata Y., Atsumi, M., Ohizumi, Y. and Nakahata, N. (2003) Mastoparan binds to glycogen phosphorylase to regulate sarcoplasmic reticulum  $Ca^{2+}$  release in skeletal muscle. *Biochem. J.* **371**, 81-88.
- [49]. Hollingworth, S., Gee, K.R. and Baylor, S.M. (2009) Low-affinity  $Ca^{2+}$  indicators compared in measurements of skeletal muscle  $Ca^{2+}$  transients. *Biophys J.* **97**, 1864-1872.
- [50]. Heizmann, C.W., Berchtold, M.W., Rowlerson, A.M. (1982) Correlation of parvalbumin concentration with relaxation speed in mammalian muscles. *Proc. Natl. Acad. Sci.* **79**: 7243-7247.
- [51]. Baylor, S.M., Hollingworth. S. (2012) Intracellular calcium movements during excitation-contraction coupling in mammalian slow-twitch and fast-twitch muscle fibers. *J. Gen. Physiol.* **13** :261–272.
- [52]. Zhou, J., Yi, J., Royer, L., Launikonis, B.S., Gonzalez, A., Garcia, J. and Rios, E. (2006) A probable role of dihydropyridine receptors in repression of  $Ca^{2+}$  sparks demonstrated in cultured mammalian muscle. *Am. J. Physiol Cell Physiol.* **290**, C539-C553.
- [53]. Jung, C.H., Ro, S.H., Cao, J., Otto, N.M. and Kim, D.H. (2010) mTOR regulation of autophagy. *FEBS Lett.* **584**, 1287-1295.
- [54]. Harston, R.K., McKillop, J.C., Moschella, P.C., Van Laer, A., Quinones, L.S., Baicu, C.F., Balasubramanian S., Zile, M.R. and Kuppaswamy, D. (2011) Rapamycin treatment augments both protein ubiquitination and Akt activation in pressure -overloaded rat myocardium. *Am. J. Physiol. Heart Circ. Physiol.* **300**, H1696-H1706.
- [55]. Delbono, O. and Meissner, G. (1996) Sarcoplasmic reticulum  $Ca^{2+}$  release in rat slow and fast-twitch muscles. *J. Membr. Biol.* **151**, 123-130.
- [56]. Zhou, H., Lillis, S., Loy, R.E., Ghassemi, F., Rose, M.R., Norwood, F., Mills, K., Al-Sarraj, S., Lane, R.J., Feng, L., Matthews, E., Sewry, C.A., Abbs, S., Buk, S.,

- Hanna, M., Treves, S., Dirksen, R.T., Meissner, G., Muntoni, F. and Jungbluth, H. (2010) Multi-minicore Disease and atypical periodic paralysis associated with novel mutations in the skeletal muscle ryanodine receptor (RYR1) gene. *Neuromuscul. Disord.* **20**,166-173.
- [57]. Al-Qusairi, L., Weiss, N., Toussaint, A., Berbey, C., Messaddeq, N., Kretz, C., Sanoudou, D., Beggs, A.H., Allard, B., Mandel, J.L., Laporte, J., Jacquemond, V. and Buj-Bello, A. (2009) T-tubule disorganization and defective excitation-contraction coupling in muscle fibers lacking myotubularin lipid phosphatase. *Proc. Natl. Acad. Sci. U.S.A.* **106**,18763-18768.
- [58]. Bevilacqua, J.A., Bitoun, M., Biancalana, V., Oldfors, A., Stoltenburg, G., Claeys, K.G., Lacène, E., Brochier, G., Manéré, L., Laforêt, P., Eymard, B., Guicheney, P., Fardeau, M. and Romero, N.B. (2009) Neclace fibers, a new histological marker of late onset MTM1-related centronuclear myopathy. *Acta Neuropathol.* **117**, 283-291
- [59]. Razidlo, G.L., Katafiasz, D. and Taylor, G.S. (2011) Myotubularin regulates Akt-dependent survival signaling via phosphatidylinositol 3-phosphate. *J. Biol. Chem.* **286**, 20005-20019.
- [60]. Bers, D.M. and Stiffel., V.M. (1993) Ratio of ryanodine to dihydropyridine receptors in cardiac and skeletal muscle and implications for E-C coupling. *Am. J. Physiol.* **264**, C1587-C1593.
- [61]. Anderson, K., Cohn, A.H. and Meissner, G. (1994) High-affinity [3H]PN200-110 and [3H]ryanodine binding to rabbit and frog skeletal muscle. *Am J Physiol.* **266**, C462-C466.
- [62]. Margreth, A., Damiani, E. and Tobaldin, G. (1993) Ratio of dihydropyridine to ryanodine receptors in mammalian and frog twitch muscles in relation to the mechanical hypothesis of excitation-contraction coupling. *Biochem. Biophys. Res. Commun.* **197**, 1303-11.
- [63]. Shirokova, N., Garcia, J. and Rios, E. (1998) Local Ca<sup>2+</sup> release in mammalian skeletal muscle. *J. Physiol.* **512**, 377-384.
- [64]. Figueroa, L., Shkryl, V.M., Zhou, J., Manno, C., Marmotake, A., Brum, G., Blatter, L.A., Elli-Davies, G.C. and Rios, E. (2012) Synthetic localized calcium transients directly probe signalling mechanisms in skeletal muscle. *J. Physiol.* **590**, 1389-1411.
- [65]. González, A., Kirsch, W.G., Shirokova, N., Pizarro G., Stern, M.D. and Ríos, E. (2000) The spark and its ember: separately gated local components of Ca<sup>2+</sup> release in skeletal muscle. *J Gen Physiol.* **115**,139-58.
-

- [66]. Peachey, L.D. (1965) The sarcoplasmic reticulum and transverse tubules of the frog's sartorius. *J. Cell Biol.* **25**, 209-231.
- [67]. Drummond, G. I., Hanwood, J. P. and Powell, C. A. (1969) Studies on the activation of phosphorylase in skeletal muscle by contraction and by epinephrine *J. Biol. Chem.* **244**, 4235-4240.
- [68]. Entman, M.L., Keslensky S.S, Chu, A. and Van Winkle, W.B. (1980) The sarcoplasmic reticulum-glycogenolytic complex in mammalian fast twitch skeletal muscle. Proposed in vitro counterpart of the contraction-activated glycogenolytic pool. *J. Biol. Chem.* **255**, 6245-6252.
- [69]. Katz, A., Andersson, D.C., Yu, J., Norman, B., Sandstrom, M.E., Wieringa, B. and Westerblad, H. (2003) Contraction-mediated glycogenolysis in mouse skeletal muscle lacking creatine kinase: the role of phosphorylase b activation. *J. Physiol.* **553**, 523-531.
- [70]. Hellstein, Y., Richter, E.A., Kiens, B. and Bangsbo, J. (1999) AMP deamination and purine exchange in human skeletal muscle during and after intense exercise. *J. Physiol.* **520**, 909-920.
- [71]. Allen, D.G., Lamb, G.D. and Westerblad, H. (2007). Impaired calcium release during fatigue. *J. Appl. Physiol.* **104**, 296-305.
- [72]. Stephenson, D.G. (2011) In pursuit of the glycogen [Ca<sup>2+</sup>] connection. *J. Physiol* **589**, 451.
- [73]. Ortenblad, N., Nielsen, J., Saltin, B. and Holmberg, H.C. (2011) Role of glycogen availability in sarcoplasmic reticulum Ca<sup>2+</sup> kinetics in human skeletal muscle. *J. Physiol* **589**, 711-725.

---



## **Manuscript II: MH-linked *RyR1* mutation and arterial smooth muscle $\text{Ca}^{2+}$ homeostasis on bleeding disorders**

### *Summary of publication 2*

Clinical observations have indicated MHS patients carrying *RyR1* have a slight but consistent bleeding disorder (Jungbluth 2015, personal communication). Interestingly, such finding was confirmed by Vuckevick (personal communication, 2014) while working with a MH mouse model knocked-in for the MH mutation  $\text{RyR1}_{\text{Y522S}}$  (Chelu et al., 2006). Curiously, patients and the animal model do not show apparent alterations of platelet or coagulation function.

Intrigued by this apparent discrepancy, we decided to assess the bleeding time in tail of the  $\text{RyR1}_{\text{Y522S}}$  MH mouse model. Surprisingly the bleeding times were increased in the knock-in mice compared to their WT littermates. Furthermore, the prolonged bleeding was reversed by treatment with Dantrolele. This result prompted us to characterize at the molecular, biochemical and physiological levels vascular smooth muscle cells (VSMCs) from the tail artery. We showed the determined *RyR1* transcripts expressed in VSMCs by Real Time Polymerase Chain Reaction (RT-PCR) and supported this by immunoblotting Western Blot assays. We then identified the subcellular localization of *RyR1* by confocal immunofluorescence microscopy. Interestingly, we found that *RyR1* distributes principally at the periphery of smooth muscle cells. We also studied  $\text{Ca}^{2+}$  homeostasis in VSMCs by fluorescence microscopy and found that cells from the MH knock-in exhibited significant more frequent discrete spontaneous calcium release events referred as ECREs (Elementary Calcium Release Events) compared to their WT littermates. Pharmacological assessments using different  $\text{Ca}^{2+}$  channels blockers confirmed that the source of ECREs was the *RyR1*. Interesting, in smooth muscle cells ECREs are important in controlling vasodilation by activating STOCs currents through the  $\text{Ca}^{2+}$  dependent potassium channels (BK channels) that hyperpolarizes the membrane potential and therefore reduce calcium entrance via the voltage dependent  $\text{Ca}^{2+}$  channel (*Cav1.2*) (Nelson et al., 1995). We evaluate the resting membrane potential of VSMCs with the potentiometric fluorescent dye BisOxonol and we found that cells isolated from the MH mice exhibit a resting membrane potential that is

hyperpolarized by 14 mV compared to that of cells from WT mice. Altogether our evidence strongly suggests that *RyR1* mutations affect not only skeletal muscle function but also vascular homeostasis and we propose that alteration of RyR1 function may be responsible for those bleeding disorders lacking a defined cause, thereby opening a potential use of Dantrolene (or analogous drugs) as an antidote for this sort of bleeding abnormalities

## *RYR1* mutations are a newly identified cause of prolonged bleeding abnormalities<sup>¶</sup>

<sup>¶</sup>Note: manuscript submitted to the Journal *Science Signalling* and is currently under revision.

<sup>1</sup>Rubén J. Lopez, <sup>2</sup>Susan Byrne, <sup>1,3</sup>Mirko Vukcevic, <sup>4</sup>Jay Alamelu, <sup>5</sup>Nicol Voermans, <sup>6</sup>Marc Snoeck, <sup>7</sup>Emma Clement, <sup>8</sup>Francesco Muntoni, <sup>8</sup>Haiyan Zhou, <sup>9</sup>Aleksandar Radunovic, <sup>7</sup>Shehla Mohammed, <sup>2</sup>Elizabeth Wraige, <sup>1,10\*</sup>Francesco Zorzato, <sup>1,10\*</sup>Susan Treves, <sup>2,11,12\*</sup>Heinz Jungbluth

<sup>1</sup>Departments of Anesthesia and of Biomedicine, Basel University Hospital, Hebelstrasse 20, 4031 Basel, Switzerland; <sup>2</sup>Department of Paediatric Neurology, Neuromuscular Service, Evelina Children's Hospital, St Thomas' Hospital, London, UK; <sup>3</sup>Department of Physiology University of Basel, Basel, Switzerland; <sup>4</sup>Department of Haematology, Evelina Children's Hospital, St Thomas' Hospital, London, UK; <sup>5</sup>Department of Neurology, Radboud University Medical Centre, Nijmegen, The Netherlands; <sup>6</sup>National MH Investigation Unit, Department of Anesthesiology, Canisius Wilhelmina Hospital, Nijmegen, The Netherlands; <sup>7</sup>Department of Clinical Genetics, Guy's Hospital, London, UK; <sup>8</sup>Dubowitz Neuromuscular Centre, Institute of Child Health, University College London; <sup>9</sup>Department of Neurology, The Royal London Hospital, London, UK; <sup>10</sup>Department of Life Sciences, General Pathology Section, University of Ferrara, Via Borsari 46, 44100 Ferrara, Italy; <sup>11</sup>Randall Division of Cell and Molecular Biophysics, Muscle Signalling Section, King's College, London, UK; <sup>12</sup>Department of Basic and Clinical Neuroscience, IoPPN, King's College London, London, U.K.

\*These authors contributed equally.

#To whom correspondence should be addressed: [susan.treves@unibas.ch](mailto:susan.treves@unibas.ch)

Abstract

**Background:** Bleeding abnormalities have been reported in some patients with *RYR1*-related Malignant Hyperthermia (MH) but the frequency and molecular basis for this observation are currently uncertain.

**Methods:** *RYR1*-mutated patients and their healthy relatives were identified through the participating tertiary neuromuscular and MH centers; bleeding was assessed by means of a standardized questionnaire (MCMDM-1VWD). Bleeding times in wild type and mice knocked in for the Malignant Hyperthermia *RYR1* mutation Y522S (MHS *RYR1*<sub>Y522S</sub>) were determined. Single tail arterial smooth muscle cells were isolated, loaded with Fluo-4 and observed by confocal microscopy for spontaneous Ca<sup>2+</sup> release events.

**Results:** 8/20 patients had abnormal bleeding scores compared to 0/11 controls (P=0.028); the mean bleeding score in patients was 2.3 and -0.5 in controls (P<0.004). MHS *RYR1*<sub>Y522S</sub> knock in mice exhibited 3 times longer bleeding times compared to their wild type littermates. The bleeding defect of MHS mice could be reversed by pre-treatment with the ryanodine receptor 1 antagonist dantrolene. Primary vascular SMCs from *RYR1*<sub>Y522S</sub> knock-in mice exhibited a higher frequency of subplasmalemmal Ca<sup>2+</sup> sparks leading to a more negative resting membrane potential. Ca<sup>2+</sup> sparks were blocked by pre-treatment with ryanodine or dantrolene.

**Conclusions:** *RYR1* mutations cause prolonged bleeding by altering vascular SMC function and, importantly, dantrolene has potential therapeutic value in the treatment of bleeding disorders.

## Overview, results and finding implications

Bleeding disorders are clinically and genetically heterogeneous and may affect all aspects of hemostasis. Mild bleeding disorders are common in the general population but their precise incidence as well as their genetic background remain often unresolved (1,2).

Mutations in *RYR1*, the gene encoding the skeletal muscle Ca<sup>2+</sup> channel ryanodine receptor 1 (RyR1), have a calculated frequency of 1:3000. Dominant *RYR1* mutations are commonly associated with Malignant Hyperthermia (MH), a severe pharmacogenetic reaction to halogenated anesthetics and muscle relaxants, exertional rhabdomyolysis/myalgia (ERM) (3) and the congenital myopathy Central Core Disease (CCD). Recessive *RYR1* mutations have been associated with the congenital myopathies Multi-minicore Disease (MmD), Centronuclear Myopathy (CNM) and Congenital Fiber Type Disproportion (CFTD) (4-6). Bleeding abnormalities have been reported in isolated patients with MH susceptibility (MHS) (7-9). Interestingly, homozygous mouse embryos knocked in for the MHS *RYR1* mutation Y522S display massive edema and subcutaneous blood effusions at birth, suggestive of a severe bleeding disorder with antenatal onset (10).

To investigate bleeding in *RYR1*-associated myopathies, we invited *RYR1*-mutated individuals and their non-mutated relatives to complete a standardized questionnaire (MCMDM-1VWD) validated for the evaluation of bleeding disorders (Table 1). Patients had neuromuscular features of MH, ERM, a congenital myopathy (CCD/MmD) or a combination of these features, associated with mainly dominant heterozygous *RYR1* missense mutations. The neuromuscular features of patients from families 1, 2, 4, 6, 7, 8 and of their relatives have been previously reported. (3,11,12(Snoeck et al., 2015). MCMDM-1VWD bleeding questionnaires were obtained from 23 *RYR1*-mutated patients (12 females, 11 males) and 11 relatives without the familial *RYR1* mutation (3 females, 8 males). Symptoms of abnormal bleeding were common in *RYR1*-mutated individuals, characterized by severe menorrhagia and postpartum hemorrhage in females and milder symptoms of epistaxis and easy bruising in males. One patient reported an additional history of recurrent and unexplained miscarriages. Interestingly, improvement of menorrhagia was reported in one female (Patient 4.2) after prescription of sodium dantrolene, a specific RyR1 antagonist used clinically to reverse acute MH reactions (13-14), for her severe ERM. Baseline haematological studies including evaluation of clotting factors and platelet aggregation studies were normal in all patients with symptoms of increased bleeding, except in patients 2.6 and 2.7 in whom abnormal von Willebrand factor (vWF) levels were found, and patient 5.1 who had evidence

---

of abnormal platelet function; bleeding scores from these patients were excluded from further statistical analysis as an alternative haematological diagnosis could not be confidently ruled out. Eight out of twenty (40%) patients included in the statistical analysis had a pathological bleeding score ( $\geq 4$ ) on the questionnaire compared to 0/11 (0%) of controls ( $P=0.028$ , Fisher exact testing with 2-tailed  $P$  value). The mean bleeding score for patients was 2.3 (range -2 to 9), and -0.5 (range -1 to 3) in controls ( $P=0.004$ , Student's  $t$ -test) (Figure 1A).

In order to gain mechanistic insight linking *RYR1* mutations to bleeding, we used the heterozygous *RYR1*<sub>Y522S</sub> MH mouse (10). Applying a standardized test to accurately determine bleeding times in mice (15), we demonstrate that bleeding times in *RYR1*<sub>Y522S</sub> mice are 2-3 longer than in their WT littermates (Figure 1B). Bleeding times in male mice were  $136.59 \pm 19.41$  sec. vs  $57.59 \pm 6.56$  sec ( $P < 0.0014$  Student's  $t$  test). Bleeding times in female mice were  $93.0 \pm 10.4$  sec vs  $48.7 \pm 4.3$  sec ( $P < 0.003$  Student's  $t$  test; *Supplementary Figure 1*). Intraperitoneal dantrolene administration (10 mg/Kg) to WT mice 60 minutes prior to the bleeding test did not affect bleeding times ( $P=0.827$  Student's  $t$  test). However, pre-treatment of *RYR1*<sub>Y522S</sub> MH mice with 10 mg/Kg dantrolene reduced bleeding to the same times as those seen in their WT littermates ( $57.15 \pm 6.90$  sec;  $P < 0.002$  Student's  $t$  test). This effect was not observed in mice treated with vehicle alone.

Bleeding times depend on the activation of circulating clotting factors, platelet number and function and on the contraction of injured blood vessels. In a previous study we found no difference in the number and function of circulating platelets between WT and *RYR1*<sub>Y522S</sub> MH (16). We also found no significant RyR1 expression in platelets, virtually excluding disturbed platelet function as a potential cause for the observed bleeding disorder. Since WT and knock-in littermates only differ in their *RYR1*, we hypothesized that these differences could be due to changes in the contraction/relaxation properties of the smooth muscle cells lining the blood vessels. Vascular SMCs (VSMC) have an elaborate  $Ca^{2+}$  homeostasis as they not only express  $InsP_3R$  but also different RyR isoforms (17-21). While  $InsP_3R$  act as channels releasing  $Ca^{2+}$  from the endo(sarco)plasmic reticulum leading to smooth muscle cell contraction, the specific role of RyR is more complex, and experimental evidence indicates that they are also involved in SMC relaxation (21-23). In the next series of experiments we verified if primary arterial VSMC express RyR1 by performing qPCR experiments using primers specific for mouse *RYR1* and normalized the expression levels in the different muscle tissues to desmin (*DES*), as this protein is present in skeletal and smooth muscle cells (24). Figure 2A shows that mouse aorta and tail artery express the *RYR1* transcript, though as expected, to a much lower extent than in skeletal muscle. Figure 2B

shows that the presence of the RYR1<sub>Y522S</sub> mutation in the heterozygous state does not affect the expression levels of RYR1. Figure 2C shows the results of RT-PCR on mRNA isolated from the tail artery confirming the expression of a mutated transcript in the heterozygous RYR1<sub>Y522S</sub> knock in mice.

We next performed confocal immunohistochemical analysis on isolated primary VSMCs. Figure 2D shows that the cells are positive for the specific smooth muscle marker actin (Fig. 2D panel b). Analysis of the subcellular distribution of RyR1 using an antibody that does not cross react with RyR2 (*Supplementary figure 2*) shows that RyR1s are localized on the cell periphery close to the plasma membrane (Figure 2E, panel b). This distribution is compatible with that of the voltage sensing dihydropyridine receptor Ca<sub>v</sub>1.2 which is expressed on the plasma membrane of VSMC (figure 2E panel c) (25-26). The subcellular distribution of RyR1 in isolated primary VSMC is similar to that reported in pulmonary artery smooth muscle cells and in vas deferens (27-29); in the latter cells localized RyR1-mediated calcium release from subplasmalemmal stores causes activation of BK channels resulting in cellular hyperpolarization leading to vasodilation (29, 30).

To investigate how *RYR1* mutations affect Ca<sup>2+</sup> homeostasis, we isolated primary VMCs from mouse tail arteries. We used this model since (i) bleeding times were assessed on this tissue and (ii) these cells are the major cells responsible for the control of the vasomotor activity in the tail (31). No changes in the resting [Ca<sup>2+</sup>] were observed between primary VSMC isolated from WT and RYR1<sub>Y522S</sub> mice (Fig.3 A and B), though the latter cells showed significantly smaller (P<0.05 Student's *t* test) total rapidly releasable Ca<sup>2+</sup> stores compared to those isolated from WT littermates (Fig.3C). In SMC local calcium release events termed "Ca<sup>2+</sup> sparks" have been ascribed to the opening of single or clusters of RyR channels; though they have little or no direct effect on contraction, they indirectly lead to vasodilation through activation of BK channels (21,22). We studied spark activity in isolated primary VSMCs loaded with the calcium dye Fluo-4. A representative image of an isolated tail VSMC is displayed on the top panel of Figure 3 D and the same cell loaded with Fluo-4 is shown in Figure 3D panel b. The bottom panels of Figure 3D show representative linescan images (*x,t*) of Ca<sup>2+</sup> sparks observed in WT and RYR1<sub>Y522S</sub> knock in mice. The grey images have been pseudocoloured and normalized to F/F<sub>0</sub>. A trace showing the detailed time course of several sparks in WT and RYR1<sub>Y522S</sub> cells is shown beneath each linescan image. Detailed analysis of spark activity from 28 SMCs isolated from 6 WT mice (n=877 sparks) and 28 SMCs from 6 RYR1<sub>Y522S</sub> knock in mice (n=1388 sparks), revealed a minor decrease in the amplitude ( $\Delta F/F_0$  in WT vs knock in mice was 0.83±0.01 vs 0.79±0.01, respectively. P<0.05

Student's *t* test), Full Duration Half Maximum (FDHM in WT vs knock in mice was  $1.72 \pm 0.04$  vs  $1.56 \pm 0.03$ , respectively.  $P < 0.05$  Student's *t* test) and Full Width Half Maximum (FWHM in WT vs knock in mice was  $22.09 \pm 0.75$  vs  $19.52 \pm 0.64$ , respectively.  $P < 0.05$  Student's *t* test). Furthermore, the frequency of sparks was significantly increased in the VSMC from the RYR1<sub>Y522S</sub> mice ( $P < 0.00001$  Student's *t* test) (*Supplementary Table 2.4 and Supplementary Videos 1 and 2*).

We next used several drugs including RyR1 blockers and the InsP<sub>3</sub>R antagonist Xestospongine C to determine the origin of these spontaneous Ca<sup>2+</sup> release events. Sparks were totally extinguished in WT and RYR1<sub>Y522S</sub> primary VSMC by pre-incubation with 10 μM Ryanodine (*Supplementary Video 3 and 4*). Additionally, pre-incubation with 20 μM dantrolene significantly decreased spark frequency in both WT and RYR1<sub>Y522S</sub> cells from  $6.33 \pm 0.91$  to  $3.38 \pm 0.70$  ( $P < 0.03$ ) and  $9.56 \pm 0.61$  to  $5.36 \pm 0.87$ , respectively ( $P < 0.0001$ ) (*Supplementary Video 5 and 6 and Supplementary Table 2.4*). This effect was not observed when cells were incubated with the InsP<sub>3</sub> antagonist Xestospongine C (250 nM) (*Supplementary video 7 and 8*). Altogether the results obtained so far confirmed that: (i) primary VSMCs express RyR1; (ii) RYR1 mutations leading to MHS are not only expressed in skeletal muscles but also in arterial SMCs; (iii) the RYR1<sub>Y522S</sub> MH mutation increases the frequency of spark events. In skeletal muscle, RYR1 mutations associated with MHS cause an increased sensitivity to activating stimuli, resulting in prolonged and sustained muscle contractions (32-35). A similar mechanism does not operate in SMCs since RYR1 mutations cause a prolonged and not a shorter bleeding time, the latter would be expected if mutated RyR1 caused a gain of function in primary VSMCs. In skeletal muscle excitation-contraction coupling depends on the mechanical interaction between the voltage sensing dihydropyridine receptor and the RyR1 (36), whereas in SMCs the functional unit is made up of dihydropyridine receptors, ryanodine receptors and BK<sub>Ca</sub> channels (21,22). RyR dependent Ca<sup>2+</sup> sparks activate BK<sub>Ca</sub> channels causing plasma membrane hyperpolarization thereby decreasing Ca<sup>2+</sup> influx via the dihydropyridine receptor and leading to smooth muscle relaxation (21,22) (see Figure 4b). Consistently, we found that the membrane potential of primary VSMCs from WT mice is  $-39.6 \pm 3.4$  mV, a value in line with previous reports (22). On the other hand that of primary VSMCs isolated from RYR1<sub>Y522S</sub> mice was significantly more hyperpolarized ( $-53.7 \pm 3.2$  mV) (Figure 4A).

In conclusion, we demonstrate that RYR1 mutations cause a mild but distinct bleeding disorder in humans and a corresponding phenotype in a murine model of MH. Although in our study we evaluated a relatively small sample size of RYR1-mutated patients and controls,



the clinical data are consistent with the data obtained from the mouse model and the demonstration of complete reversibility of the observed bleeding phenotype through administration of dantrolene. Our findings are important for the surveillance and anticipatory management of patients with *RYR1*-related myopathies, particularly females as SMCs play an important role in uterine vasoregulation and myometrial contraction (37, 38). Moreover, considering that MH-related *RYR1* mutations are frequent but often asymptomatic, they may account for common mild bleeding abnormalities in humans that are currently without genetic explanation and, more importantly, may be amenable to dantrolene treatment. Lastly, our findings may also lead to further investigations into the role of *RYR1*-mediated vasoregulation in other organ systems, including the CNS and the lungs.

## Methods

### Patients

Patients were identified through the participating tertiary neuromuscular and malignant hyperthermia (MH) centers. Genetic testing and haematological studies including evaluation of clotting factors and platelet aggregation were performed as part of the routine diagnostic workup. Patients were invited to complete the MCMDM-1VWD (= Molecular and Clinical Markers for the Diagnosis and Management of Type 1 Von Willebrand's Disease) bleeding questionnaire, a validated and widely used diagnostic tool in the evaluation of bleeding disorders (39). MCMDM1-VWD bleeding questionnaires were scored independently by two clinicians blinded to the genetic status (mutated vs non-mutated) of the proband. The study received UK Research Ethics Committee approval (15/WS/204, granted by the West of Scotland REC 5). Patients gave informed consent for anonymized publication of their clinical information.

### Animal Model

Experiments were carried out on 7-12 week old heterozygous *RYR1*<sub>Y522S</sub> knock-in mice (MHS) and their wild type littermates. The mouse model was generated by Chelu et al. (10) and was a generous gift of Dr. Susan Hamilton, Baylor College of Medicine, Houston, Texas USA. Experimental procedures were approved by the Veterinary Cantonal Authorities

(Permit numbers 1728 and 1729).

#### Bleeding time assay

Bleeding time was determined according to Liu et al. (15). Intraperitoneal injections with dantrolene (10 mg/kg) or vehicle alone (saline solution) were administered 1 h prior to bleeding time determination.

#### Isolation of single smooth muscle cells

Primary vascular smooth muscle cells were isolated essentially as described (40) using an enzymatic cocktail containing 9.6 U/ml papain (Sigma # P4762), 1200U/ml collagenase (Worthington # LS004176), 2.58U/ml elastase (Worthington # LS002292), 0.6% bovine serum albumin (BSA) and 1 mg/ml soybean trypsin inhibitor (Worthington # LS003587).

#### Calcium imaging and Spark analysis

The resting calcium fluorescence was measured using the calcium indicator fura-2 AM (Invitrogen) (16) and the total amount of  $Ca^{2+}$  present in the rapidly releasable intracellular stores was determined as previously described (41). Calcium sparks were measured in cells loaded with 5  $\mu$ M Fluo-4 using a Nikon A1R laser scanning confocal microscope (Nikon Instruments Inc. Melville, USA) with a 60 $\times$  oil immersion Plan Apo VC Nikon objective (NA 1.4). Five sec duration linescan images (x,t) were acquired in resonant mode at super high temporal resolution (7680 fps) with 512 pixels (0.05  $\mu$ m/pixel) in the x- and 39936 pixels (0.126 ms/pixel) in the t-direction using a pinhole size of 72.27  $\mu$ m. Four to five images were taken at different positions across each cell. Fluo-4 was excited with a laser at 487 nm and the fluorescence emitted at 525 $\pm$ 25 nm was recorded. Images were analysed using the open source image processor software Fiji (42). After binning 4X in the temporal axes, linescan images were run with the automated sparks processor plugin SparkMaster (43).

#### Immunofluorescence

Cells were fixed with ice-cold methanol: acetone (1:1) for 30 min and processed as previously described (41). The primary antibodies used were: mouse anti-smooth muscle actin (Sigma #A5228), mouse anti-RyR1 (Thermo Scientific #MA3-925), rabbit anti-Ca<sub>v</sub>1.2 (Santa Cruz # sc-25686) and the secondary conjugates were anti-mouse Alexa Fluor 568 and chicken anti-rabbit Alexa Fluor 488 (Lubio science). Nuclei were counterstained with DAPI (25-30 μM) for 5 min prior to mounting. Cells were examined by confocal microscopy using a Nikon A1R laser scanning confocal microscope with a 60× oil immersion Plan Apo objective.

#### Real Time qPCR and RT PCR

Total RNA was extracted and treated with deoxyribonuclease I (Invitrogen) as previously described (16). After reverse transcription using 1000-1500 ng of RNA, cDNA was amplified by quantitative real-time PCR with a 7500 Fast Real-Time PCR system (Applied Biosystems) using SYBR Green technology (fast SYBR green master mix, Applied Biosystems) and the following primers: RYR1 F: 5'-TCA CTC ACA ATG GAA AGC AG-3'; R: 5'-AGC AGA ATG ACG ATA ACG AA-3'; Desmin F: 5'-TGA GAC CAT CGC GGC TAA GA-3' and R: 5'-GTG TCG GTA TTC CAT CAT CTC C-3'. Gene expression was normalized to desmin (*DES*) content as this marker is specifically expressed in muscle cells (24, 44). RYR1 expression levels in mouse aorta, tail artery and mesenteric artery were compared to RYR1 expression levels in *Extensor Digitorum Longus* (EDL), that latter being the reference tissue set to 1. RYR1 expression in aorta was also investigated by semi-quantitative RT PCR as previously described (16).

#### Membrane potential measurements

Membrane potential measurements were performed using the potentiometric fluorescence dye Bis-Oxonol as described (45). Briefly, isolated arterial smooth muscle cells (SMC) were plated on laminin: gelatin (1:10 ratio) pre-coated coverslips and allowed to attach for 20 min in a modified Krebs-Ringer solution (in mM: NaCl: 140; CaCl<sub>2</sub>: 0.5; KCl: 5; MgSO<sub>4</sub>: 1; HEPES: 10; Na<sub>2</sub>HPO<sub>4</sub>: 1; Glucose: 5.5 and Albumin 1%). Cells were loaded with the potentiometric fluorescence dye Bis-Oxonol (Molecular Probes, B438) at room temperature for 30-40 min. To calibrate the membrane potential cells were incubated with the Na<sup>+</sup>

ionophore gramicidin (10  $\mu$ M) (Sigma, G 5002) and then exposed to different Na<sup>+</sup> containing solutions (*Supplementary Figure 3a*). The concentration ratios of Na<sup>+</sup> and Choline were varied in order to maintain [Na<sup>+</sup>] + [Choline] = 144 mM. Theoretical values for membrane potential (*Supplementary Figure 3b*) were calculated according to the formula:

$$E_m = 60 \text{ Log}([\text{Na}^+]_o + [\text{K}^+]_o) / ([\text{Na}^+]_i + [\text{K}^+]_i) \quad (\text{Eq 1})$$

and considering the internal concentration of Na<sup>+</sup> and K<sup>+</sup> as described by Nelson et al. (22). Fluorescence was recorded every 0.5 min with a Nikon A1 plus confocal microscope, using a 60X oil objective. Samples were illuminated with a Sapphire Laser at 488 nm and the fluorescence emitted at 525/50 nm was recorded. Fluorescence images were processed using the open source software Fiji.

#### Statistical analysis and graphical software

Statistical analysis on the MCMDM1-VWD bleeding questionnaires was performed by converting raw bleeding scores to binary numbers for use in Fisher exact testing with 2-tailed p value (negative screening test  $\leq 3$ , positive screening test  $\geq 4$ ). Mean scores were compared using Student's *t* test. For all other experiments statistical analysis was performed using the Student's *t* test; means were considered statistically significant when the P value was  $< 0.05$ . Data was processed, analysed and plotted using the software OriginPro 8.6.0 (OriginLab Corporation). Images were assembled using Adobe Photoshop CS (version 8.0).

Figures, legends and Table

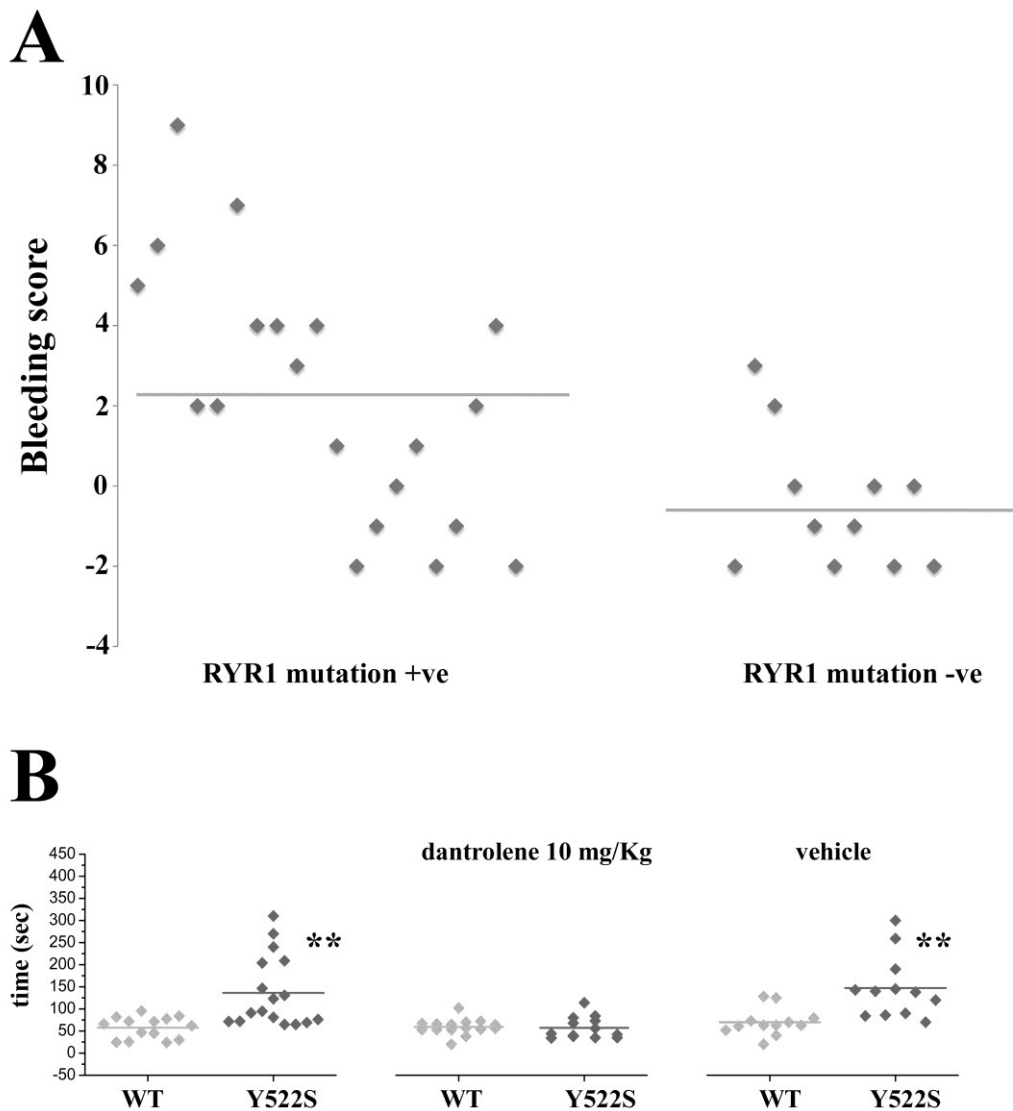


Figure 1. *RYR1* mutations are associated with prolonged bleeding times.

**A.** Scatterplot of MCMDM-1VWD bleeding scores for *RYR1*-mutated patients compared to related controls without the familial *RYR1* mutation(s) (mean score 2.3 in cases compared to -0.5 in controls,  $P < 0.0001$ ). **B.** *RYR1*<sub>Y522S</sub> knock in MHS mice show prolonged bleeding times that are reversed by dantrolene. Each symbol represents the bleeding time (in sec) of a singly wild type (light grey) and *RYR1*<sub>Y522S</sub> (dark grey) mouse. Mice were either untreated (left panel), pre-treated with 10 mg/Kg dantrolene prior to the experiment (central panel) or pre-treated with vehicle alone right panel. \* $P < 0.05$  Students *t*-test.

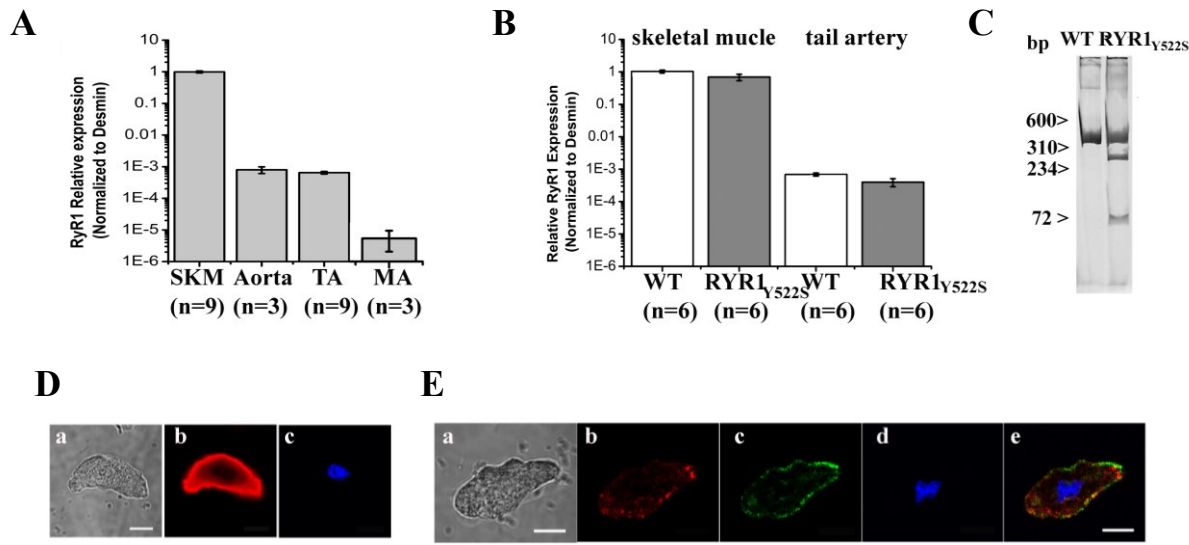


Figure 2. RyR1 is expressed in aorta and tail arteries and has a sub-plasma membrane localization.

**A.** RYR1 expression in skeletal muscle (SKL), aorta, tail and mesenteric artery was normalized to DES content, which is present in skeletal and smooth muscle cells (24). The numbers below the bars indicate number of mice used in the experiment. **B.** The presence of the Y522S mutation does not affect the levels of *RYR1* expression as determined by qPCR. The numbers below the bars indicate number of mice used in the experiment. **C.** Total RNA was extracted from purified aortas and the expression of RYR1 was evaluated by RT-PCR. Digestion of the amplified RYR1 cDNA from wild-type mice (wt) yields the uncut band of about 376 bp, whereas digestion of the cDNA from heterozygous RYR1<sub>Y522S</sub> (het) yields two bands of 276 bp and 100 bp plus the uncut 376 bp band from the wild-type allele **D.** Phase contrast of an isolated primary VSMC (a); confocal immunofluorescence on the same cell using a mouse antibody specific for smooth muscle actin followed by anti-mouse Alexa Fluor 569 (panel b) or DAPI to localize the nucleus (panel c). **E.** Phase contrast on an isolated primary VSMC (panel a); Confocal immunofluorescence of the same cell stained with mouse monoclonal anti-RyR1 mAb followed by anti-mouse Alexa Fluor-568 (red, b), rabbit anti-Ca<sub>v</sub>1.2 followed by anti-rabbit Alexa Fluor-488 (green, c), DAPI (panel d). Composite image showing co-localization of RyR1 and Ca<sub>v</sub>1.2 (panel e). Images were acquired with a Nikon AIR confocal microscope using a 60× oil immersion Plan Apo objective. Scale bar = 10 μm.

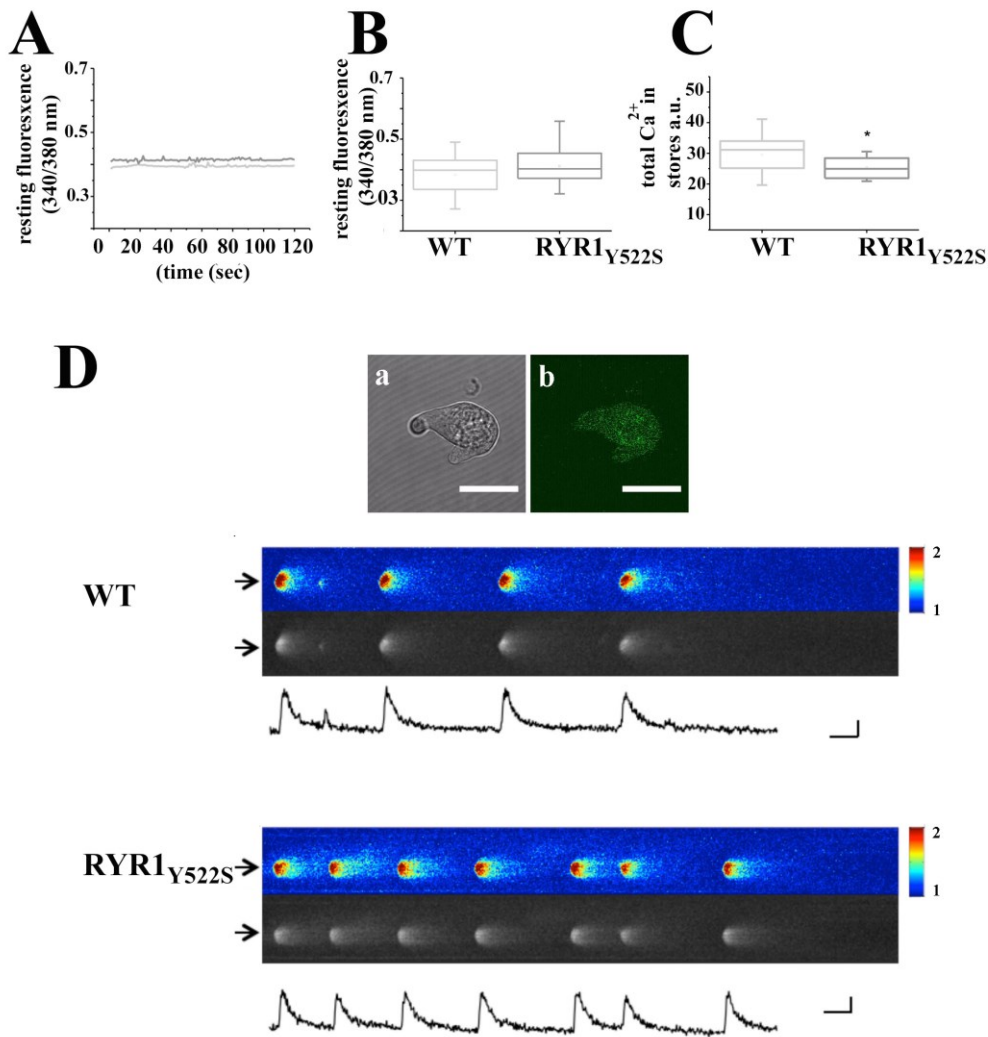


Figure 3. Arterial SMC from the *RYR1<sub>Y522S</sub>* mouse exhibit smaller intracellular  $\text{Ca}^{2+}$  stores and a higher frequency of spontaneous  $\text{Ca}^{2+}$  sparks.

**A.** Fura-2 traces of resting fluorescence ratios (340/380 nm) of primary VSMC isolated from WT (light grey) and *RYR1<sub>Y522S</sub>* knock in (dark grey) mice. **B** Resting fluorescence ratios from primary VSMC isolated from WT (n=20) and *RYR1<sub>Y522S</sub>* knock in (n=20) mice. The values were not significantly different. **C.** Total amount of  $\text{Ca}^{2+}$  in the thapsigargin/ionomycin-sensitive stores was significantly lower in VSMC from *RYR1<sub>Y522S</sub>* mice (n=20 cells) compared to those from WT (n=20 cells) littermates.  $P < 0.05$  Student's *t* test. Experiments were performed as described in (41). **D.** Top images show a brightfield image (a) and fluo-4 fluorescent image (b) photomicrograph of isolated SMC. Bar indicates 10  $\mu\text{m}$ . Bottom pseudocolour and greyscale linescan images of spontaneous localized calcium release events (sparks) in SMC from a WT (top) and a *RYR1<sub>Y522S</sub>* (bottom) mouse.

The color scale indicates the fluorescence change expressed as the ratio of  $F/F_0$ . The traces under the linescan images show the time course of the calcium sparks. Scale bars: vertical 10  $\mu\text{m}$ , horizontal 100 ms, pseudocolor  $F/F_0$ . Note the higher frequency of sparks in the knock in compared to its WT littermate.



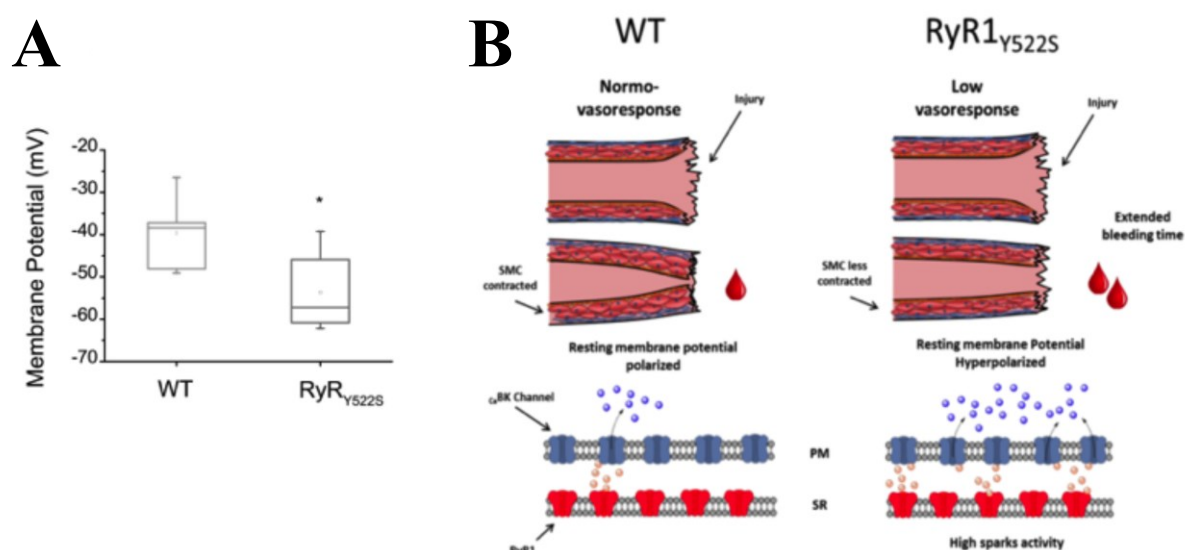


Figure 4. The resting membrane potential in SMC from the  $\text{RYR1}_{Y522S}$  mouse is significantly different from that of WT cells. Schematic representation of RyR1 function in arterial smooth muscle cells.

**A.** The resting membrane potential was measured using the potentiometric probe Bis-Oxonol in 6 WT (6 mice) and 8 MHS (6 mice) smooth muscle cells (See Methods and Supplementary Figure 1 for details). \* Mean resting membrane potential was significantly different (Student's  $t$ -test  $P < 0.05$ ). **B.** Schematic representation of the mechanism leading to prolonged bleeding time due to  $\text{RYR1}$  mutations. In normal conditions (left panel), early vasospasm occurring immediately after injury, reduces bleeding (in coordination with platelets and coagulation factors not shown here). Mutation and the  $\text{RYR1}$  (right panel) results in hyperpolarization of the SMC membrane potential, reducing the ability of vessels to contract and ultimately increasing the bleeding time. PM: Plasma Membrane, SR: Sarcoplasmic Reticulum, RyR1: Ryanodine Receptor Type 1,  $\text{Ca}_v\text{BK}$ : Calcium activated Potassium Channel. Blue balls: Potassium, Yellow balls: calcium sparks, WT: Wild Type,  $\text{RyR1}_{Y522S}$ : MH knock-in condition.

Table 1. Genetic details, neuromuscular features, MCMDM-1VWD bleeding questionnaire scores and bleeding phenotypes from patients with *RYR1*-related myopathies and their non-mutated relatives.

<b>F</b>	<b>P/C</b>	<b>S</b>	<b><i>RYR1</i> mutation(s)</b>	<b>I</b>	<b>NM</b>	<b><i>RYR1</i> +/-</b>	<b>BS</b>	<b>Bleeding phenotype</b>
<b>1</b>	<b>1.1</b>	F	p.R2241X, p.D708N; p.R2939K	AR	MmD/M H	<b>+</b>	<b>5</b>	Severe menorrhagia; Postpartum bleeding
	<b>2.1</b>	F	p.G4638D	AD	CCD/MH S	<b>+</b>	<b>6</b>	Severe menorrhagia; Postpartum bleeding
	<b>2.2</b>	F	p.G4638D	AD	CCD/MH S	<b>+</b>	<b>9</b>	Severe menorrhagia; Postpartum bleeding
	<b>2.3</b>	M	-	-	-	<b>-</b>	<b>-2</b>	not applicable
	<b>2.4</b>	M	-	-	-	<b>-</b>	<b>3</b>	Rectal bleeding (diverticulitis?); Bleeding after dental extraction
<b>2</b>	<b>2.5</b>	M	-	-	-	<b>-</b>	<b>2</b>	Rectal bleeding (colitis?)
	<b>2.6</b>	M	p.G4638D	AD	CCD/MH S	<b>+</b>	<b>4</b>	Epistaxis; Easy bruising*
	<b>2.7</b>	M	p.G4638D	AD	CCD/MH S	<b>+</b>	<b>1</b>	Easy bruising*
	<b>2.8</b>	M	-	-	-	<b>-</b>	<b>0</b>	not applicable
	<b>2.9</b>	F	-	-	-	<b>-</b>	<b>-1</b>	not applicable
	<b>2.10</b>	F	-	-	-	<b>-</b>	<b>-2</b>	not applicable
	<b>2.11</b>	M	-	-	-	<b>-</b>	<b>-1</b>	not applicable
<b>3</b>	<b>3.1</b>	F	p.S1342G, p.A1352G, p.T2787S	AD	ERM	<b>+</b>	<b>2</b>	Menorrhagia; Epistaxis
	<b>3.2</b>	F	p.S1342G, p.A1352G, p.T2787S	AD	ERM	<b>+</b>	<b>2</b>	Menorrhagia; Oral cavity bleeding
	<b>4.1</b>	F	p.G2434R	AD	ERM, MHS	<b>+</b>	<b>7</b>	Severe menorrhagia; Epistaxis
	<b>4.2</b>	F	p.G2434R	AD	ERM, MHS	<b>+</b>	<b>4</b>	Severe menorrhagia#
<b>4</b>	<b>4.3</b>	M	-	-	-	<b>-</b>	<b>0</b>	Epistaxis
	<b>4.4</b>	F	-	-	-	<b>-</b>	<b>-2</b>	not applicable

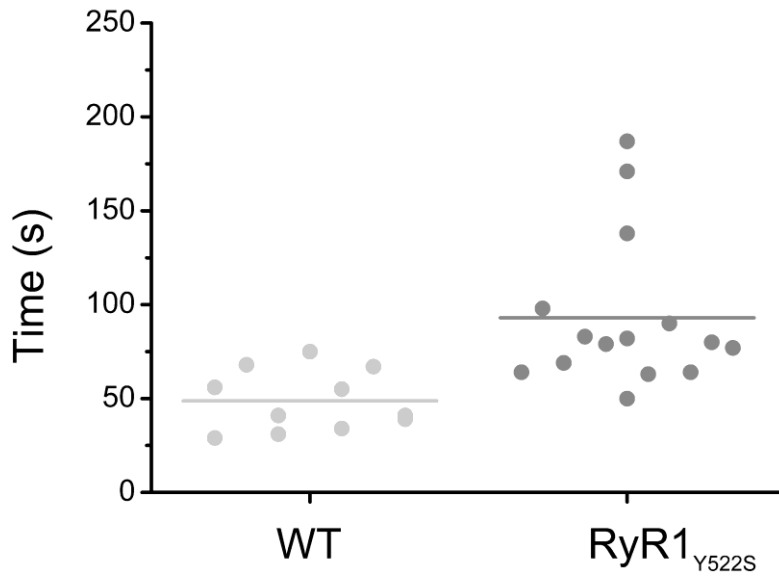
	<b>4.5</b>	M	p.G2434R	AD	ERM, MHS	+	<b>3</b>	Epistaxis; Bleeding after dental extraction
<b>5</b>	<b>5.1</b>	F	p.H3981Y	AD	ERM	+	<b>13</b>	Severe menorrhagia; Postpartum bleeding*
	<b>6.1</b>	F	p.T4288_A4290dup	AD	ERM	+	<b>4</b>	Menorrhagia; Postpartum bleeding
<b>6</b>	<b>6.2</b>	F	p.T4288_A4290dup	AD	ERM	+	<b>4</b>	Easy bruising; Oral cavity bleeding; GI bleeding
	<b>6.3</b>	M	p.T4288_A4290dup	AD	ERM	+	<b>1</b>	Bleeding from minor wounds
	<b>7.1</b>	M	p.V4849I	AD	ERM	+	<b>-2</b>	not applicable
<b>7</b>	<b>7.2</b>	M	p.V4849I	AD	ERM	+	<b>-1</b>	not applicable
	<b>7.3</b>	M	p.I2321V; p.V4849I	AD	ERM	+	<b>0</b>	not applicable
	<b>7.4</b>	M	-	-	-	-	<b>0</b>	not applicable
	<b>8.1</b>	M	p.R614C	AD	MHS	+	<b>1</b>	Oral cavity bleeding
	<b>8.2</b>	M	p.R2676W	AD	MHS	+	<b>-2</b>	not applicable
<b>8</b>	<b>8.3</b>	M	p.R614C	AD	MHS	+	<b>-1</b>	not applicable
	<b>8.4</b>	M	-	-	-	-	<b>-2</b>	not applicable
	<b>8.5</b>	F	p.R2676W	AD	MHS	+	<b>2</b>	Menorrhagia
<b>9</b>	<b>9.1</b>	F	p.R2454H	AD	MHS	+	<b>4</b>	Easy bruising; Postpartum bleeding; Muscle hematoma
	<b>9.2</b>	M	p.R2454H	AD	MHS	+	<b>-2</b>	not applicable

Abnormal MCMDM-1VWD bleeding scores ( $\geq 4$ ) are highlighted in red. Patient 1.1 was deceased and the MCMDM-1VWD bleeding questionnaire was completed retrospectively based on information derived from the patient medical notes. \*Three patients (2.6, 2.7, 5.1) were excluded from further statistical analysis because of abnormal von Willebrand factor levels (2.6, 2.7) and evidence of abnormal platelet function (5.1), respectively. #Patient 4.2 reported improvement of bleeding symptoms following commencement of dantrolene treatment, prescribed for exertional myalgia. Two dominant heterozygous MHS-related *RYR1* mutations were running independently in families 5, 7 and 8. Neuromuscular features from families 1, 2, 4, 6, 7 and 8 have been previously reported. F = Family; P/C = Patient/Control; I = Inheritance; NM = Neuromuscular phenotype; *RYR1* +/- = *RYR1* mutation carrier state; BS = MCMDM-1VWD.

Supplementary material

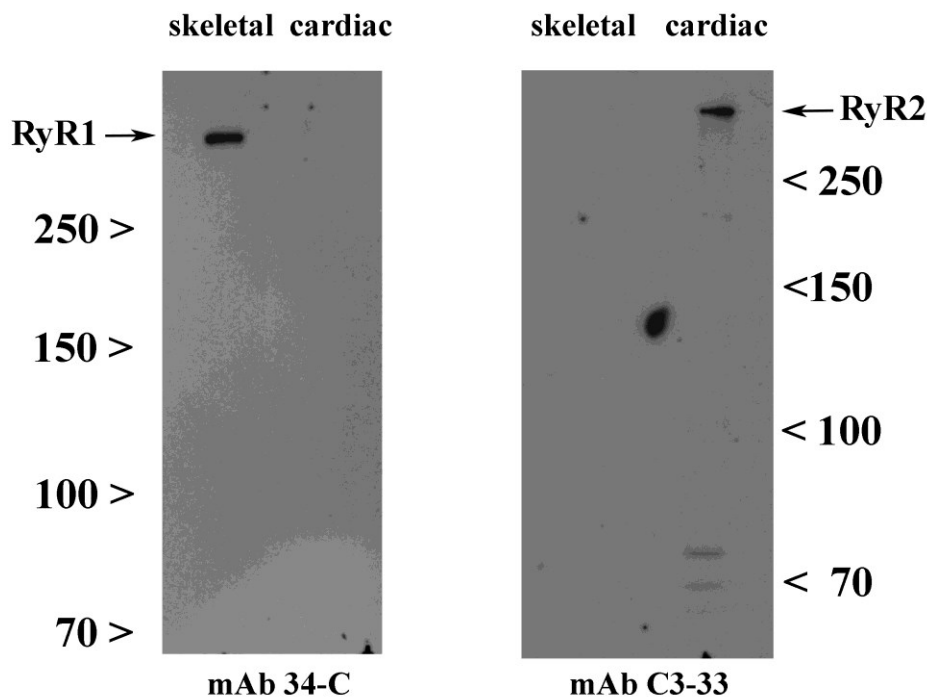
This manuscript contains 3 Supplementary Figure, 1 Supplementary Table and 10 Supplementary videos.

Supplementary Figures



Supplementary Figure 1. Female RYR1<sub>Y522S</sub> knock in MHS mice show prolonged bleeding times.

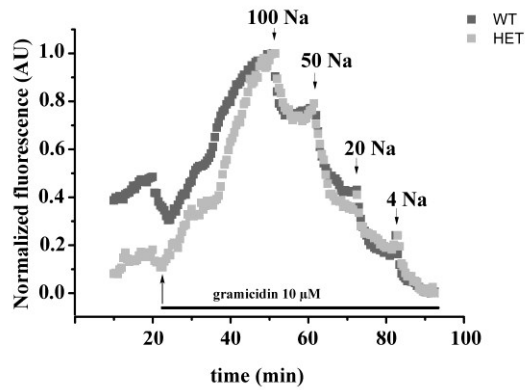
Each symbol represents the bleeding time (in sec) of a singly wild type (light grey) and RYR1<sub>Y522S</sub> (dark grey) mouse. \*P<0.005 Students *t*-test.



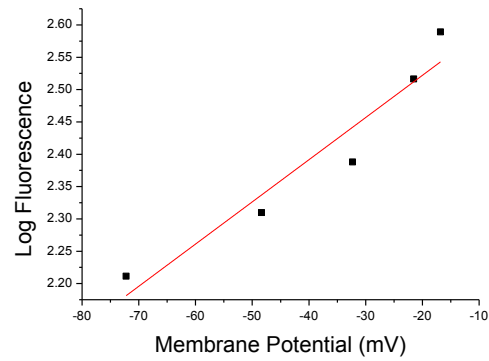
Supplementary Figure 2. Specificity of the anti-RyR1 antibodies used for IHC: western blots of skeletal and cardiac total sarcoplasmic reticulum membranes using isoform specific anti-RyR antibodies.

Thirty micrograms of sarcoplasmic reticulum proteins were separated on a 6% SDS PAG and blotted onto nitrocellulose. Blots were blocked with 1% blocking buffer (Roche) in TBS for 60 min and probed with 1:5000 dilution monoclonal anti-RyR1 specific mAb34-C (left panel) or anti-RyR2 mAb C3-33 (right panel) for 60 min in TBST, rinsed 3 times with TBST, incubated with peroxidase-conjugate anti-mouse IgG (1:200,000 in TBST), rinsed 3 times and developed using the enhanced chemiluminescence kit from Thermo Scientific. As shown, the anti-RyR1 mAb does not cross react with cardiac RyR2. The blot on the right shows a positive control for cardiac RyR2.

**A**



**B**



Supplementary Figure 3. Membrane potential measurements using the fluorescence potentiometric probe Bis-Oxonol.

**A** Representative trace of the changes in fluorescence obtained in primary VSMC, expressed as Arbitrary Units (AU). The arrows indicate addition of Gramicidin or the indicated  $[Na^+]$  in mM. Dark squares VSMC from WT mice, grey squares VSMC from  $RyR1_{Y522S}$  mice. **B** Values derived from Equation 1 (Methods section) with the best linear fitting regression ( $R^2=0.90$ ;  $Y = 0.0065X + 2.6525$ ) of the log of the fluorescence obtained at each  $[Na^+]$ .

Supplementary Table

Supplementary Table 2.4. Effect of Dantrolene and Ryanodine on the frequency of spontaneous Ca<sup>2+</sup> Sparks

	Spark Frequency (Sparks/image)					
	No treatment	Dantrolene 20 μM	<i>N</i>	No treatment	Ryanodine 10 μM	<i>N</i>
<sup>1</sup> WT	6.33±0.91	3.38±0.70*	81	6.69±1.30	0.00±0.00	107
<sup>2</sup> RYR1 <sub>Y522S</sub>	9.56±0.61	5.36±0.87**	236	10.75±1.00	0.00±0.00	215

Values are expressed as Mean ± SEM. \* P< 0.03 \*\*P<0.0001 Student's *t*-test. *N* represent the number of sparks analyzed in 20 images taken from cells isolated from 5-10 different WT and RYR1<sub>Y522S</sub> mice respectively, before and after drug application.

<sup>1</sup>Cells were isolated from 10 and 5 WT mice for the experiments ± 20 μM dantrolene and ± 10 μM ryanodine, respectively.

<sup>2</sup>Cells were isolated from 16 and 5 RYR1<sub>Y522S</sub> heterozygous mice for the experiments ± 20 μM dantrolene and ± 10 μM ryanodine, respectively.

## Supplementary Videos

The Videos 1 and 2 show the white-field and calcium fluorescence signal of spontaneous ECREs activity of a WT and knock-in RYR1<sub>Y522S</sub> VSMC respectively. ECREs activity of knock-in RYR1<sub>Y522S</sub> VSMCs before and after incubation with the RyR blockers Ryanodine 10  $\mu$ M (Videos 3 and 4), Dantrolene 20  $\mu$ M (Videos 5 and 6) and the InsP<sub>3</sub> antagonist Xestospongin C 250 nM (Videos 7 and 8) can be visualized in the following videos respectively. Scale bar for videos = 10  $\mu$ M.

### Supplementary video 1

File name: ***WT Spontaneous ECREs.avi***

<https://www.dropbox.com/s/j1lvec63bblsv9y/WT%20Spontaneous%20ECREs.avi?dl=0>

### Supplementary video 2

File name: ***RyR1Y522S Spontaneous ECREs.avi***

<https://www.dropbox.com/s/rgvcx0pdz13swb/RyR1Y522S%20Spontaneous%20ECREs.avi?dl=0>

### Supplementary video 3

File name: ***RyR1Y522S Pre-Ryanodine treatment ECREs.avi***

<https://www.dropbox.com/s/strrhxyg9vvb7a3/RyR1Y522S%20Pre-Ryanodine%20treatment%20ECREs.avi?dl=0>

### Supplementary video 4

File name: ***RyR1Y522S Post-Ryanodine treatment ECREs.avi***

<https://www.dropbox.com/s/hns7thv61qnruy4/RyR1Y522S%20Post-Ryanodine%20treatment%20ECREs.avi?dl=0>

### Supplementary video 5

File name: ***RyR1Y522S Pre-Dantrolene treatment ECREs.avi***

<https://www.dropbox.com/s/5pygnnwoiw03nzn/RyR1Y522S%20Pre-Dantrolene%20treatment%20ECREs.avi?dl=0>

### Supplementary video 6

File name: ***RyR1Y522S Post-Dantrolene treatment ECREs.avi***

---



<https://www.dropbox.com/s/ufxpjn0gogsaoif/RyR1Y522S%20Post-Dantrolene%20treatment%20ECREs.avi?dl=0>

Supplementary video 7

File name: ***RyR1Y522S Pre-XeC treatment ECREs.avi***

<https://www.dropbox.com/s/vkfpop47je3eo6s/RyR1Y522S%20Pre-XeC%20treatment%20ECREs.avi?dl=0>

Supplementary video 8

File name: ***RyR1Y522S Post-XeC treatment ECREs.avi***

<https://www.dropbox.com/s/uy0irqh8ckrks48/RyR1Y522S%20Post-XeC%20treatment%20ECREs.avi?dl=0>

### Author Contribution

R.J.L designed and performed the experiments and analysed the results with guidance from F.Z. and S.T.; M.V. performed the first bleeding experiments in the mice and helped measure membrane potential. H.Z. investigated RyR1 expression in platelets. S.B., M.S., E.C, H.J., J.A., N.V., F.M., A.R., S.M., E.W. were involved in patients selection, identification of mutations, phenotypic and genetic characterization and characterization of bleeding properties. F.Z. and S.T. designed the experiments on the mouse model, oversaw the project and wrote the paper together with H.J.; H.J. made the initial observation of bleeding abnormalities in the patients.

### Acknowledgements

The support of the Department of Anesthesia Basel University Hospital and the technical support of Anne-Sylvie Monnet are gratefully acknowledged. We would like to thank our patients for their participation.

### Funding

This work was supported by a grant from the Swiss National Science Foundation (SNF N° 31003A-146198).

## References

1. Tosetto A, Castman G, Rodeghiero F. Bleeders, bleeding rates, and bleeding score. *J Thromb Haemost* 2013; 11 (Suppl 1): 142-150.
2. Shaw PH, Reynolds S, Gunawardena S, Krishnamurti L, Ritchey AK. The prevalence of bleeding disorders among healthy pediatric patients with abnormal preprocedural coagulation studies. *J Pediatr Hematol Oncol* 2008; 30: 135-141.
3. Dlamini N, Voermans NC, Lillis S, Stewart K, Kamsteeg EJ, Drost G, et al. Mutations in RYR1 are a common cause of exertional myalgia and rhabdomyolysis. *Neuromuscul Disord* 2013; 23:540-548.
4. Treves S, Jungbluth H, Muntoni F, Zorzato F. Congenital muscle disorders with cores: the ryanodine receptor calcium channel paradigm. *Curr Opin Pharmacol* 2008; 8:319-326.
5. Colombo I, Scoto M, Robb SA, Maggi L, Gowda V, Cullup T, et al. Congenital myopathies: natural history of a large pediatric cohort. *Neurology* 2015; 84: 28-35.
6. Denborough M. Malignant Hyperthermia. *Lancet* 1998; 352: 1131-1135.
7. Stephen CR. Fulminant hyperthermia during anaesthesia and surgery. *JAMA* 1967; 202:178-182.
8. Cullen WG. Malignant Hyperpyrexia during general anaesthesia: a report of two cases. *Canad Anaesth Soc J* 1966; 13:437-443.
9. Daniels JC, Polayes IM, Villar R, Hehre FW. Malignant Hyperthermia with disseminated intravascular coagulation during general anaesthesia: a case report. *Anesth Analg* 1969; 48:877-883.
10. Chelu M, Goonasekera S, Durham W, Tang W, Lueck J, Riehl J, et al. Heat- and anesthesia-induced malignant hyperthermia in an RyR1 knock-in mouse. *FASEB J* 2006; 20, 329-30.
11. Snoeck M., van Engelen BG, Kusters B, Lammens M, Meijer R, Molenaar JP, Raaphorst J, Verschuuren-Bemelmans CC, Straathof CS, Sie LT, de Coo IF, van der Pol WL, de Visser M, Scheffer H, Treves S, Jungbluth H, Voermans NC, Kamsteeg EJ. 2015. RYR1-related myopathies: a wide spectrum of phenotypes throughout life. *Eur J Neurol* 2015; 22:1094-1112.
12. Zhou H, Lillis S, Loy RE, Ghassemi F, Rose MR, Norwood F. Multi-minicore disease and atypical periodic paralysis associated with novel mutations in the

- skeletal muscle ryanodine receptor (RYR1) gene. *Neuromuscul Disord* 2010; 20: 166-173.
13. Krause T, Gerbershagen MU, Fiege M, Weisshorn R, Wappler F. Dantrolene-a review of its pharmacology, therapeutic use and new developments. *Anaesthesia* 2004; 59: 364–373.
  14. Fruen BR, Mickelson JR, Louis CF. Dantrolene inhibition of sarcoplasmic reticulum Ca<sup>2+</sup> release by direct and specific action at skeletal muscle ryanodine receptors. *J Biol Chem* 1997; 272: 26965-26971.
  15. Liu Y, Jennings NL, Dart AM, Du XJ. Standardizing a simpler, more sensitive and accurate tail bleeding assay in mice. *World J Exp Med* 2012; 2: 30-36.
  16. Vukcevic M, Zorzato F, Keck S, Tsakiris DA, Keiser J, Maizels RM, et al. Gain of function in the immune system caused by a ryanodine receptor 1 mutation. *J. Cell. Sci.* 2013; 126: 3485-3492.
  17. Zheng YM, Wang QS, Liu QH, Rathore R, Yadav V, Wang YX. Heterogeneous gene expression and functional activity of ryanodine receptors in resistance and conduit pulmonary as well as mesenteric artery smooth muscle cells. *J Vasc Res* 2008; 45: 469-479.
  18. Vaithianathan T, Narayanan D, Asuncion-Chin MT, Jeyakumar LH, Liu J, Fleischer S, et al. Subtype identification and functional characterization of ryanodine receptors in rat cerebral artery myocytes. *Am J Physiol Cell Physiol* 2010; 299: C264-C278.
  19. Li XQ, Zheng YM, Rathore R, Ma J, Takeshima H, Wang YX. Genetic evidence for functional role of ryanodine receptor 1 in pulmonary smooth muscle cells. *Pflugers Arch* 2009; 457: 771-783.
  20. Westcott EB, Goodwin EL, Segal SS, Jackson WE. Function and expression of ryanodine receptors and inositol 1,4,5-trisphosphate receptors in smooth muscle cells of murine feed arteries and arterioles. *J. Physiol* 2012; 590:1849-1869.
  21. Berridge MJ. Smooth muscle cell calcium activation mechanisms. *J Physiol* 2008; 586: 5047-5061.
  22. Nelson M T, Cheng H, Rubart M, Santana LF, Bonev AD, Knot HJ, et al. Relaxation of arterial smooth muscle by calcium sparks. *Science* 1995; 270: 633-637.
  23. Jaggar JH, Porter VA, Lederer JW, Nelson MT. Calcium sparks in smooth muscle. *Am J Physiol Cell Physiol* 2000; 278: C235-C256.

24. Paulin D, Li Z. Desmin: a major intermediate filament protein essential for the structural integrity and function of muscle. *Exp Cell Res* 2004; 301: 1-7.
25. Navedo MF, Amberg GC, Westenbroeck RE, Sinnegger-Brauns MJ, Catterall WA, Striessnig J, Santana LF. Cav1.3 channels produce persistent calcium sparklets, but Cav1.2 channels are responsible for sparklets in mouse arterial smooth muscle. *Am J Physiol Heart Circ Physiol* 2007; 293: H1359-H1370.
26. Gollasch M, Haase H, Ried C, Lindschau C, Morano I, Luft FC, Haller H L-type calcium channel expression depends on the differentiated state of vascular smooth muscle cells. *FASEB J* 1998; 12: 593-601.
27. Yang XR, Lin MJ, Yip KP, Jeyakumar LH, Fleischer S, Leing GPH, Sham JSK. Multiple ryanodine receptor subtypes and heterogeneous ryanodine receptor-gated  $Ca^{2+}$  stores in pulmonary arterial smooth muscle cells. *Am J Physiol Lung Cell Mol Physiol* 2005; 289: L338-L349.
28. Lesh RE, Nixon GF, Fleischer S, Airey JA, Somplyo AP, Somlyo AV. Localization of ryanodine receptors in smooth muscle. *Circ Res* 1998; 82:175-185.
29. Lifshitz LM, Carmichael JD, Lai FA, Sorrentino V, Bellvé K, Fogarty KE, ZhuGe R. Spatial organization of RYRs and BK channels underlying the activation of STOCs by  $Ca^{2+}$  sparks in airway myocytes. *J Gen Physiol* 2011; 138: 195-209.
30. Clark JH, Kinnear NP, Kalujnaia S, Cramb G, Fleischer S, Jeyakumar LH, et al. Identification of functionally segregated sarcoplasmic reticulum calcium stores in pulmonary arterial smooth muscle cells. *J Biol Chem* 2010; 285: 13542-13549.
31. Nowiki PT, Flavahan S, Hassanain H, Mitra S, Holland S, Goldschmidt-Clemont PJ, et al. Redox signalling of the arteriolar myogenic response. *Circ Res* 2001; 9:114-116.
32. Treves S, Anderson AA, Ducreux S, Divet A, Bleunven C, Grasso C, et al. Ryanodine receptor 1 mutation, dysregulation of calcium homeostasis and neuromuscular disorders. *Neuromuscul Disord* 2005; 15: 577-587.
33. Robinson R, Carpenter D, Shaw MA, Halsall J, Hopkins P. Mutations in RYR1 in malignant hyperthermia and central core disease. *Hum Mutat* 2006; 27: 977-989.
34. Lyfenko AD, Goonasekera SA, Dirksen RT. Dynamic alterations in myoplasmic  $Ca^{2+}$  in malignant hyperthermia and central core disease. *Biochem Biophys Res Commun* 2004; 322: 1256-1266.
35. Girard T, Cavagna D, Padovan E, Spagnoli G, Urwuyler A, Zorzato F, et al. B-lymphocytes from malignant hyperthermia-susceptible patients have an increased

- sensitivity to skeletal muscle ryanodine receptor activators. *J Biol Chem* 2001; 276: 48077–48082.
36. Fleischer S, Inui M. Biochemistry and biophysics of excitation–contraction coupling. *Annu Rev Biophys Biophys Chem* 1989; 18: 333–364.
  37. Li Y, Lorca RA, Ma X, Rhodes A, England SK. BK channels regulate myometrial contraction by modulating nuclear translocation of NFκB. *Endocrinology* 2014; 155: 1055-1063.
  38. Rosenfeld CR, Roy T. Large conductance Ca<sup>2+</sup>-activated and voltage-activated K<sup>+</sup> channels contribute to the rise and maintenance of estrogen-induced uterine vasodilation and maintenance of blood pressure. *Endocrinology* 2012; 153: 6012-6020.
  39. Bowman M, Mundell G, Grabell J, Hopman WM, Rapson D, Lillicrap D, et al. Generation and validation of the Condensed MCMDM-1VWD bleeding questionnaire for von Willebrand disease. *J Thromb Haemost* 2008; 6: 2062-2066.
  40. Tao S, Yamazaki D, Komazaki S, Zhao C, Iida T, Kakizawa S, et al. Facilitated hyperpolarization signalling in vascular smooth muscle-overexpressing TRIC-A channels. *J Biol Chem* 2013; 288: 15581-15589.
  41. Sekulic-Jablanovic M, Palmowski-Wolfe A, Zorzato F, Treves S. Characterization of excitation-contraction coupling components in human extraocular muscles. *Biochem J* 2015; 466:29-36.
  42. Schindelin J, Arganda-Carreras I, Frise E, Kaynig V, Longair M, Pietzsch T, et al. Fiji: an open-source platform for biological-image analysis. *Nature Methods* 2012; 9: 676-682.
  43. Picht E, Zima AV, Blatter A, Bers DM. SparkMaster: automated calcium spark analysis with ImageJ. *Am J Physiol Cell Physiol* 2007; 293: C1073-C1081.
  44. Zhou H, Rokach O, Feng L, Munteanu I, Mamchaoui K, Wilmshurst J, et al. RyR1 deficiency in congenital myopathies disrupts excitation-contraction coupling. *Hum Mutat* 2013; 34: 986-96.
  45. Dell’Asta V, Gatt R, Orlandini G, Rossi P, Rotoli BM, Sala R, et al. Membrane Potential Changes Visualized in Complete Growth Media through Confocal Laser Scanning Microscopy of bis-Oxonol-Loaded Cells. *Exp Cell Res* 1997; 231: 260-268.

---

## CONCLUSIONS AND PERSPECTIVES

Discrete calcium releases events namely ECREs are complex and diverse among different excitable tissues. Since Cheng and colleagues described in 1993 for the first time the so called “calcium sparks” in cardiomyocytes, much has advanced in our understanding the nature of this phenomenon and its participation in EC coupling in normal and pathological conditions. In this thesis we have studied ECREs and characterize in detail their role in calcium hemostasis in two different systems: skeletal muscles and arterial smooth muscles.

Regarding skeletal muscle, study of the biochemistry and molecular composition of the SR membranes in the RamKO animals revealed an important change in the stoichiometry of the two most important players of EC coupling: RyR1 and Cav1.1. This finding not only demonstrates the importance of mTORC1 as a master regulator for the integrity of the protein composition of skeletal muscle as finely described by Bentzinger et al. (2008) and confirmed and extended by Risson et al. (2009), but also open a new perspective in understanding the EC coupling mechanism under particular conditions occurring when there is a reduced control of RyR1 by the voltage sensor DHPR. Interesting, this particular finding recalls the uncoupling of the RyR1-Cav1.1 proteins observed in aging mice by Renganathan et al (1997) by a similar decrease in the Cav1.1 expression, interpreted as an important cause of loss of strength.

Although these observations provide an important contribution on our understanding the role of mTORC1 in muscle biology and particularly in EC coupling, a number of questions arise from this study that still require to be answered, for example how does mTORC1 control Cav1.1 expression? Can the increase in calcium spark frequency and mass observed in RamKO mice be reverted by restoration of functional Cav1.1? Is this reversion directly mTORC1 dependent or are there other unknown factors involved in governing Cav1.1 expression?

As far as my results on ECREs in smooth muscle cells are concerned, unpaired ECREs activity as seen in the MH mouse model knocked-in for the *RYR1* Y522S mutation leads to a prolonged bleeding disorder. Interestingly, this bleeding abnormality is similarly observed in some patients who are MH susceptible. These findings place RyR1 in a new

---

physiological perspective and highlight how disturbances of calcium homeostasis could go beyond skeletal muscle myopathies and incur in other(s) physiological process such as primary hemostasis.

Although we postulate a mechanistic model of a bleeding disorder supported by strong biochemical, molecular and functional evidence at the cellular level, direct studies on the reactivity of the intact blood vessels using different RyR1 agonist/antagonist would provide additional evidence of the pathological mechanism observed in the bleeding disorder we described. This is particular important in order to have a complete picture of this vascular disorder at a multiscale level.

Another important point that should be mentioned is that although the patient's bleeding scores correlate strongly with the bleeding abnormalities of the MH animal model, the small number of patients analyzed in this study might be another limitation. A larger number of patients with RYR1-associated myopathies may be required to further support our hypothesis.

Several technical limitations of this study must also be pointed out for future considerations. Although the use of potentiometric fluorescent dyes was suitable to reveal the resting membrane potential of smooth muscles, the results were at times variable and it took many attempts before I was able to set up the appropriate experimental conditions. As an alternative approach, electrophysiological measurements as determined by patch clamp experiments would have been a potentially more accurate method. I would like to mention that we did attempt to patch isolated smooth muscle cells but we encountered many problems that could not be overcome. For example we could not adequately restrain the isolated cells and achieve a Giga seal with the glass pipette. This was probably due to the nature of the cell preparation (small size, membrane surface properties, etc).

Finally, although skeletal muscle and smooth muscle cells differ significantly in their calcium homeostasis, in both systems calcium is probably the most important regulator of contraction and relaxation. We demonstrate that proteins controlling directly or indirectly calcium homeostasis are of critical importance for the maintenance of a normal physiological balance. Thus, the study of ECREs in other tissues that functionally express RyR1 deserves further attention particularly when investigating the underlying mechanisms of different pathologies of unknown origin.



---

## APPENDIX

### *Blood pressure assessment in RyR1<sup>Y522S</sup> mice*

In order to explore the effect of altered calcium homeostasis of VSMCs of the MH mouse model on vascular hemodynamics, we evaluated the blood pressure of the animals in resting conditions. Additionally, we investigated if the blood pressure in MH susceptible animals is affected by the MH trigger agent isoflurane.

Blood pressure was monitored in conscious and anesthetized mice using a non-invasive method by a tail-cuff photoplethysmography system (BP-2000 Blood Pressure Analysis System, Visitech Systems). Because the system could not accurately estimate the diastolic pressure, we considered systolic pressure only.

The blood pressure of the animals was assessed one time per day for a period of 7 days prior to the real measurements, in a quiet environment and at the same time of day in order to allow the mice to adjust to the protocol. For the anesthetized group of animals, inhaled isoflurane was administered (1,5-3%, 900 cc/min O<sub>2</sub>) for a period no longer than 15 min so the animals were asleep but an MH crisis was avoided.

Figure A1 shows the blood pressure of WT and MH (RyR1<sup>Y522S</sup>) susceptible animals in conscious, untreated animals (left side). We found no statistical difference between 9 WT and 9 RyR1<sup>Y522S</sup> mice (Mean ± SEM: WT= 128.68±2.31; RyR1<sup>Y522S</sup>= 126.10±2.76). When the mice were lightly anesthetized, the blood pressure was consistently depressed in both WT and MH susceptible mice (Figure A1, right panel). Although a consistent depression of blood pressure was observed (Figure A1, right panel), statistical analysis revealed no differences between the MH susceptible animals and the control group (Mean ± SEM: WT= 96.11±3.87; RyR1<sup>Y522S</sup>= 93.85±4.87).

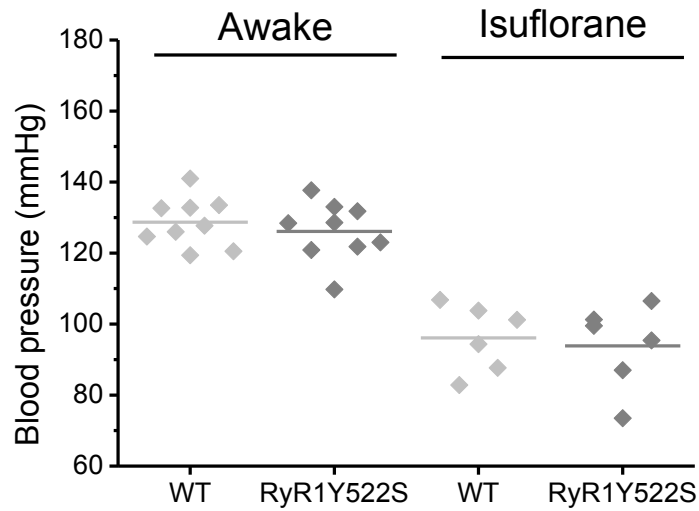


Figure A1. Isoflurane reduces the blood pressure of both WT and RyR1<sub>Y522S</sub> animals to similar levels. The blood pressure of MH susceptible RyR1<sub>Y522S</sub> and WT mice was not different under normal conditions (conscious animals, left panel: Awake). Animals under anesthesia (right panel of the figure: Isoflurane) exhibited a lower blood pressure compared to wakeful animals but there was no difference between the WT and MH susceptible groups.

---

*Detailed kinetics Analysis of ECREs activity in VSMCs*

Table A1. Detailed Analysis of full kinetics parameters of ECREs activity quantified in VSMCs from WT and RyR1Y522S animals respectively.

Morphology of ECREs in Arterial Smooth Muscle Cells									
	Amplitude (DF/F <sub>0</sub> )	FWHM ( $\mu$ m)	FDHM (ms)	Full Widht ( $\mu$ m)	Full Dur (ms)	TtP (ms)	Tau (ms)	Freq (Sparks/image)	N <sup>†</sup>
WT	0.83±0.01	1.72±0.04	22.09±0.75	4.38±0.10	69.93±2.05	20.72±0.64	128.56±33.66	6.96±0.49	877
RyR1 <sub>Y522S</sub>	0.79±0.01*	1.56±0.03*	19.52±0.64*	4.04±0.07*	59.32±1.32*	19.76±0.54	72.81±9.13	10.68±0.55*	1388

\* Statistic significance with T-Test (p<0.05).

Table A2. Detailed Analysis of full kinetics parameters of ECREs activity quantified in VSMCs from WT and RyR1Y522S animals respectively treated with Dantrolene.

Morphology of ECREs in Arterial Smooth Muscle Cells										
		Amplitude (DF/F <sub>0</sub> )	FWHM ( $\mu$ m)	FDHM (ms)	Full Widht ( $\mu$ m)	Full Dur (ms)	TtP (ms)	Tau (ms)	Freq (Sparks/image)	N <sup>†</sup>
Dantrolene 20 $\mu$ M	WT	0.55±0.02	1.21±0.09	15.72±2.14	4.76±0.31	82.68±7.70	25.34±2.91	120.18±55.59	3.38±0.70	81
	RyR1 <sub>Y522S</sub>	0.78±0.03*	1.31±0.05	19.75±1.18	4.52±0.13	87.18±4.12	23.95±1.22	59.33±3.98	5.36±0.87	236

\* Statistic significance with T-Test (p<0.05) compared with the control untreated group respectively.

---

***Effect of Tetracain 150  $\mu$ M on ECREs activity in VSMCs***

Video A1

File name: ***RyR1Y522S Pre-TTC treatment ECREs.avi***

<https://www.dropbox.com/s/cv6jvlbjgmcqxz2/RyR1Y522S%20Pre-TTC%20treatment%20ECREs.avi?dl=0>

Video A2

File name: ***RyR1Y522S Post-TTC treatment ECREs.avi***

<https://www.dropbox.com/s/gs2yn87vdzwiq0k/RyR1Y522S%20Post-TTC%20treatment%20ECREs.avi?dl=0>

---

## REFERENCES

- Administration, U.S.F.a.D. 2015. Rapamune (sirolimus) Oral Solution, Tablets Prescribing Information.
- Agency, E.M. 2015. European public assessment report (EPAR) for Rapamune.
- Albert, V., and M.N. Hall. 2015. mTOR signaling in cellular and organismal energetics. *Curr Opin Cell Biol.* 33:55-66.
- Anderson, A.A., S. Treves, D. Biral, R. Betto, D. Sandona, M. Ronjat, and F. Zorzato. 2003. The novel skeletal muscle sarcoplasmic reticulum JP-45 protein. Molecular cloning, tissue distribution, developmental expression, and interaction with alpha 1.1 subunit of the voltage-gated calcium channel. *J Biol Chem.* 278:39987-39992.
- Apostol, S., D. Ursu, F. Lehmann-Horn, and W. Melzer. 2009. Local calcium signals induced by hyper-osmotic stress in mammalian skeletal muscle cells. *J Muscle Res Cell Motil.* 30:97-109.
- Augustine, G.J., and H. Kasai. 2007. Bernard Katz, quantal transmitter release and the foundations of presynaptic physiology. *J Physiol.* 578:623-625.
- Bankhead, P., C.N. Scholfield, T.M. Curtis, and J.G. McGeown. 2011. Detecting Ca<sup>2+</sup> sparks on stationary and varying baselines. *Am J Physiol Cell Physiol.* 301:C717-728.
- Baretic, D., and R.L. Williams. 2014. PIKKs--the solenoid nest where partners and kinases meet. *Curr Opin Struct Biol.* 29:134-142.
- Barone, V., D. Randazzo, V. Del Re, V. Sorrentino, and D. Rossi. 2015. Organization of junctional sarcoplasmic reticulum proteins in skeletal muscle fibers. *J Muscle Res Cell Motil.*
- Baselga, J., M. Campone, M. Piccart, H.A. Burris, 3rd, H.S. Rugo, T. Sahmoud, S. Noguchi, M. Gnant, K.I. Pritchard, F. Lebrun, J.T. Beck, Y. Ito, D. Yardley, I. Deleu, A. Perez, T. Bachelot, L. Vittori, Z. Xu, P. Mukhopadhyay, D. Lebwohl, and G.N. Hortobagyi. 2012. Everolimus in postmenopausal hormone-receptor-positive advanced breast cancer. *N Engl J Med.* 366:520-529.
- Beard, N.A., M.G. Casarotto, L. Wei, M. Varsanyi, D.R. Laver, and A.F. Dulhunty. 2005. Regulation of ryanodine receptors by calsequestrin: effect of high luminal Ca<sup>2+</sup> and phosphorylation. *Biophys J.* 88:3444-3454.

- 
- Beard, N.A., D.R. Laver, and A.F. Dulhunty. 2004. Calsequestrin and the calcium release channel of skeletal and cardiac muscle. *Prog Biophys Mol Biol.* 85:33-69.
- Beard, N.A., L. Wei, and A.F. Dulhunty. 2009. Ca(2+) signaling in striated muscle: the elusive roles of triadin, junctin, and calsequestrin. *Eur Biophys J.* 39:27-36.
- Ben-Sahra, I., J.J. Howell, J.M. Asara, and B.D. Manning. 2013. Stimulation of de novo pyrimidine synthesis by growth signaling through mTOR and S6K1. *Science.* 339:1323-1328.
- Benham, C.D., and T.B. Bolton. 1986. Spontaneous transient outward currents in single visceral and vascular smooth muscle cells of the rabbit. *J Physiol.* 381:385-406.
- Bentzinger, C.F., S. Lin, K. Romanino, P. Castets, M. Guridi, S. Summermatter, C. Handschin, L.A. Tintignac, M.N. Hall, and M.A. Rugg. 2013. Differential response of skeletal muscles to mTORC1 signaling during atrophy and hypertrophy. *Skelet Muscle.* 3:6.
- Bentzinger, C.F., K. Romanino, D. Cloetta, S. Lin, J.B. Mascarenhas, F. Oliveri, J. Xia, E. Casanova, C.F. Costa, M. Brink, F. Zorzato, M.N. Hall, and M.A. Rugg. 2008. Skeletal muscle-specific ablation of raptor, but not of rictor, causes metabolic changes and results in muscle dystrophy. *Cell Metab.* 8:411-424.
- Berridge, M.J. 2006. Calcium microdomains: organization and function. *Cell Calcium.* 40:405-412.
- Berridge, M.J., M.D. Bootman, and H.L. Roderick. 2003. Calcium signalling: dynamics, homeostasis and remodelling. *Nat Rev Mol Cell Biol.* 4:517-529.
- Beurg, M., C.A. Ahern, P. Vallejo, M.W. Conklin, P.A. Powers, R.G. Gregg, and R. Coronado. 1999a. Involvement of the carboxy-terminus region of the dihydropyridine receptor beta1a subunit in excitation-contraction coupling of skeletal muscle. *Biophys J.* 77:2953-2967.
- Beurg, M., M. Sukhareva, C.A. Ahern, M.W. Conklin, E. Perez-Reyes, P.A. Powers, R.G. Gregg, and R. Coronado. 1999b. Differential regulation of skeletal muscle L-type Ca<sup>2+</sup> current and excitation-contraction coupling by the dihydropyridine receptor beta subunit. *Biophys J.* 76:1744-1756.
- Biral, D., P. Volpe, E. Damiani, and A. Margreth. 1992. Coexistence of two calsequestrin isoforms in rabbit slow-twitch skeletal muscle fibers. *FEBS Lett.* 299:175-178.
- Block, B.A., T. Imagawa, K.P. Campbell, and C. Franzini-Armstrong. 1988. Structural evidence for direct interaction between the molecular components of the transverse
-



- 
- tubule/sarcoplasmic reticulum junction in skeletal muscle. *J Cell Biol.* 107:2587-2600.
- Bodine, S.C., T.N. Stitt, M. Gonzalez, W.O. Kline, G.L. Stover, R. Bauerlein, E. Zlotchenko, A. Scrimgeour, J.C. Lawrence, D.J. Glass, and G.D. Yancopoulos. 2001a. Akt/mTOR pathway is a crucial regulator of skeletal muscle hypertrophy and can prevent muscle atrophy in vivo. *Nat Cell Biol.* 3:1014-1019.
- Bodine, S.C., T.N. Stitt, M. Gonzalez, W.O. Kline, G.L. Stover, R. Bauerlein, E. Zlotchenko, A. Scrimgeour, J.C. Lawrence, D.J. Glass, and G.D. Yancopoulos. 2001b. Akt/mTOR pathway is a crucial regulator of skeletal muscle hypertrophy and can prevent muscle atrophy in vivo. *Nature Cell Biology.* 3:1014-1019.
- Bolton, T.B. 1979. MECHANISMS OF ACTION OF TRANSMITTERS AND OTHER SUBSTANCES ON SMOOTH-MUSCLE. *Physiological Reviews.* 59:606-718.
- Bottinelli, R., and C. Reggiani. 2000. Human skeletal muscle fibres: molecular and functional diversity. *Prog Biophys Mol Biol.* 73:195-262.
- Brattstrom, C., J. Sawe, B. Jansson, A. Lonnebo, J. Nordin, J.J. Zimmerman, J.T. Burke, and C.G. Groth. 2000. Pharmacokinetics and safety of single oral doses of sirolimus (rapamycin) in healthy male volunteers. *Ther Drug Monit.* 22:537-544.
- Broos, K., H.B. Feys, S.F. De Meyer, K. Vanhoorelbeke, and H. Deckmyn. 2011. Platelets at work in primary hemostasis. *Blood Rev.* 25:155-167.
- Buraei, Z., and J. Yang. 2013. Structure and function of the beta subunit of voltage-gated Ca(2+)(+) channels. *Biochim Biophys Acta.* 1828:1530-1540.
- Burk, S.E., J. Lytton, D.H. MacLennan, and G.E. Shull. 1989. cDNA cloning, functional expression, and mRNA tissue distribution of a third organellar Ca<sup>2+</sup> pump. *J Biol Chem.* 264:18561-18568.
- Calderon, J.C., P. Bolanos, and C. Caputo. 2010. Myosin heavy chain isoform composition and Ca(2+) transients in fibres from enzymatically dissociated murine soleus and extensor digitorum longus muscles. *J Physiol.* 588:267-279.
- Calne, R.Y., D.S. Collier, S. Lim, S.G. Pollard, A. Samaan, D.J. White, and S. Thiru. 1989. Rapamycin for immunosuppression in organ allografting. *Lancet.* 2:227.
- Capacchione, J.F., N. Sambuughin, S. Bina, L.P. Mulligan, T.D. Lawson, and S.M. Muldoon. 2010. Exertional rhabdomyolysis and malignant hyperthermia in a patient with ryanodine receptor type 1 gene, L-type calcium channel alpha-1 subunit gene, and calsequestrin-1 gene polymorphisms. *Anesthesiology.* 112:239-244.
-

- 
- Cardamone, M., D. Flanagan, D. Mowat, S.E. Kennedy, M. Chopra, and J.A. Lawson. 2014. Mammalian target of rapamycin inhibitors for intractable epilepsy and subependymal giant cell astrocytomas in tuberous sclerosis complex. *J Pediatr.* 164:1195-1200.
- Cartwright, E.J., D. Oceandy, C. Austin, and L. Neyses. 2011. Ca<sup>2+</sup> signalling in cardiovascular disease: the role of the plasma membrane calcium pumps. *Sci China Life Sci.* 54:691-698.
- Cassens, R.G., and C.C. Cooper. 1971. Red and white muscle. *Adv Food Res.* 19:1-74.
- Catterall, W.A. 1991. Excitation-contraction coupling in vertebrate skeletal muscle: a tale of two calcium channels. *Cell.* 64:871-874.
- Catterall, W.A. 1995. Structure and function of voltage-gated ion channels. *Annu Rev Biochem.* 64:493-531.
- Chapin, J.C., and K.A. Hajjar. 2015. Fibrinolysis and the control of blood coagulation. *Blood Rev.* 29:17-24.
- Chelu, M.G., S.A. Goonasekera, W.J. Durham, W. Tang, J.D. Lueck, J. Riehl, I.N. Pessah, P. Zhang, M.B. Bhattacharjee, R.T. Dirksen, and S.L. Hamilton. 2006. Heat- and anesthesia-induced malignant hyperthermia in an RyR1 knock-in mouse. *FASEB J.* 20:329-330.
- Chen, J., X.F. Zheng, E.J. Brown, and S.L. Schreiber. 1995. Identification of an 11-kDa FKBP12-rapamycin-binding domain within the 289-kDa FKBP12-rapamycin-associated protein and characterization of a critical serine residue. *Proc Natl Acad Sci U S A.* 92:4947-4951.
- Cheng, H., and W.J. Lederer. 2008. Calcium sparks. *Physiol Rev.* 88:1491-1545.
- Cheng, H., W.J. Lederer, and M.B. Cannell. 1993. Calcium sparks: elementary events underlying excitation-contraction coupling in heart muscle. *Science.* 262:740-744.
- Chetty, R., S. Batitang, and R. Nair. 2000. Large artery vasculopathy in HIV-positive patients: another vasculitic enigma. *Hum Pathol.* 31:374-379.
- Clapp, L.H., M.B. Vivaudou, J.V. Walsh, and J.J. Singer. 1987. ACETYLCHOLINE INCREASES VOLTAGE-ACTIVATED CA-2+ CURRENT IN FRESHLY DISSOCIATED SMOOTH-MUSCLE CELLS. *Proceedings of the National Academy of Sciences of the United States of America.* 84:2092-2096.
- Clarke, N.F., L.B. Waddell, S.T. Cooper, M. Perry, R.L. Smith, A.J. Kornberg, F. Muntoni, S. Lillis, V. Straub, K. Bushby, M. Guglieri, M.D. King, M.A. Farrell, I. Marty, J. Lunardi, N. Monnier, and K.N. North. 2010. Recessive mutations in RYR1 are a common cause of congenital fiber type disproportion. *Hum Mutat.* 31:E1544-1550.
-

- 
- Collier, M.L., A.P. Thomas, and J.R. Berlin. 1999. Relationship between L-type Ca<sup>2+</sup> current and unitary sarcoplasmic reticulum Ca<sup>2+</sup> release events in rat ventricular myocytes. *J Physiol.* 516 ( Pt 1):117-128.
- Colman, R.W. 2006. Hemostasis and thrombosis : basic principles and clinical practice. Lippincott Williams & Wilkins, Philadelphia, PA. xxiv, 1827 p. pp.
- Cornu, M., V. Albert, and M.N. Hall. 2013. mTOR in aging, metabolism, and cancer. *Curr Opin Genet Dev.* 23:53-62.
- Costello, B., C. Chadwick, A. Saito, A. Chu, A. Maurer, and S. Fleischer. 1986. Characterization of the junctional face membrane from terminal cisternae of sarcoplasmic reticulum. *J Cell Biol.* 103:741-753.
- Csernoch, L., J. Zhou, M.D. Stern, G. Brum, and E. Rios. 2004. The elementary events of Ca<sup>2+</sup> release elicited by membrane depolarization in mammalian muscle. *J Physiol.* 557:43-58.
- Cunningham, J.T., J.T. Rodgers, D.H. Arlow, F. Vazquez, V.K. Mootha, and P. Puigserver. 2007. mTOR controls mitochondrial oxidative function through a YY1-PGC-1alpha transcriptional complex. *Nature.* 450:736-740.
- Curtis, B.M., and W.A. Catterall. 1984. Purification of the calcium antagonist receptor of the voltage-sensitive calcium channel from skeletal muscle transverse tubules. *Biochemistry.* 23:2113-2118.
- Czarnecki, R.B.M.C.P.J. 2008. Hemostasis and Hemorrhagic Disorders. Fermentation-Biotech GmbH.
- Damiani, E., R. Betto, S. Salvatori, P. Volpe, G. Salviati, and A. Margreth. 1981. Polymorphism of sarcoplasmic-reticulum adenosine triphosphatase of rabbit skeletal muscle. *Biochem J.* 197:245-248.
- Damiani, E., and A. Margreth. 1994. Characterization study of the ryanodine receptor and of calsequestrin isoforms of mammalian skeletal muscles in relation to fibre types. *J Muscle Res Cell Motil.* 15:86-101.
- Damiani, E., C. Spamer, C. Heilmann, S. Salvatori, and A. Margreth. 1988. Endoplasmic reticulum of rat liver contains two proteins closely related to skeletal sarcoplasmic reticulum Ca-ATPase and calsequestrin. *J Biol Chem.* 263:340-343.
- Damiani, E., P. Volpe, and A. Margreth. 1990. Coexpression of two isoforms of calsequestrin in rabbit slow-twitch muscle. *J Muscle Res Cell Motil.* 11:522-530.
- de Maat, S., P.G. de Groot, and C. Maas. 2014. Contact system activation on endothelial cells. *Semin Thromb Hemost.* 40:887-894.
-

- 
- DeFoor, P.H., D. Levitsky, T. Biryukova, and S. Fleischer. 1980. Immunological dissimilarity of the calcium pump protein of skeletal and cardiac muscle sarcoplasmic reticulum. *Arch Biochem Biophys.* 200:196-205.
- Del Castillo, J., and B. Katz. 1954. Action, and spontaneous release, of acetylcholine at an inexcitable nerve-muscle junction. *J Physiol.* 126:27P.
- Delbono, O., K.S. O'Rourke, and W.H. Ettinger. 1995. Excitation-calcium release uncoupling in aged single human skeletal muscle fibers. *J Membr Biol.* 148:211-222.
- Delbono, O., J. Xia, S. Treves, Z.M. Wang, R. Jimenez-Moreno, A.M. Payne, M.L. Messi, A. Briguet, F. Schaerer, M. Nishi, H. Takeshima, and F. Zorzato. 2007. Loss of skeletal muscle strength by ablation of the sarcoplasmic reticulum protein JP45. *Proc Natl Acad Sci U S A.* 104:20108-20113.
- Demuro, A., and I. Parker. 2008. Multi-dimensional resolution of elementary Ca<sup>2+</sup> signals by simultaneous multi-focal imaging. *Cell Calcium.* 43:367-374.
- Denborough, M. 1998. Malignant hyperthermia. *Lancet.* 352:1131-1136.
- Dibble, C.C., and B.D. Manning. 2013. Signal integration by mTORC1 coordinates nutrient input with biosynthetic output. *Nat Cell Biol.* 15:555-564.
- Dietze, B., J. Henke, H.M. Eichinger, F. Lehmann-Horn, and W. Melzer. 2000. Malignant hyperthermia mutation Arg615Cys in the porcine ryanodine receptor alters voltage dependence of Ca<sup>2+</sup> release. *J Physiol.* 526 Pt 3:507-514.
- Dittus, C., M. Streiff, and J. Ansell. 2015. Bleeding and clotting in hereditary hemorrhagic telangiectasia. *World J Clin Cases.* 3:330-337.
- Dolphin, A.C. 2012. Calcium channel auxiliary alpha2delta and beta subunits: trafficking and one step beyond. *Nat Rev Neurosci.* 13:542-555.
- Duvel, K., J.L. Yecies, S. Menon, P. Raman, A.I. Lipovsky, A.L. Souza, E. Triantafellow, Q. Ma, R. Gorski, S. Cleaver, M.G. Vander Heiden, J.P. MacKeigan, P.M. Finan, C.B. Clish, L.O. Murphy, and B.D. Manning. 2010. Activation of a metabolic gene regulatory network downstream of mTOR complex 1. *Mol Cell.* 39:171-183.
- Ebashi, S. 1972. Calcium ions and muscle contraction. *Nature.* 240:217-218.
- Ehninger, D., F. Neff, and K. Xie. 2014. Longevity, aging and rapamycin. *Cell Mol Life Sci.* 71:4325-4346.
- European Malignant Hyperthermia, G. 2016. Mutations in RyR1.
- Fabiato, A. 1983. Calcium-induced release of calcium from the cardiac sarcoplasmic reticulum. *Am J Physiol.* 245:C1-14.
-

- 
- Fatt, P., and B. Katz. 1951. An analysis of the end-plate potential recorded with an intracellular electrode. *J Physiol.* 115:320-370.
- Ferreiro, A., N. Monnier, N.B. Romero, J.P. Leroy, C. Bonnemann, C.A. Haenggeli, V. Straub, W.D. Voss, Y. Nivoche, H. Jungbluth, A. Lemainque, T. Voit, J. Lunardi, M. Fardeau, and P. Guicheney. 2002. A recessive form of central core disease, transiently presenting as multi-minicore disease, is associated with a homozygous mutation in the ryanodine receptor type 1 gene. *Ann Neurol.* 51:750-759.
- Fliegel, L., E. Newton, K. Burns, and M. Michalak. 1990. Molecular cloning of cDNA encoding a 55-kDa multifunctional thyroid hormone binding protein of skeletal muscle sarcoplasmic reticulum. *J Biol Chem.* 265:15496-15502.
- Floyd, R., and S. Wray. 2007. Calcium transporters and signalling in smooth muscles. *Cell Calcium.* 42:467-476.
- Fok, W.C., Y. Chen, A. Bokov, Y. Zhang, A.B. Salmon, V. Diaz, M. Javors, W.H. Wood, 3rd, Y. Zhang, K.G. Becker, V.I. Perez, and A. Richardson. 2014. Mice fed rapamycin have an increase in lifespan associated with major changes in the liver transcriptome. *PLoS One.* 9:e83988.
- Fosset, M., E. Jaimovich, E. Delpont, and M. Lazdunski. 1983. [3H]nitrendipine receptors in skeletal muscle. *J Biol Chem.* 258:6086-6092.
- Franzini-Armstrong, C. 1980. Structure of sarcoplasmic reticulum. *Fed Proc.* 39:2403-2409.
- Franzini-Armstrong, C., L.J. Kenney, and E. Varriano-Marston. 1987. The structure of calsequestrin in triads of vertebrate skeletal muscle: a deep-etch study. *J Cell Biol.* 105:49-56.
- Franzini-Armstrong, C., M. Pincon-Raymond, and F. Rieger. 1991. Muscle fibers from dysgenic mouse in vivo lack a surface component of peripheral couplings. *Dev Biol.* 146:364-376.
- Fritz, N., J.L. Morel, L.H. Jeyakumar, S. Fleischer, P.D. Allen, J. Mironneau, and N. Macrez. 2007. RyR1-specific requirement for depolarization-induced Ca<sup>2+</sup> sparks in urinary bladder smooth muscle. *J Cell Sci.* 120:3784-3791.
- Fritzsche, T., M. Schnolzer, S. Fiedler, M. Weigand, M. Wiessler, and E. Frei. 2004. Isolation and identification of heterogeneous nuclear ribonucleoproteins (hnRNP) from purified plasma membranes of human tumour cell lines as albumin-binding proteins. *Biochem Pharmacol.* 67:655-665.
- Gallant, E.M., and L.R. Lentz. 1992. Excitation-contraction coupling in pigs heterozygous for malignant hyperthermia. *Am J Physiol.* 262:C422-426.
-

- 
- Gangloff, Y.G., M. Mueller, S.G. Dann, P. Svoboda, M. Sticker, J.F. Spetz, S.H. Um, E.J. Brown, S. Cereghini, G. Thomas, and S.C. Kozma. 2004. Disruption of the mouse mTOR gene leads to early postimplantation lethality and prohibits embryonic stem cell development. *Mol Cell Biol.* 24:9508-9516.
- Ganitkevich, V., and G. Isenberg. 1990. Isolated guinea pig coronary smooth muscle cells. Acetylcholine induces hyperpolarization due to sarcoplasmic reticulum calcium release activating potassium channels. *Circ Res.* 67:525-528.
- Giannini, G., A. Conti, S. Mammarella, M. Scrobogna, and V. Sorrentino. 1995. The ryanodine receptor/calcium channel genes are widely and differentially expressed in murine brain and peripheral tissues. *J Cell Biol.* 128:893-904.
- Gillies, R.L., A.R. Bjorksten, D. Du Sart, and B.M. Hockey. 2015. Analysis of the entire ryanodine receptor type 1 and alpha 1 subunit of the dihydropyridine receptor (CACNA1S) coding regions for variants associated with malignant hyperthermia in Australian families. *Anaesth Intensive Care.* 43:157-166.
- Glossmann, H., D.R. Ferry, A. Goll, and M. Rombusch. 1984. Molecular pharmacology of the calcium channel: evidence for subtypes, multiple drug-receptor sites, channel subunits, and the development of a radioiodinated 1,4-dihydropyridine calcium channel label, [125I]iodipine. *J Cardiovasc Pharmacol.* 6 Suppl 4:S608-621.
- Gollasch, M., and M.T. Nelson. 1997. Voltage-dependent Ca<sup>2+</sup> channels in arterial smooth muscle cells. *Kidney Blood Press Res.* 20:355-371.
- Gonsalves, S.G., D. Ng, J.J. Johnston, J.K. Teer, P.D. Stenson, D.N. Cooper, J.C. Mullikin, L.G. Biesecker, and N.C.S. Program. 2013. Using exome data to identify malignant hyperthermia susceptibility mutations. *Anesthesiology.* 119:1043-1053.
- Gonzalez-Serratos, H., D.W. Hilgemann, M. Rozycka, A. Gauthier, and H. Rasgado-Flores. 1996. Na-Ca exchange studies in sarcolemmal skeletal muscle. *Ann N Y Acad Sci.* 779:556-560.
- Grabner, M., R.T. Dirksen, N. Suda, and K.G. Beam. 1999. The II-III loop of the skeletal muscle dihydropyridine receptor is responsible for the Bi-directional coupling with the ryanodine receptor. *J Biol Chem.* 274:21913-21919.
- Gregg, R.G., A. Messing, C. Strube, M. Beurg, R. Moss, M. Behan, M. Sukhareva, S. Haynes, J.A. Powell, R. Coronado, and P.A. Powers. 1996. Absence of the beta subunit (cchb1) of the skeletal muscle dihydropyridine receptor alters expression of the alpha 1 subunit and eliminates excitation-contraction coupling. *Proc Natl Acad Sci U S A.* 93:13961-13966.
-

- 
- Guertin, D.A., D.M. Stevens, C.C. Thoreen, A.A. Burds, N.Y. Kalaany, J. Moffat, M. Brown, K.J. Fitzgerald, and D.M. Sabatini. 2006. Ablation in mice of the mTORC components raptor, rictor, or mLST8 reveals that mTORC2 is required for signaling to Akt-FOXO and PKC $\alpha$ , but not S6K1. *Dev Cell*. 11:859-871.
- Gunteski-Hamblin, A.M., J. Greeb, and G.E. Shull. 1988. A novel Ca<sup>2+</sup> pump expressed in brain, kidney, and stomach is encoded by an alternative transcript of the slow-twitch muscle sarcoplasmic reticulum Ca-ATPase gene. Identification of cDNAs encoding Ca<sup>2+</sup> and other cation-transporting ATPases using an oligonucleotide probe derived from the ATP-binding site. *J Biol Chem*. 263:15032-15040.
- Gusev, N.B. 2001. Some properties of caldesmon and calponin and the participation of these proteins in regulation of smooth muscle contraction and cytoskeleton formation. *Biochemistry (Mosc)*. 66:1112-1121.
- Halevy, O., and O. Lerman. 1993. Retinoic acid induces adult muscle cell differentiation mediated by the retinoic acid receptor- $\alpha$ . *J Cell Physiol*. 154:566-572.
- Hall, M.N. 2008. mTOR-what does it do? *Transplant Proc*. 40:S5-8.
- Harrison, D.E., R. Strong, Z.D. Sharp, J.F. Nelson, C.M. Astle, K. Flurkey, N.L. Nadon, J.E. Wilkinson, K. Frenkel, C.S. Carter, M. Pahor, M.A. Javors, E. Fernandez, and R.A. Miller. 2009. Rapamycin fed late in life extends lifespan in genetically heterogeneous mice. *Nature*. 460:392-395.
- Hasselbach, W. 1980. Quantitative aspects of the calcium concept of excitation contraction coupling--a critical evaluation. *Basic Res Cardiol*. 75:2-12.
- Hayashi, T. 1952. Contractile properties of compressed monolayers of actomyosin. *J Gen Physiol*. 36:139-152.
- He, Z., A.K. Dunker, C.R. Wesson, and W.R. Trumble. 1993. Ca<sup>2+</sup>-induced folding and aggregation of skeletal muscle sarcoplasmic reticulum calsequestrin. The involvement of the trifluoperazine-binding site. *J Biol Chem*. 268:24635-24641.
- Heitman, J., N.R. Movva, and M.N. Hall. 1991. Targets for cell cycle arrest by the immunosuppressant rapamycin in yeast. *Science*. 253:905-909.
- Hill, J. 2012. Muscle: fundamental biology and mechanisms of disease. Academic Press, S.I. 1 online resource. pp.
- Hill, R.W., G.A. Wyse, and M. Anderson. 2012. Animal physiology. Sinauer, Sunderland, Mass. 800 p. pp.
-

- 
- Hirano, K., M. Hirano, and H. Kanaide. 2004. Regulation of myosin phosphorylation and myofilament Ca<sup>2+</sup> sensitivity in vascular smooth muscle. *J Smooth Muscle Res.* 40:219-236.
- Hopkins, P.M., F.R. Ellis, and P.J. Halsall. 1991. Evidence for related myopathies in exertional heat stroke and malignant hyperthermia. *Lancet.* 338:1491-1492.
- Hopkins, P.M., H. Ruffert, M.M. Snoeck, T. Girard, K.P. Glahn, F.R. Ellis, C.R. Muller, A. Urwyler, and G. European Malignant Hyperthermia. 2015. European Malignant Hyperthermia Group guidelines for investigation of malignant hyperthermia susceptibility. *Br J Anaesth.* 115:531-539.
- Huxley, H.E. 1957. The double array of filaments in cross-striated muscle. *J Biophys Biochem Cytol.* 3:631-648.
- Huxley, H.E. 1969. The mechanism of muscular contraction. *Science.* 164:1356-1365.
- Hwang, J.H., F. Zorzato, N.F. Clarke, and S. Treves. 2012. Mapping domains and mutations on the skeletal muscle ryanodine receptor channel. *Trends Mol Med.* 18:644-657.
- Iadevaia, V., Y. Huo, Z. Zhang, L.J. Foster, and C.G. Proud. 2012. Roles of the mammalian target of rapamycin, mTOR, in controlling ribosome biogenesis and protein synthesis. *Biochem Soc Trans.* 40:168-172.
- Ikemoto, N., M. Ronjat, L.G. Meszaros, and M. Koshita. 1989. Postulated role of calsequestrin in the regulation of calcium release from sarcoplasmic reticulum. *Biochemistry.* 28:6764-6771.
- Ikura, M. 1996. Calcium binding and conformational response in EF-hand proteins. *Trends Biochem Sci.* 21:14-17.
- Inesi, G. 1985. Mechanism of calcium transport. *Annu Rev Physiol.* 47:573-601.
- Inoki, K., J. Kim, and K.L. Guan. 2012. AMPK and mTOR in cellular energy homeostasis and drug targets. *Annu Rev Pharmacol Toxicol.* 52:381-400.
- Inoue, M., and J.H. Bridge. 2003. Ca<sup>2+</sup> sparks in rabbit ventricular myocytes evoked by action potentials: involvement of clusters of L-type Ca<sup>2+</sup> channels. *Circ Res.* 92:532-538.
- Jacinto, E., R. Loewith, A. Schmidt, S. Lin, M.A. Ruegg, A. Hall, and M.N. Hall. 2004. Mammalian TOR complex 2 controls the actin cytoskeleton and is rapamycin insensitive. *Nat Cell Biol.* 6:1122-1128.
- Jaggar, J.H., G.C. Wellman, T.J. Heppner, V.A. Porter, G.J. Perez, M. Gollasch, T. Kleppisch, M. Rubart, A.S. Stevenson, W.J. Lederer, H.J. Knot, A.D. Bonev, and M.T. Nelson. 1998. Ca<sup>2+</sup> channels, ryanodine receptors and Ca(2+)-activated K<sup>+</sup>
-



- 
- channels: a functional unit for regulating arterial tone. *Acta Physiol Scand.* 164:577-587.
- Jiang, Y.H., M.G. Klein, and M.F. Schneider. 1999. Numerical simulation of Ca<sup>2+</sup> "sparks" in skeletal muscle. *Biophys J.* 77:2333-2357.
- Jiao, Q., H. Takeshima, Y. Ishikawa, and S. Minamisawa. 2012. Sarcalumenin plays a critical role in age-related cardiac dysfunction due to decreases in SERCA2a expression and activity. *Cell Calcium.* 51:31-39.
- Johnson, S.C., G.M. Martin, P.S. Rabinovitch, and M. Kaerberlein. 2013. Preserving youth: does rapamycin deliver? *Sci Transl Med.* 5:211fs240.
- Jorgensen, A.O., W. Arnold, D.R. Pepper, S.D. Kahl, F. Mandel, and K.P. Campbell. 1988. A monoclonal antibody to the Ca<sup>2+</sup>-ATPase of cardiac sarcoplasmic reticulum cross-reacts with slow type I but not with fast type II canine skeletal muscle fibers: an immunocytochemical and immunochemical study. *Cell Motil Cytoskeleton.* 9:164-174.
- Jorgensen, A.O., and L.R. Jones. 1986. Localization of phospholamban in slow but not fast canine skeletal muscle fibers. An immunocytochemical and biochemical study. *J Biol Chem.* 261:3775-3781.
- Jurkat-Rott, K., T. McCarthy, and F. Lehmann-Horn. 2000. Genetics and pathogenesis of malignant hyperthermia. *Muscle Nerve.* 23:4-17.
- Kahan, B.D., J. Podbielski, K.L. Napoli, S.M. Katz, H.U. Meier-Kriesche, and C.T. Van Buren. 1998. Immunosuppressive effects and safety of a sirolimus/cyclosporine combination regimen for renal transplantation. *Transplantation.* 66:1040-1046.
- Kang, S.A., M.E. Pacold, C.L. Cervantes, D. Lim, H.J. Lou, K. Ottina, N.S. Gray, B.E. Turk, M.B. Yaffe, and D.M. Sabatini. 2013. mTORC1 phosphorylation sites encode their sensitivity to starvation and rapamycin. *Science.* 341:1236566.
- Kawamoto, R.M., J.P. Brunschwig, K.C. Kim, and A.H. Caswell. 1986. Isolation, characterization, and localization of the spanning protein from skeletal muscle triads. *J Cell Biol.* 103:1405-1414.
- Khurana, T.S., and K.E. Davies. 2003. Pharmacological strategies for muscular dystrophy. *Nat Rev Drug Discov.* 2:379-390.
- Kirsch, W.G., D. Uttenweiler, and R.H. Fink. 2001. Spark- and ember-like elementary Ca<sup>2+</sup> release events in skinned fibres of adult mammalian skeletal muscle. *J Physiol.* 537:379-389.
-

- 
- Knudson, C.M., and K.P. Campbell. 1989. Albumin is a major protein component of transverse tubule vesicles isolated from skeletal muscle. *J Biol Chem.* 264:10795-10798.
- Kolb, M.E., M.L. Horne, and R. Martz. 1982. Dantrolene in human malignant hyperthermia. *Anesthesiology.* 56:254-262.
- Koltin, Y., L. Faucette, D.J. Bergsma, M.A. Levy, R. Cafferkey, P.L. Koser, R.K. Johnson, and G.P. Livi. 1991. Rapamycin sensitivity in *Saccharomyces cerevisiae* is mediated by a peptidyl-prolyl cis-trans isomerase related to human FK506-binding protein. *Mol Cell Biol.* 11:1718-1723.
- Krause, T., M.U. Gerbershagen, M. Fiege, R. Weisshorn, and F. Wappler. 2004. Dantrolene-- a review of its pharmacology, therapeutic use and new developments. *Anaesthesia.* 59:364-373.
- Kugler, G., R.G. Weiss, B.E. Flucher, and M. Grabner. 2004. Structural requirements of the dihydropyridine receptor alpha1S II-III loop for skeletal-type excitation-contraction coupling. *J Biol Chem.* 279:4721-4728.
- Lacampagne, A., M.G. Klein, C.W. Ward, and M.F. Schneider. 2000. Two mechanisms for termination of individual Ca<sup>2+</sup> sparks in skeletal muscle. *Proc Natl Acad Sci U S A.* 97:7823-7828.
- Lamming, D.W., and D.M. Sabatini. 2013. A Central role for mTOR in lipid homeostasis. *Cell Metab.* 18:465-469.
- Lanner, J.T. 2012. Ryanodine receptor physiology and its role in disease. *Adv Exp Med Biol.* 740:217-234.
- Lanner, J.T., D.K. Georgiou, A.D. Joshi, and S.L. Hamilton. 2010. Ryanodine receptors: structure, expression, molecular details, and function in calcium release. *Cold Spring Harb Perspect Biol.* 2:a003996.
- Laplante, M., and D.M. Sabatini. 2009. An emerging role of mTOR in lipid biosynthesis. *Curr Biol.* 19:R1046-1052.
- Laplante, M., and D.M. Sabatini. 2012. mTOR signaling in growth control and disease. *Cell.* 149:274-293.
- Large, W.A. 2002. Receptor-operated Ca<sup>2+</sup>(+)-permeable nonselective cation channels in vascular smooth muscle: a physiologic perspective. *J Cardiovasc Electrophysiol.* 13:493-501.
-

- 
- Launikonis, B.S., J.S. Zhou, L. Royer, T.R. Shannon, G. Brum, and E. Rios. 2006. Depletion "skraps" and dynamic buffering inside the cellular calcium store. *Proceedings of the National Academy of Sciences of the United States of America*. 103:2982-2987.
- Laver, D.R., G.K. Lenz, and G.D. Lamb. 2001. Regulation of the calcium release channel from rabbit skeletal muscle by the nucleotides ATP, AMP, IMP and adenosine. *J Physiol*. 537:763-778.
- Lawrence, J.C., Jr. 2001. mTOR-dependent control of skeletal muscle protein synthesis. *Int J Sport Nutr Exerc Metab*. 11 Suppl:S177-185.
- Le Rumeur, E. 2015. Dystrophin and the two related genetic diseases, Duchenne and Becker muscular dystrophies. *Bosn J Basic Med Sci*. 15:14-20.
- Leberer, E., B.G. Timms, K.P. Campbell, and D.H. MacLennan. 1990. Purification, calcium binding properties, and ultrastructural localization of the 53,000- and 160,000 (sarcalumenin)-dalton glycoproteins of the sarcoplasmic reticulum. *J Biol Chem*. 265:10118-10124.
- Ledbetter, M.W., J.K. Preiner, C.F. Louis, and J.R. Mickelson. 1994. Tissue distribution of ryanodine receptor isoforms and alleles determined by reverse transcription polymerase chain reaction. *J Biol Chem*. 269:31544-31551.
- Leger, B., R. Cartoni, M. Praz, S. Lamon, O. Deriaz, A. Crettenand, C. Gobelet, P. Rohmer, M. Konzelmann, F. Luthi, and A.P. Russell. 2006. Akt signalling through GSK-3beta, mTOR and Foxo1 is involved in human skeletal muscle hypertrophy and atrophy. *J Physiol*. 576:923-933.
- Liden, M., and U. Eriksson. 2006. Understanding retinol metabolism: structure and function of retinol dehydrogenases. *J Biol Chem*. 281:13001-13004.
- Lorber, M.I., S. Mulgaonkar, K.M. Butt, E. Elkhammas, R. Mendez, P.R. Rajagopalan, B. Kahan, H. Sollinger, Y. Li, N. Cretin, H. Tedesco, and B.S. Group. 2005. Everolimus versus mycophenolate mofetil in the prevention of rejection in de novo renal transplant recipients: a 3-year randomized, multicenter, phase III study. *Transplantation*. 80:244-252.
- Loscalzo, J. 1995. Endothelial injury, vasoconstriction, and its prevention. *Tex Heart Inst J*. 22:180-184.
- Lu, X., L. Xu, and G. Meissner. 1994. Activation of the skeletal muscle calcium release channel by a cytoplasmic loop of the dihydropyridine receptor. *J Biol Chem*. 269:6511-6516.
-

- 
- Lukyanenko, V., and S. Gyorke. 1999. Ca<sup>2+</sup> sparks and Ca<sup>2+</sup> waves in saponin-permeabilized rat ventricular myocytes. *J Physiol.* 521 Pt 3:575-585.
- Lytton, J., A. Zarain-Herzberg, M. Periasamy, and D.H. MacLennan. 1989. Molecular cloning of the mammalian smooth muscle sarco(endo)plasmic reticulum Ca<sup>2+</sup>-ATPase. *J Biol Chem.* 264:7059-7065.
- Ma, X.M., and J. Blenis. 2009. Molecular mechanisms of mTOR-mediated translational control. *Nat Rev Mol Cell Biol.* 10:307-318.
- Mackrill, J.J., R.A. Challiss, A. O'Connell D, F.A. Lai, and S.R. Nahorski. 1997. Differential expression and regulation of ryanodine receptor and myo-inositol 1,4,5-trisphosphate receptor Ca<sup>2+</sup> release channels in mammalian tissues and cell lines. *Biochem J.* 327 ( Pt 1):251-258.
- MacLennan, D.H. 2000. Ca<sup>2+</sup> signalling and muscle disease. *Eur J Biochem.* 267:5291-5297.
- MacLennan, D.H., C. Duff, F. Zorzato, J. Fujii, M. Phillips, R.G. Korneluk, W. Frodis, B.A. Britt, and R.G. Worton. 1990. Ryanodine receptor gene is a candidate for predisposition to malignant hyperthermia. *Nature.* 343:559-561.
- MacLennan, D.H., and E.G. Kranias. 2003. Phospholamban: a crucial regulator of cardiac contractility. *Nat Rev Mol Cell Biol.* 4:566-577.
- MacLennan, D.H., and P.T. Wong. 1971. Isolation of a calcium-sequestering protein from sarcoplasmic reticulum. *Proc Natl Acad Sci U S A.* 68:1231-1235.
- Malfait, F., and A. De Paepe. 2014. The Ehlers-Danlos syndrome. *Adv Exp Med Biol.* 802:129-143.
- Manring, H., E. Abreu, L. Brotto, N. Weisleder, and M. Brotto. 2014. Novel excitation-contraction coupling related genes reveal aspects of muscle weakness beyond atrophy-new hopes for treatment of musculoskeletal diseases. *Front Physiol.* 5:37.
- Margreth, A., E. Damiani, and E. Bortoloso. 1999. Sarcoplasmic reticulum in aged skeletal muscle. *Acta Physiol Scand.* 167:331-338.
- Marx, S.O., K. Ondrias, and A.R. Marks. 1998. Coupled gating between individual skeletal muscle Ca<sup>2+</sup> release channels (ryanodine receptors). *Science.* 281:818-821.
- Mascioni, A., C. Karim, G. Barany, D.D. Thomas, and G. Veglia. 2002. Structure and orientation of sarcolipin in lipid environments. *Biochemistry.* 41:475-482.
- McCarron, J.G., M.L. Olson, C. Wilson, M.E. Sandison, and S. Chalmers. 2013. Examining the Role of Mitochondria in Ca<sup>2+</sup> Signaling in Native Vascular Smooth Muscle. *Microcirculation.* 20:317-329.
-

- 
- McCarthy, T.V., J.M. Healy, J.J. Heffron, M. Lehane, T. Deufel, F. Lehmann-Horn, M. Farrall, and K. Johnson. 1990. Localization of the malignant hyperthermia susceptibility locus to human chromosome 19q12-13.2. *Nature*. 343:562-564.
- Meissner, G. 1975. Isolation and characterization of two types of sarcoplasmic reticulum vesicles. *Biochim Biophys Acta*. 389:51-68.
- Meissner, G., E. Darling, and J. Eveleth. 1986. Kinetics of rapid Ca<sup>2+</sup> release by sarcoplasmic reticulum. Effects of Ca<sup>2+</sup>, Mg<sup>2+</sup>, and adenine nucleotides. *Biochemistry*. 25:236-244.
- Meissner, G., E. Rios, A. Tripathy, and D.A. Pasek. 1997. Regulation of skeletal muscle Ca<sup>2+</sup> release channel (ryanodine receptor) by Ca<sup>2+</sup> and monovalent cations and anions. *J Biol Chem*. 272:1628-1638.
- Merlot, A.M., D.S. Kalinowski, and D.R. Richardson. 2014. Unraveling the mysteries of serum albumin-more than just a serum protein. *Front Physiol*. 5:299.
- Michalak, M., E.F. Corbett, N. Mesaeli, K. Nakamura, and M. Opas. 1999. Calreticulin: one protein, one gene, many functions. *Biochem J*. 344 Pt 2:281-292.
- Mosca, B., O. Delbono, M. Laura Messi, L. Bergamelli, Z.M. Wang, M. Vukcevic, R. Lopez, S. Treves, M. Nishi, H. Takeshima, C. Paolini, M. Martini, G. Rispoli, F. Protasi, and F. Zorzato. 2013. Enhanced dihydropyridine receptor calcium channel activity restores muscle strength in JP45/CASQ1 double knockout mice. *Nat Commun*. 4:1541.
- Muller, G., and C.W. Heizmann. 1982. Albumin in chicken skeletal muscle. *Eur J Biochem*. 123:577-582.
- Mumford, A.D., J. O'Donnell, J.D. Gillmore, R.A. Manning, P.N. Hawkins, and M. Laffan. 2000. Bleeding symptoms and coagulation abnormalities in 337 patients with AL-amyloidosis. *Br J Haematol*. 110:454-460.
- Murakami, M., T. Ichisaka, M. Maeda, N. Oshiro, K. Hara, F. Edenhofer, H. Kiyama, K. Yonezawa, and S. Yamanaka. 2004. mTOR is essential for growth and proliferation in early mouse embryos and embryonic stem cells. *Mol Cell Biol*. 24:6710-6718.
- Muscat, G.E., L. Mynett-Johnson, D. Dowhan, M. Downes, and R. Griggs. 1994. Activation of myoD gene transcription by 3,5,3'-triiodo-L-thyronine: a direct role for the thyroid hormone and retinoid X receptors. *Nucleic Acids Res*. 22:583-591.
- Nakamura, K., A. Zuppini, S. Arnaudeau, J. Lynch, I. Ahsan, R. Krause, S. Papp, H. De Smedt, J.B. Parys, W. Muller-Esterl, D.P. Lew, K.H. Krause, N. Demaurex, M. Opas,
-

- 
- and M. Michalak. 2001. Functional specialization of calreticulin domains. *J Cell Biol.* 154:961-972.
- Nakayama, K., and Y. Tanaka. 1994. Stretch-induced contraction and Ca<sup>2+</sup> mobilization in vascular smooth muscle. *Biological Signals.* 2:241-252.
- Napoli, J.L. 1996. Biochemical pathways of retinoid transport, metabolism, and signal transduction. *Clin Immunol Immunopathol.* 80:S52-62.
- Nazer, M.A., and C. van Breemen. 1998. Functional linkage of Na<sup>(+)</sup>-Ca<sup>2+</sup> exchange and sarcoplasmic reticulum Ca<sup>2+</sup> release mediates Ca<sup>2+</sup> cycling in vascular smooth muscle. *Cell Calcium.* 24:275-283.
- Nelson, D.A., and E.S. Benson. 1963. On the structural continuities of the transverse tubular system of rabbit and human myocardial cells. *J Cell Biol.* 16:297-313.
- Nelson, M.T., H. Cheng, M. Rubart, L.F. Santana, A.D. Bonev, H.J. Knot, and W.J. Lederer. 1995. Relaxation of arterial smooth muscle by calcium sparks. *Science.* 270:633-637.
- Neuhuber, B., U. Gerster, F. Doring, H. Glossmann, T. Tanabe, and B.E. Flucher. 1998. Association of calcium channel alpha1S and beta1a subunits is required for the targeting of beta1a but not of alpha1S into skeletal muscle triads. *Proc Natl Acad Sci U S A.* 95:5015-5020.
- Neylon, C.B., S.M. Richards, M.A. Larsen, A. Agrotis, and A. Bobik. 1995. Multiple types of ryanodine receptor/Ca<sup>2+</sup> release channels are expressed in vascular smooth muscle. *Biochem Biophys Res Commun.* 215:814-821.
- Niggli, E., and N. Shirokova. 2007. A guide to sparkology: the taxonomy of elementary cellular Ca<sup>2+</sup> signaling events. *Cell Calcium.* 42:379-387.
- Novak, P., and T. Soukup. 2011. Calsequestrin distribution, structure and function, its role in normal and pathological situations and the effect of thyroid hormones. *Physiol Res.* 60:439-452.
- Obermair, G.J., P. Tuluc, and B.E. Flucher. 2008. Auxiliary Ca(2+) channel subunits: lessons learned from muscle. *Curr Opin Pharmacol.* 8:311-318.
- Odermatt, A., S. Becker, V.K. Khanna, K. Kurzydowski, E. Leisner, D. Pette, and D.H. MacLennan. 1998. Sarcolipin regulates the activity of SERCA1, the fast-twitch skeletal muscle sarcoplasmic reticulum Ca<sup>2+</sup>-ATPase. *J Biol Chem.* 273:12360-12369.
- Ohanna, M., A.K. Sobering, T. Lapointe, L. Lorenzo, C. Praud, E. Petroulakis, N. Sonenberg, P.A. Kelly, A. Sotiropoulos, and M. Pende. 2005. Atrophy of S6K1(-/-) skeletal
-

- 
- muscle cells reveals distinct mTOR effectors for cell cycle and size control. *Nat Cell Biol.* 7:286-294.
- Olesen, C., M. Picard, A.M. Winther, C. Gyruup, J.P. Morth, C. Oxvig, J.V. Moller, and P. Nissen. 2007. The structural basis of calcium transport by the calcium pump. *Nature.* 450:1036-1042.
- Owen, V.J., N.L. Taske, and G.D. Lamb. 1997. Reduced Mg<sup>2+</sup> inhibition of Ca<sup>2+</sup> release in muscle fibers of pigs susceptible to malignant hyperthermia. *Am J Physiol.* 272:C203-211.
- Paul-Pletzer, K., T. Yamamoto, M.B. Bhat, J. Ma, N. Ikemoto, L.S. Jimenez, H. Morimoto, P.G. Williams, and J. Parness. 2002. Identification of a dantrolene-binding sequence on the skeletal muscle ryanodine receptor. *J Biol Chem.* 277:34918-34923.
- Perez, G.J., A.D. Bonev, J.B. Patlak, and M.T. Nelson. 1999. Functional coupling of ryanodine receptors to KCa channels in smooth muscle cells from rat cerebral arteries. *J Gen Physiol.* 113:229-238.
- Periasamy, M., and A. Kalyanasundaram. 2007. SERCA pump isoforms: their role in calcium transport and disease. *Muscle Nerve.* 35:430-442.
- Picht, E., A.V. Zima, L.A. Blatter, and D.M. Bers. 2007. SparkMaster: automated calcium spark analysis with ImageJ. *Am J Physiol Cell Physiol.* 293:C1073-1081.
- Podolsky, R.J. 1961. The myocardium-its biochemistry and biophysics. II. Biochemistry. Muscle physiology and contraction theories. *Circulation.* 24:399-409.
- Porter, K.R., and G.E. Palade. 1957. Studies on the endoplasmic reticulum. III. Its form and distribution in striated muscle cells. *J Biophys Biochem Cytol.* 3:269-300.
- Prins, D., and M. Michalak. 2011. Organellar calcium buffers. *Cold Spring Harb Perspect Biol.* 3.
- Proenza, C., J. O'Brien, J. Nakai, S. Mukherjee, P.D. Allen, and K.G. Beam. 2002. Identification of a region of RyR1 that participates in allosteric coupling with the alpha(1S) (Ca(V)1.1) II-III loop. *J Biol Chem.* 277:6530-6535.
- Pulido-Perez, A., J.A. Aviles-Izquierdo, and R. Suarez-Fernandez. 2012. [Cutaneous vasculitis]. *Actas Dermosifiliogr.* 103:179-191.
- Qin, J., G. Valle, A. Nani, H. Chen, J. Ramos-Franco, A. Nori, P. Volpe, and M. Fill. 2009. Ryanodine receptor luminal Ca<sup>2+</sup> regulation: swapping calsequestrin and channel isoforms. *Biophys J.* 97:1961-1970.
- Quiroga, T., and D. Mezzano. 2012. Is my patient a bleeder? A diagnostic framework for mild bleeding disorders. *Hematology Am Soc Hematol Educ Program.* 2012:466-474.
-

- 
- Reho, J.J., X. Zheng, and S.A. Fisher. 2014. Smooth muscle contractile diversity in the control of regional circulations. *Am J Physiol Heart Circ Physiol.* 306:H163-172.
- Rembold, C.M. 1992. Regulation of contraction and relaxation in arterial smooth muscle. *Hypertension.* 20:129-137.
- Renganathan, M., M.L. Messi, and O. Delbono. 1997. Dihydropyridine receptor-ryanodine receptor uncoupling in aged skeletal muscle. *J Membr Biol.* 157:247-253.
- Ribeiro, C.B., D.C. Christofolletti, V.A. Pezolato, R. de Cassia Marqueti Durigan, J. Prestes, R.A. Tibana, E.C. Pereira, I.V. de Sousa Neto, J.L. Durigan, and C.A. da Silva. 2015. Leucine minimizes denervation-induced skeletal muscle atrophy of rats through akt/mTOR signaling pathways. *Front Physiol.* 6:73.
- Rios, E., and G. Brum. 1987. Involvement of dihydropyridine receptors in excitation-contraction coupling in skeletal muscle. *Nature.* 325:717-720.
- Risson, V., L. Mazelin, M. Roceri, H. Sanchez, V. Moncollin, C. Corneloup, H. Richard-Bulteau, A. Vignaud, D. Baas, A. Defour, D. Freyssenet, J.F. Tanti, Y. Le-Marchand-Brustel, B. Ferrier, A. Conjard-Duplany, K. Romanino, S. Bauche, D. Hantai, M. Mueller, S.C. Kozma, G. Thomas, M.A. Ruegg, A. Ferry, M. Pende, X. Bigard, N. Koulmann, L. Schaeffer, and Y.G. Gangloff. 2009. Muscle inactivation of mTOR causes metabolic and dystrophin defects leading to severe myopathy. *J Cell Biol.* 187:859-874.
- Robitaille, A.M., S. Christen, M. Shimobayashi, M. Cornu, L.L. Fava, S. Moes, C. Prescianotto-Baschong, U. Sauer, P. Jenoe, and M.N. Hall. 2013. Quantitative phosphoproteomics reveal mTORC1 activates de novo pyrimidine synthesis. *Science.* 339:1320-1323.
- Rommel, C., S.C. Bodine, B.A. Clarke, R. Rossman, L. Nunez, T.N. Stitt, G.D. Yancopoulos, and D.J. Glass. 2001. Mediation of IGF-1-induced skeletal myotube hypertrophy by PI(3)K/Akt/mTOR and PI(3)K/Akt/GSK3 pathways. *Nat Cell Biol.* 3:1009-1013.
- Rosenberg, H., M. Davis, D. James, N. Pollock, and K. Stowell. 2007. Malignant hyperthermia. *Orphanet J Rare Dis.* 2:21.
- Rosenberg, H., N. Pollock, A. Schiemann, T. Bulger, and K. Stowell. 2015. Malignant hyperthermia: a review. *Orphanet J Rare Dis.* 10:93.
- Rosenberg, H., N. Sambuughin, S. Riazi, and R. Dirksen. 2003. GeneReviews® [Internet]. P. RA, A. MP, A. HH, and e. al., editors. Seattle (WA): University of Washington, Seattle.
-



- 
- Rossi, A.E., and R.T. Dirksen. 2006. Sarcoplasmic reticulum: the dynamic calcium governor of muscle. *Muscle Nerve*. 33:715-731.
- Sabatini, D.M., H. Erdjument-Bromage, M. Lui, P. Tempst, and S.H. Snyder. 1994. RAFT1: a mammalian protein that binds to FKBP12 in a rapamycin-dependent fashion and is homologous to yeast TORs. *Cell*. 78:35-43.
- Saito, A., S. Seiler, A. Chu, and S. Fleischer. 1984. Preparation and morphology of sarcoplasmic reticulum terminal cisternae from rabbit skeletal muscle. *J Cell Biol*. 99:875-885.
- Sandow, A. 1952. Excitation-contraction coupling in muscular response. *Yale J Biol Med*. 25:176-201.
- Sandri, M. 2008. Signaling in muscle atrophy and hypertrophy. *Physiology (Bethesda)*. 23:160-170.
- Sarbassov, D.D., S.M. Ali, D.H. Kim, D.A. Guertin, R.R. Latek, H. Erdjument-Bromage, P. Tempst, and D.M. Sabatini. 2004. Rictor, a novel binding partner of mTOR, defines a rapamycin-insensitive and raptor-independent pathway that regulates the cytoskeleton. *Curr Biol*. 14:1296-1302.
- Sarbassov, D.D., S.M. Ali, S. Sengupta, J.H. Sheen, P.P. Hsu, A.F. Bagley, A.L. Markhard, and D.M. Sabatini. 2006. Prolonged rapamycin treatment inhibits mTORC2 assembly and Akt/PKB. *Mol Cell*. 22:159-168.
- Sasaguri, T., M. Hirata, and H. Kuriyama. 1985. Dependence on Ca<sup>2+</sup> of the activities of phosphatidylinositol 4,5-bisphosphate phosphodiesterase and inositol 1,4,5-trisphosphate phosphatase in smooth muscles of the porcine coronary artery. *Biochem J*. 231:497-503.
- Satoh, H., L.A. Blatter, and D.M. Bers. 1997. Effects of [Ca<sup>2+</sup>]<sub>i</sub>, SR Ca<sup>2+</sup> load, and rest on Ca<sup>2+</sup> spark frequency in ventricular myocytes. *Am J Physiol*. 272:H657-668.
- Schiaffino, S., and C. Reggiani. 2011. FIBER TYPES IN MAMMALIAN SKELETAL MUSCLES. *Physiological Reviews*. 91:1447-1531.
- Schoneich, C., R.I. Viner, D.A. Ferrington, and D.J. Bigelow. 1999. Age-related chemical modification of the skeletal muscle sarcoplasmic reticulum Ca-ATPase of the rat. *Mech Ageing Dev*. 107:221-231.
- Schredelseker, J., V. Di Biase, G.J. Obermair, E.T. Felder, B.E. Flucher, C. Franzini-Armstrong, and M. Grabner. 2005. The beta 1a subunit is essential for the assembly of dihydropyridine-receptor arrays in skeletal muscle. *Proc Natl Acad Sci U S A*. 102:17219-17224.
-

- 
- Schuler, W., R. Sedrani, S. Cottens, B. Haberlin, M. Schulz, H.J. Schuurman, G. Zenke, H.G. Zerwes, and M.H. Schreier. 1997. SDZ RAD, a new rapamycin derivative: pharmacological properties in vitro and in vivo. *Transplantation*. 64:36-42.
- Scott, B.T., H.K. Simmerman, J.H. Collins, B. Nadal-Ginard, and L.R. Jones. 1988. Complete amino acid sequence of canine cardiac calsequestrin deduced by cDNA cloning. *J Biol Chem*. 263:8958-8964.
- Sheridan, D.C., H. Takekura, C. Franzini-Armstrong, K.G. Beam, P.D. Allen, and C.F. Perez. 2006. Bidirectional signaling between calcium channels of skeletal muscle requires multiple direct and indirect interactions. *Proc Natl Acad Sci U S A*. 103:19760-19765.
- Shimura, M., S. Minamisawa, H. Takeshima, Q. Jiao, Y. Bai, S. Umemura, and Y. Ishikawa. 2008. Sarcalumenin alleviates stress-induced cardiac dysfunction by improving Ca<sup>2+</sup> handling of the sarcoplasmic reticulum. *Cardiovasc Res*. 77:362-370.
- Shirokova, N., J. Garcia, and E. Rios. 1998. Local calcium release in mammalian skeletal muscle. *J Physiol*. 512 ( Pt 2):377-384.
- Slavik, K.J., J.P. Wang, B. Aghdasi, J.Z. Zhang, F. Mandel, N. Malouf, and S.L. Hamilton. 1997. A carboxy-terminal peptide of the alpha 1-subunit of the dihydropyridine receptor inhibits Ca(2+)-release channels. *Am J Physiol*. 272:C1475-1481.
- Snoeck, M., B.G. van Engelen, B. Kusters, M. Lammens, R. Meijer, J.P. Molenaar, J. Raaphorst, C.C. Verschuuren-Bemelmans, C.S. Straathof, L.T. Sie, I.F. de Coo, W.L. van der Pol, M. de Visser, H. Scheffer, S. Treves, H. Jungbluth, N.C. Voermans, and E.J. Kamsteeg. 2015. RYR1-related myopathies: a wide spectrum of phenotypes throughout life. *European journal of neurology : the official journal of the European Federation of Neurological Societies*. 22:1094-1112.
- Somlyo, A.V., M. Bond, A.P. Somlyo, and A. Scarpa. 1985. INOSITOL TRISPHOSPHATE-INDUCED CALCIUM RELEASE AND CONTRACTION IN VASCULAR SMOOTH-MUSCLE. *Proceedings of the National Academy of Sciences of the United States of America*. 82:5231-5235.
- Stern, M.D. 1992. Theory of excitation-contraction coupling in cardiac muscle. *Biophys J*. 63:497-517.
- Suematsu, E., M. Hirata, T. Hashimoto, and H. Kuriyama. 1984. Inositol 1,4,5-trisphosphate releases Ca<sup>2+</sup> from intracellular store sites in skinned single cells of porcine coronary artery. *Biochem Biophys Res Commun*. 120:481-485.
- Takuwa, Y. 1996. Regulation of vascular smooth muscle contraction. The roles of Ca<sup>2+</sup>, protein kinase C and myosin light chain phosphatase. *Jpn Heart J*. 37:793-813.
-

- 
- Tanabe, T., K.G. Beam, B.A. Adams, T. Niidome, and S. Numa. 1990. Regions of the skeletal muscle dihydropyridine receptor critical for excitation-contraction coupling. *Nature*. 346:567-569.
- Theodosiou, M., V. Laudet, and M. Schubert. 2010. From carrot to clinic: an overview of the retinoic acid signaling pathway. *Cell Mol Life Sci*. 67:1423-1445.
- Thoreen, C.C., L. Chantranupong, H.R. Keys, T. Wang, N.S. Gray, and D.M. Sabatini. 2012. A unifying model for mTORC1-mediated regulation of mRNA translation. *Nature*. 485:109-113.
- Timchenko, L. 2013. Molecular mechanisms of muscle atrophy in myotonic dystrophies. *Int J Biochem Cell Biol*. 45:2280-2287.
- Tosetto, A., G. Castaman, and F. Rodeghiero. 2013. Bleeders, bleeding rates, and bleeding score. *J Thromb Haemost*. 11 Suppl 1:142-150.
- Toyoshima, C., M. Nakasako, H. Nomura, and H. Ogawa. 2000. Crystal structure of the calcium pump of sarcoplasmic reticulum at 2.6 Å resolution. *Nature*. 405:647-655.
- Treves, S., A.A. Anderson, S. Ducreux, A. Divet, C. Bleunven, C. Grasso, S. Paesante, and F. Zorzato. 2005. Ryanodine receptor 1 mutations, dysregulation of calcium homeostasis and neuromuscular disorders. *Neuromuscul Disord*. 15:577-587.
- Treves, S., M. De Mattei, M. Landfredi, A. Villa, N.M. Green, D.H. MacLennan, J. Meldolesi, and T. Pozzan. 1990. Calreticulin is a candidate for a calsequestrin-like function in Ca<sup>2+</sup>(+)-storage compartments (calciosomes) of liver and brain. *Biochem J*. 271:473-480.
- Treves, S., H. Jungbluth, F. Muntoni, and F. Zorzato. 2008. Congenital muscle disorders with cores: the ryanodine receptor calcium channel paradigm. *Curr Opin Pharmacol*. 8:319-326.
- Treves, S., R. Thurnheer, B. Mosca, M. Vukcevic, L. Bergamelli, R. Voltan, V. Oberhauser, M. Ronjat, L. Csernoch, P. Szentesi, and F. Zorzato. 2012. SRP-35, a newly identified protein of the skeletal muscle sarcoplasmic reticulum, is a retinol dehydrogenase. *Biochem J*. 441:731-741.
- Treves, S., M. Vukcevic, M. Maj, R. Thurnheer, B. Mosca, and F. Zorzato. 2009. Minor sarcoplasmic reticulum membrane components that modulate excitation-contraction coupling in striated muscles. *J Physiol*. 587:3071-3079.
- Triggle, D.J. 2006. L-type calcium channels. *Curr Pharm Des*. 12:443-457.
- Trombetta, E.S. 2003. The contribution of N-glycans and their processing in the endoplasmic reticulum to glycoprotein biosynthesis. *Glycobiology*. 13:77R-91R.
-

- 
- Vazquez-Martin, A., S. Cufi, C. Oliveras-Ferraros, and J.A. Menendez. 2011. Raptor, a positive regulatory subunit of mTOR complex 1, is a novel phosphoprotein of the rDNA transcription machinery in nucleoli and chromosomal nucleolus organizer regions (NORs). *Cell Cycle*. 10:3140-3152.
- Versteeg, H.H., J.W. Heemskerk, M. Levi, and P.H. Reitsma. 2013. New fundamentals in hemostasis. *Physiol Rev*. 93:327-358.
- Vezina, C., A. Kudelski, and S.N. Sehgal. 1975. Rapamycin (AY-22,989), a new antifungal antibiotic. I. Taxonomy of the producing streptomycete and isolation of the active principle. *J Antibiot (Tokyo)*. 28:721-726.
- Vivaudou, M.B., L.H. Clapp, J.V. Walsh, and J.J. Singer. 1988. REGULATION OF ONE TYPE OF CA-2+ CURRENT IN SMOOTH-MUSCLE CELLS BY DIACYLGLYCEROL AND ACETYLCHOLINE. *Faseb Journal*. 2:2497-2504.
- Volpe, P., B.H. Alderson-Lang, L. Madeddu, E. Damiani, J.H. Collins, and A. Margreth. 1990. Calsequestrin, a component of the inositol 1,4,5-trisphosphate-sensitive Ca<sup>2+</sup> store of chicken cerebellum. *Neuron*. 5:713-721.
- Volpe, P., A. Martini, S. Furlan, and J. Meldolesi. 1994. Calsequestrin is a component of smooth muscles: the skeletal- and cardiac-muscle isoforms are both present, although in highly variable amounts and ratios. *Biochem J*. 301 ( Pt 2):465-469.
- Wagenknecht, T., C.E. Hsieh, B.K. Rath, S. Fleischer, and M. Marko. 2002. Electron tomography of frozen-hydrated isolated triad junctions. *Biophys J*. 83:2491-2501.
- Wang, S., W.R. Trumble, H. Liao, C.R. Wesson, A.K. Dunker, and C.H. Kang. 1998. Crystal structure of calsequestrin from rabbit skeletal muscle sarcoplasmic reticulum. *Nat Struct Biol*. 5:476-483.
- Wang, X., N. Weisleder, C. Collet, J. Zhou, Y. Chu, Y. Hirata, X. Zhao, Z. Pan, M. Brotto, H. Cheng, and J. Ma. 2005. Uncontrolled calcium sparks act as a dystrophic signal for mammalian skeletal muscle. *Nat Cell Biol*. 7:525-530.
- Ward, C.W., and W.J. Lederer. 2005. Ghost sparks. *Nat Cell Biol*. 7:457-459.
- Weber, A., and S. Winicur. 1961. The role of calcium in the superprecipitation of actomyosin. *J Biol Chem*. 236:3198-3202.
- Weisleder, N., M. Brotto, S. Komazaki, Z. Pan, X. Zhao, T. Nosek, J. Parness, H. Takeshima, and J. Ma. 2006. Muscle aging is associated with compromised Ca<sup>2+</sup> spark signaling and segregated intracellular Ca<sup>2+</sup> release. *J Cell Biol*. 174:639-645.
- Weisleder, N., and J.J. Ma. 2006. Ca<sup>2+</sup> sparks as a plastic signal for skeletal muscle health, aging, and dystrophy. *Acta Pharmacol Sin*. 27:791-798.
-

- 
- Weisleder, N., J. Zhou, and J. Ma. 2012. Detection of calcium sparks in intact and permeabilized skeletal muscle fibers. *Methods Mol Biol.* 798:395-410.
- Wilmshurst, J.M., S. Lillis, H. Zhou, K. Pillay, H. Henderson, W. Kress, C.R. Muller, A. Ndong, V. Cloke, T. Cullup, E. Bertini, C. Boennemann, V. Straub, R. Quinlivan, J.J. Dowling, S. Al-Sarraj, S. Treves, S. Abbs, A.Y. Manzur, C.A. Sewry, F. Muntoni, and H. Jungbluth. 2010. RYR1 mutations are a common cause of congenital myopathies with central nuclei. *Ann Neurol.* 68:717-726.
- Wray, S., and T. Burdyga. 2010. Sarcoplasmic reticulum function in smooth muscle. *Physiol Rev.* 90:113-178.
- Wu, D., A. Katz, C.H. Lee, and M.I. Simon. 1992. Activation of phospholipase C by alpha 1-adrenergic receptors is mediated by the alpha subunits of Gq family. *J Biol Chem.* 267:25798-25802.
- Wu, S., M.C. Ibarra, M.C. Malicdan, K. Murayama, Y. Ichihara, H. Kikuchi, I. Nonaka, S. Noguchi, Y.K. Hayashi, and I. Nishino. 2006. Central core disease is due to RYR1 mutations in more than 90% of patients. *Brain.* 129:1470-1480.
- Yao, Y., J. Choi, and I. Parker. 1995. Quantal puffs of intracellular Ca<sup>2+</sup> evoked by inositol trisphosphate in *Xenopus* oocytes. *J Physiol.* 482 ( Pt 3):533-553.
- Yao, Y., and I. Parker. 1994. Ca<sup>2+</sup> influx modulation of temporal and spatial patterns of inositol trisphosphate-mediated Ca<sup>2+</sup> liberation in *Xenopus* oocytes. *J Physiol.* 476:17-28.
- Yasuda, T., O. Delbono, Z.M. Wang, M.L. Messi, T. Girard, A. Urwyler, S. Treves, and F. Zorzato. 2013. JP-45/JSRP1 variants affect skeletal muscle excitation-contraction coupling by decreasing the sensitivity of the dihydropyridine receptor. *Hum Mutat.* 34:184-190.
- Yoshida, M., S. Minamisawa, M. Shimura, S. Komazaki, H. Kume, M. Zhang, K. Matsumura, M. Nishi, M. Saito, Y. Saeki, Y. Ishikawa, T. Yanagisawa, and H. Takeshima. 2005. Impaired Ca<sup>2+</sup> store functions in skeletal and cardiac muscle cells from sarcalumenin-deficient mice. *J Biol Chem.* 280:3500-3506.
- Yu, X., S. Carroll, J.L. Rigaud, and G. Inesi. 1993. H<sup>+</sup> countertransport and electrogenicity of the sarcoplasmic reticulum Ca<sup>2+</sup> pump in reconstituted proteoliposomes. *Biophys J.* 64:1232-1242.
- Zalk, R., O.B. Clarke, A. des Georges, R.A. Grassucci, S. Reiken, F. Mancina, W.A. Hendrickson, J. Frank, and A.R. Marks. 2015. Structure of a mammalian ryanodine receptor. *Nature.* 517:44-49.
-

- 
- Zalk, R., S.E. Lehnart, and A.R. Marks. 2007. Modulation of the ryanodine receptor and intracellular calcium. *Annu Rev Biochem.* 76:367-385.
- Zhang, L., J. Kelley, G. Schmeisser, Y.M. Kobayashi, and L.R. Jones. 1997. Complex formation between junctin, triadin, calsequestrin, and the ryanodine receptor. Proteins of the cardiac junctional sarcoplasmic reticulum membrane. *J Biol Chem.* 272:23389-23397.
- Zhao, F., P. Li, S.R. Chen, C.F. Louis, and B.R. Fruen. 2001. Dantrolene inhibition of ryanodine receptor Ca<sup>2+</sup> release channels. Molecular mechanism and isoform selectivity. *J Biol Chem.* 276:13810-13816.
- Zhao, Y., P.M. Vanhoutte, and S.W. Leung. 2015. Vascular nitric oxide: Beyond eNOS. *J Pharmacol Sci.*
- Zhou, J., B.S. Launikonis, E. Rios, and G. Brum. 2004. Regulation of Ca<sup>2+</sup> sparks by Ca<sup>2+</sup> and Mg<sup>2+</sup> in mammalian and amphibian muscle. An RyR isoform-specific role in excitation-contraction coupling? *J Gen Physiol.* 124:409-428.
- Zhu, Z.M., M. Tepel, M. Neusser, and W. Zidek. 1994. ROLE OF NA<sup>+</sup>-CA<sup>2+</sup> EXCHANGE IN AGONIST-INDUCED CHANGES IN CYTOSOLIC CA<sup>2+</sup> IN VASCULAR SMOOTH-MUSCLE CELLS. *American Journal of Physiology.* 266:C794-C799.
- Zinzalla, V., D. Stracka, W. Oppliger, and M.N. Hall. 2011. Activation of mTORC2 by association with the ribosome. *Cell.* 144:757-768.
- Zorzato, F., A.A. Anderson, K. Ohlendieck, G. Froemming, R. Guerrini, and S. Treves. 2000. Identification of a novel 45 kDa protein (JP-45) from rabbit sarcoplasmic-reticulum junctional-face membrane. *Biochem J.* 351 Pt 2:537-543.
- Zorzato, F., A. Margreth, and P. Volpe. 1986. Direct photoaffinity labeling of junctional sarcoplasmic reticulum with [<sup>14</sup>C]doxorubicin. *J Biol Chem.* 261:13252-13257.
- Zubrzycka-Gaarn, E., G. MacDonald, L. Phillips, A.O. Jorgensen, and D.H. MacLennan. 1984. Monoclonal antibodies to the Ca<sup>2+</sup> + Mg<sup>2+</sup>-dependent ATPase of sarcoplasmic reticulum identify polymorphic forms of the enzyme and indicate the presence in the enzyme of a classical high-affinity Ca<sup>2+</sup> binding site. *J Bioenerg Biomembr.* 16:441-464.
- Zucchi, R., and S. Ronca-Testoni. 1997. The sarcoplasmic reticulum Ca<sup>2+</sup> channel/ryanodine receptor: modulation by endogenous effectors, drugs and disease states. *Pharmacol Rev.* 49:1-51.

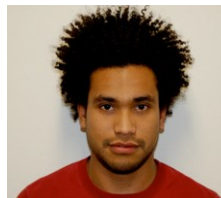
---

# CURRICULUM VITAE

Ruben Lopez

23. 09.1988 - Venezuela

Tlf: 0041786938595  
E-mail: rlopez2@gmail.com  
Kleinhuenerstrasse 139  
Basel 4057  
Switzerland



## Education

University of Carabobo, Venezuela —B. Sc. in Biology, 2011

Basel University, Switzerland —PhD, Cell Biology, currently finishing the 4th year, waiting for the final examination.

## Positions Held

PHD RESEARCHER, DEPARTMENT OF BIOMEDICINE AND ANAESTHESIA - BASEL UNIVERSITY HOSPITAL; BASEL, SWITZERLAND —2012-PRESENT

My current research project focuses on understanding the pathophysiologic mechanisms of neuromuscular diseases including malignant hyperthermia, multi minicore disease, central core disease and other ryanodine receptor-associated myopathies affecting the skeletal muscle calcium homeostasis.

TEACHING ASSISTANT IN THE COURSE PHYSICAL-CHEMISTRY FOR BIOLOGISTS, DEPARTMENT OF BIOLOGY; VALENCIA, VENEZUELA —2007-2009

I was in charge of preparing teaching material such as lectures and exercise as well as correcting exams and training students for the course themes.

## Conference Presentation

“34th Annual Scientific Meeting European Malignant Hyperthermia Group” Lille, France. June 11-13, 2015. Oral presentation.

“Gordon Research Conference: Muscle: Excitation-Contraction Coupling (GRC)” Sunday River in Newry, US. May 31- June 05, 2015. Poster presentation.

“Gordon Research Seminar: Muscle: Excitation-Contraction Coupling (GRS)” Sunday River in Newry, US. May 30-31, 2015. Poster presentation.

“6th Basel Symposium on Skeletal Muscle” Basel, Switzerland. May 15th, 2015. Attendance.

“10th Swiss Meeting on Muscle Research” Magglingen, Switzerland. November 9-10, 2014. Poster presentation.

“3rd Symposium der Jungen Physiologen”, Bonn, Germany. September 25-26, 2014. Oral presentation.

“5th Basel Symposium on Skeletal Muscle” Basel, Switzerland. May 24th, 2013. Attendance.

“Biophysical Society 57th Annual Meeting”, Philadelphia, US. February 2-6, 2013. Poster presentation

“XI Colombian Congress of Phytochemistry”, Antioquia University, Colombia. October 5-7, 2011. Poster presentation.

---

## Publications

Raptor ablation in skeletal muscle decreases Cav1.1 expression and affects the function of the excitation-contraction coupling supramolecular complex. **Lopez R**, Mosca B, Treves S, Maj M, Bergamelli L, Calderon J, Bentzinger C, Romanino K, Hall M, Rüegg M, Delbono O, Caputo C, Zorzato F. *Biochem J*. 2015;466(1):123.

Enhanced dihydropyridine receptor calcium channel activity restores muscle strength in JP45/CASQ1 double knockout mice. Mosca B, Delbono O, Laura Messi M, Bergamelli L, Wang ZM, Vukcevic M, **Lopez R**, Treves S, Nishi M, Takeshima H, Paolini C, Martini M, Rispoli G, Protasi F, Zorzato F. *Nat Commun*. 2013;4:1541.

## Additional Education

Writing to Be Published for the Natural Sciences. March 02- May 18, 2015. Basel Switzerland.

Transferable Skills for Doctoral Students: The Messenger is the Message. Sep 30- Oct 01, 2013. Basel Switzerland.

LTK Module 1: Introductory Course in Laboratory Animal Science. October 22-31, 2012. Basel Switzerland.

## Volunteer Experience

Assistantship in the Haemostasis and Vascular Genetic Laboratory of Biophysics and Biochemistry Center of the Venezuelan Institute of Scientific Research, under Dr. Omar Estrada supervision, 2009.

Assistantship in The Neurochemistry Laboratory of Biophysics and Biochemistry Center of the Venezuelan Institute of Scientific Research, under Dr. Erica Jaffé supervision, 2008.

## Languages

Spanish (Native), English (Fluent), German (Basic).

## Computer Skills

Solid knowledge on standard Microsoft Office software, statistic analysis software, Origin, Prism-GraphPad.

Considerable knowledge in analysis and processing images with the open source software ImageJ, Fiji.

Basic knowledge in data analysis with R.

## Profile

Curious, respectful, critical, social, enthusiastic, disciplined, sensitive. Willing to learn and teach something useful not only professionally, but also in everyday life.

## Interests and Activities

I enjoy to meet new, remote and exotic places, people and cultures around the world. I like to try new and curious tastes from world wide dishes. I love to do exercise, group sports, hiking, but also swimming, among other sports. Reading a good book is always enjoyable for me. I love nature and learning from it. I enjoy very much gardening and plants in general and I am particularly interested on learning about sustainable agriculture with application in urban systems.